Theoretical Development and Numerical Implementation of a Domain-Boundary Integral Equation for Two-Dimensional Electromagnetic Scattering

Jian-Ming Jin and Valdis V. Liepa

Radiation Laboratory
Department of Electrical Engineering
and Computer Science
The University of Michigan
Ann Arbor, MI 48109

April 6, 1989

SUMMARY

This report describes the theoretical development and numerical implementation of a domain-boundary integral equation (DBIE) for two-dimensional electromagnetic scattering. More specifically, it contains the following:

- Derivation of the DBIE using two different approaches;
- Interpretation of the DBIE from a physical point of view;
- Moment method solution of the DBIE using pulse basis expansion and point-matching technique (code included);
- Moment method solution of the DBIE using isoparametric elements and point-matching technique (code included).

Of particular importance are the two distinct properties of the DBIE: it is based on only one field component and does not involve derivatives of the field. The first property allows the use of a minimum number of discretized unknowns. The second allows an easy application of pulse basis expansion functions. The further development of isoparametric elements for the moment method results in a numerical solution of high accuracy.

PREFACE

This report consists of three papers and two numerical codes which represent our research work conducted during October 1987-October 1988 on the domain-boundary integral equation. In order to maintain consistency with the frequently-used phrases "Volume Integral Equation (VIE)" and "Surface Integral Equation (SIE)", we had originally named our new equation the "Volume-Surface Integral Equation (VSIE)". Though the phrases VIE and SIE are often used for the two-dimensional case, strictly speaking they belong to the three-dimensional case. On the other hand, the phrase "Domain-Boundary Integral Equation (DBIE)" is suited for both two- and three-dimensional cases. Since this report primarily deals with two-dimensional scattering, we decided to use DBIE for its title. It is, therefore, understood that the DBIE used in the title and summary is equivalent to the VSIE in the text.

The authors wish to acknowledge the discussions and suggestions of Professors C. T. Tai and J. L. Volakis in relation to this work.

TABLE OF CONTENTS

A VOLUME-SURFACE INTEGRAL EQUATION FOR ELECTROMAGNETIC SCATTERING BY INHOMOGENEOUS CYLINDERS

Jian-Ming Jin, Valdis V. Liepa, and Chen-To Tai

Radiation Laboratory

Department of Electrical Engineering and Computer Science

The University of Michigan

Ann Arbor, Michigan 48109

(published in *The Journal of Electromagnetic Waves and Applications*, vol. 2, no. 5/6)

ABSTRACT

This paper presents an integral equation formulation for electromagnetic scattering by inhomogeneous infinite cylinders having arbitrary scalar permittivities and permeabilities. The formulation involves both volume and surface integrals with only one unknown field component, and is applicable to both transverse electric and transverse magnetic cases. This volume-surface integral equation is well-suited for numerical implementation. In this paper, the integral equation is first derived by integrating the wave equation with the aid of the free-space Green's function, and then analyzed from the physical point of view, resulting in a new interpretation for the scattering mechanism. Finally, the equation is programmed using the method of moments with pulse expansion functions and point-matching.

Numerical results are shown to demonstrate the validity of the formulation and the new interpretation of the scattering mechanism.

1. Introduction

The problem of electromagnetic scattering by inhomogeneous cylinders can be formulated in terms of equivalent polarized currents (see, e.g., [1]-[4]). The formulation leads to a volume integral equation which involves three unknown current components for a scatterer having both permittivity ϵ and permeability μ different from their free-space values. If the cross section of a cylinder is divided into N cells for numerical analysis, one has $3N$ unknowns; consequently a matrix equation of size $3N \times 3N$ needs to be solved. However, the three unknown current components are not independent; they are related by Maxwell's equations. Using such relations, one should be able to reduce the number of unknowns. Recently, a compact formulation has been developed by modifying the equivalent currents, reducing the three current components to two and thus resulting in $2N$ unknowns for numerical analysis [5].

In this paper, the problem is formulated directly using the field concept, instead of the equivalent polarized currents, by integrating the wave equation with the aid of the free-space Green's function. The resultant equation contains both volume and surface integrals but involves only one unknown field component. This volume-surface integral equation provides an alternative physical interpretation for electromagnetic scattering, and is well-suited for numerical implementation. Using this equation, if the circumference of the cylinder is divided into M segments, we

have only $N+M$ unknowns and thus the resultant matrix size is $(N+M)\times(N+M)$. It is noted that a similar idea has been employed by Tai to formulate the scattering by a homogeneous electromagnetically permeable body and by an inhomogeneous dielectric body for the general three-dimensional case [6].

2. Derivation of the Integral Equation

Consider transverse electric (TE) and transverse magnetic (TM) wave scattering by an inhomogeneous cylinder having its infinite dimension along the z-direction (see Figure 1). The complex relative permittivity $\epsilon_r(\bar{r})$ and permeability $\mu_r(\bar{r})$ are continuous functions of position, where $\bar{r}$ is the position vector in the xy-plane. Let Ω denote the region inside the cylinder, Ω_∞ the region outside the cylinder, and Γ the boundary of the cylinder separating Ω and Ω_∞. In the region Ω, the z-directed electric or magnetic field, denoted by F, satisfies the wave equation

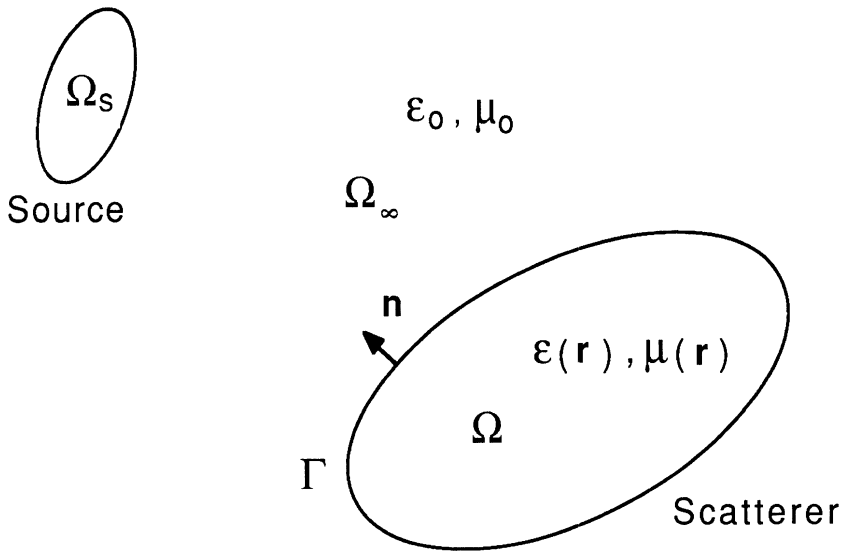

Figure 1: Geometry of wave scattering by an inhomogeneous cylinder.

$$\nabla \cdot [u(\bar{r})\nabla F(\bar{r})] + k_0^2 v(\bar{r}) F(\bar{r}) = 0 \tag{1}$$

where for TM incidence

$$F(\bar{r}) = E_z(\bar{r}) \,, \quad u(\bar{r}) = \frac{1}{\mu_r(\bar{r})} \,, \quad v(\bar{r}) = \epsilon_r(\bar{r})$$

and for TE incidence

$$F(\bar{r}) = H_z(\bar{r}) \,, \quad u(\bar{r}) = \frac{1}{\epsilon_r(\bar{r})} \,, \quad v(\bar{r}) = \mu_r(\bar{r})$$

In the above, ∇ is a two-dimensional operator defined in the rectangular coordinate system by $\nabla = \hat{x}(\partial/\partial x) + \hat{y}(\partial/\partial y)$ and k_0 is the free-space wavenumber.

To find an integral equation for F, we integrate (1) over the region Ω with the aid of the two-dimensional free-space Green's function $G_0(\bar{r}|\bar{r}')$, which satisfies the equation

$$\nabla^2 G_0(\bar{r}|\bar{r}') + k_0^2 G_0(\bar{r}|\bar{r}') = -\delta(\bar{r} - \bar{r}') \tag{2}$$

This leads to the equation

$$\int\int_\Omega \left\{ G_0(\bar{r}|\bar{r}')\nabla \cdot [u(\bar{r})\nabla F(\bar{r})] + k_0^2 v(\bar{r}) G_0(\bar{r}|\bar{r}') F(\bar{r}) \right\} ds = 0 \tag{3}$$

Then, using the identity

$$\nabla \cdot (G_0 u \nabla F) = G_0 \nabla \cdot (u \nabla F) + u \nabla F \cdot \nabla G_0$$

and the two-dimensional divergence theorem, (3) can be written as

$$\begin{aligned} &\int\int_\Omega \left[k_0^2 v(\bar{r}) G_0(\bar{r}|\bar{r}') F(\bar{r}) - u(\bar{r}) \nabla F(\bar{r}) \cdot \nabla G_0(\bar{r}|\bar{r}') \right] ds \\ &+ \oint_\Gamma G_0(\bar{r}|\bar{r}') u(\bar{r}) \frac{\partial F(\bar{r})}{\partial n} dl = 0 \end{aligned} \tag{4}$$

where $\hat{n}$ is the outward unit vector normal to the cylinder's surface. Substituting the identity

$$\nabla \cdot (uF\nabla G_0) = uF\nabla^2 G_0 + u\nabla F \cdot \nabla G_0 + \nabla u \cdot (F\nabla G_0)$$

into (4) and applying again the two-dimensional divergence theorem, we obtain

$$\int\int_\Omega \left\{k_0^2 v(\bar{r})G_0(\bar{r}|\bar{r}')F(\bar{r}) + u(\bar{r})F(\bar{r})\nabla^2 G_0(\bar{r}|\bar{r}') + \nabla u(\bar{r}) \cdot [F(\bar{r})\nabla G_0(\bar{r}|\bar{r}')]\right\} ds$$
$$+ \oint_\Gamma \left[u(\bar{r})G_0(\bar{r}|\bar{r}')\frac{\partial F(\bar{r})}{\partial n} - u(\bar{r})F(\bar{r})\frac{\partial G_0(\bar{r}|\bar{r}')}{\partial n}\right] dl = 0 \tag{5}$$

Substitution of (2) into the above equation gives

$$k_0^2 \int\int_\Omega [v(\bar{r}) - u(\bar{r})]F(\bar{r})G_0(\bar{r}|\bar{r}')ds + \int\int_\Omega \nabla u(\bar{r}) \cdot [F(\bar{r})\nabla G_0(\bar{r}|\bar{r}')]ds$$
$$+ \oint_\Gamma \left[u(\bar{r})G_0(\bar{r}|\bar{r}')\frac{\partial F(\bar{r})}{\partial n} - u(\bar{r})F(\bar{r})\frac{\partial G_0(\bar{r}|\bar{r}')}{\partial n}\right] dl$$
$$= \begin{cases} u(\bar{r}')F(\bar{r}') & \text{for } \bar{r}' \in \Omega \\ \frac{1}{2}u(\bar{r}')F(\bar{r}') & \text{for } \bar{r}' \text{ on } \Gamma \\ 0 & \text{for } \bar{r}' \in \Omega_\infty \end{cases} \tag{6}$$

Note that the line integral is understood to be a principal value integral when r' is on Γ, i.e., the singular point $r = r'$ is excluded from the integration.

Interchanging the unprimed and primed coordinates and using the symmetry property of the Green's function $G_0(\bar{r}|\bar{r}')$, the above equation can be written as

$$k_0^2 \int\int_\Omega [v(\bar{r}') - u(\bar{r}')]F(\bar{r}')G_0(\bar{r}|\bar{r}')ds' + \int\int_\Omega \nabla' u(\bar{r}') \cdot [F(\bar{r}')\nabla' G_0(\bar{r}|\bar{r}')]ds'$$
$$+ \oint_\Gamma \left[u(\bar{r}')G_0(\bar{r}|\bar{r}')\frac{\partial F(\bar{r}')}{\partial n'} - u(\bar{r}')F(\bar{r}')\frac{\partial G_0(\bar{r}|\bar{r}')}{\partial n'}\right] dl'$$
$$= \begin{cases} u(\bar{r})F(\bar{r}) & \text{for } \bar{r} \in \Omega \\ \frac{1}{2}u(\bar{r})F(\bar{r}) & \text{for } \bar{r} \text{ on } \Gamma \\ 0 & \text{for } \bar{r} \in \Omega_\infty \end{cases} \tag{7}$$

This is the equation resulting from the integration over the interior region Ω.

Now let us consider the exterior region Ω_∞. In this infinite region the field is governed by the wave equation

$$\nabla^2 F(\bar{r}) + k_0^2 F(\bar{r}) = j\omega S(\bar{r}) \tag{8}$$

and the radiation condition at infinity. The function $S(\bar{r})$ is related to the z-directed electric or magnetic current by $S(\bar{r}) = \mu_0 J_z(\bar{r})$ for E-polarization and $S(\bar{r}) = \epsilon_0 M_z(\bar{r})$ for H-polarization. Let us assume that the source distribution is confined within a region Ω_s. Integrating (8) over Ω_∞ with the function $G_0(\bar{r}|\bar{r}')$, we obtain

$$\begin{aligned} & F^{INC}(\bar{r}) - \oint_\Gamma \left[G_0(\bar{r}|\bar{r}') \frac{\partial F(\bar{r}')}{\partial n'} - F(\bar{r}') \frac{\partial G_0(\bar{r}|\bar{r}')}{\partial n'} \right] dl' \\ = & \begin{cases} 0 & \text{for } \bar{r} \in \Omega \\ \frac{1}{2} F(\bar{r}) & \text{for } \bar{r} \text{ on } \Gamma \\ F(\bar{r}) & \text{for } \bar{r} \in \Omega_\infty \end{cases} \end{aligned} \tag{9}$$

where F^{INC} is the incident field given by

$$F^{INC}(\bar{r}) = -j\omega \int\int_{\Omega_s} S(\bar{r}') G_0(\bar{r}|\bar{r}') ds'$$

Equation (9) is the well-known surface integral equation.

Since the boundary conditions require the field F and the quantity $u(\partial F/\partial n)$ to be continuous across Γ, we can combine (7) and (9) to obtain an integral equation which does not involve the normal derivative of the field. The resultant equation is then

$$F^{INC}(\bar{r}) + k_0^2 \int\int_\Omega [v(\bar{r}') - u(\bar{r}')] F(\bar{r}') G_0(\bar{r}|\bar{r}') ds'$$

$$+\int\int_{\Omega}\nabla' u(\bar{r}')\cdot[F(\bar{r}')\nabla' G_0(\bar{r}|\bar{r}')]ds' + \oint_{\Gamma}[1-u(\bar{r}')]\,F(\bar{r}')\frac{\partial G_0(\bar{r}|\bar{r}')}{\partial n'}dl'$$

$$= \begin{cases} u(\bar{r})F(\bar{r}) & \text{for } \bar{r}\in\Omega \\ \frac{1}{2}[1+u(\bar{r})]F(\bar{r}) & \text{for } \bar{r} \text{ on } \Gamma \\ F(\bar{r}) & \text{for } \bar{r}\in\Omega_{\infty} \end{cases} \tag{10}$$

and we call it the *Volume-Surface Integral Equation* (VSIE). It should be noted that the above method is not the only way to derive this equation; it can be also derived using the method of equivalent polarized currents. Such a derivation is given in Appendix I to show the difference between the two methods.

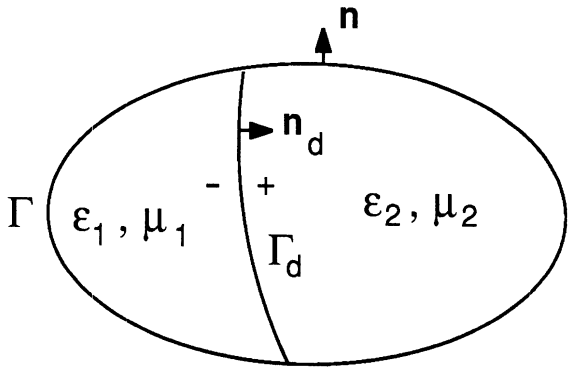

Figure 2: A cylinder consisting of two inhomogeneous media.

The above integral equation (10) is valid for problems with $u(\bar{r})$ continuous in Ω. For cylinders consisting of two or more continuous inhomogeneous media, but having step discontinuities in $u(\bar{r})$ at their interfaces denoted by Γ_d (see Figure 2), a line integral

$$\int_{\Gamma_d}\left[u(\bar{r}'_+)-u(\bar{r}'_-)\right]F(\bar{r}')\frac{\partial G_0(\bar{r}|\bar{r}')}{\partial n'_d}dl' \tag{11}$$

where $\hat{n}_d$ points from the $-$ side to the $+$ side, must be included in the left-hand side of equation (10).

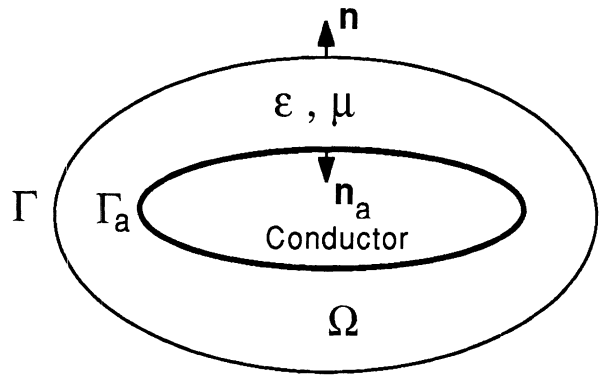

Figure 3: A conducting cylinder coated with inhomogeneous material.

To deal with scatterers containing perfect conductors, such as coated cylinders (see Figure 3), a line integral

$$\oint_{\Gamma_a} \left[\delta_e u(\bar{r}') G_0(\bar{r}|\bar{r}') \frac{\partial F(\bar{r}')}{\partial n'_a} - \delta_h u(\bar{r}') F(\bar{r}') \frac{\partial G_0(\bar{r}|\bar{r}')}{\partial n'_a} \right] dl' \tag{12}$$

along the conducting surface Γ_a must be included, where $\hat{n}_a$ points toward the inside of the conductor, and δ_h and δ_e are polarization factors defined as

$$\begin{cases} \delta_h = 0 \quad \text{for } E\text{-polarization} ; \quad 1 \quad \text{for } H\text{-polarization} \\ \delta_e = 1 \quad \text{for } E\text{-polarization} ; \quad 0 \quad \text{for } H\text{-polarization} \end{cases}$$

3. Physical Interpretation

In this section, we use the concepts of electric currents and dipoles to gain insight into the individual terms of the volume-surface integral equation and interpret it from the physical point of view. For this, let us rewrite (10) for the TM

case as follows

$$k_0^2 \int\int_\Omega [\epsilon_r(\bar{r}') - 1] E_z(\bar{r}') G_0(\bar{r}|\bar{r}') ds' + k_0^2 \int\int_\Omega \frac{\mu_r(\bar{r}') - 1}{\mu_r(\bar{r}')} E_z(\bar{r}') G_0(\bar{r}|\bar{r}') ds'$$
$$+ \int\int_\Omega \nabla' \left[\frac{1}{\mu_r(\bar{r}')} \right] \cdot [E_z(\bar{r}') \nabla' G_0(\bar{r}|\bar{r}')] ds' + \oint_\Gamma \frac{\mu_r(\bar{r}') - 1}{\mu_r(\bar{r}')} E_z(\bar{r}') \nabla' G_0(\bar{r}|\bar{r}') \cdot \hat{n}' dl'$$
$$+ E_z^{INC}(\bar{r}) = \begin{cases} [1/\mu_r(\bar{r})]\, E_z(\bar{r}) & \text{for } \bar{r} \in \Omega \\ \frac{1}{2}[1 + 1/\mu_r(\bar{r})] E_z(\bar{r}) & \text{for } \bar{r} \text{ on } \Gamma \\ E_z(\bar{r}) & \text{for } \bar{r} \in \Omega_\infty \end{cases} \tag{13}$$

Recalling that a z-directed two-dimensional electric current, denoted by J_z, produces a field

$$E_z(\bar{r}) = -j\omega\mu_0 \int\int J_z(\bar{r}') G_0(\bar{r}|\bar{r}') ds' \tag{14}$$

and a volume distribution of electric dipole moment, denoted by $\bar{p}_v$, produces a field [7]

$$E_z(\bar{r}) = j\omega\mu_0 \int\int \bar{p}_v(\bar{r}') \cdot \nabla G_0(\bar{r}|\bar{r}') ds' \tag{15}$$

and also that a surface distribution of electric dipole moment, denoted by $\bar{p}_s$, produces a field

$$E_z(\bar{r}) = j\omega\mu_0 \int \bar{p}_s(\bar{r}') \cdot \nabla G_0(\bar{r}|\bar{r}') dl' \,, \tag{16}$$

by comparing these with (13) we see that the scattered field results from the superposition of the fields produced by four sources. The first source term is an equivalent electric current

$$J_z^{(1)} = j\omega\epsilon_0(\epsilon_r - 1) E_z \tag{17}$$

the second is another equivalent electric current

$$J_z^{(2)} = j\omega\epsilon_0 \frac{\mu_r - 1}{\mu_r} E_z \tag{18}$$

the third is an equivalent volume electric dipole

$$\bar{p}_v = -\frac{1}{j\omega\mu_0} E_z \nabla \left(\frac{1}{\mu_r}\right) \tag{19}$$

and the fourth is an equivalent surface electric dipole

$$\bar{p}_s = -\frac{\mu_r - 1}{j\omega\mu_0\mu_r} E_z \hat{n} \tag{20}$$

The second electric current $J_z^{(2)}$ differs from the first one $J_z^{(1)}$ in that it produces an additional term at the source; the Green's function, denoted by $G(\bar{r}|\bar{r}')$, applied to $J_z^{(2)}$ is

$$G(\bar{r}|\bar{r}') = \frac{\delta(\bar{r} - \bar{r}')}{k_0^2} + G_0(\bar{r}|\bar{r}') \tag{21}$$

rather than $G_0(\bar{r}|\bar{r}')$ that is applied to $J_z^{(1)}$. From (17) - (20), we see clearly how each source is introduced.

We believe that the above interpretation offers a more physically realistic picture for wave scattering than the picture that follows from the conventional volume integral equations which interpret the scattered field as the superposition of the fields produced by equivalent electric and magnetic currents.

To interpret equation (10) for the TE case, it is convenient to use magnetic current and magnetic dipole concepts. The interpretation is similar to that for the TM case; the scattered field results from the superposition of the fields produced

by magnetic current sources and magnetic dipole moments of volume and surface distributions. Such an interpretation, however, falls back to the nonexistent magnetic sources again as do the conventional volume integral equations.

4. Numerical Implementation and Results

This section deals with the programming of equation (10), which is solved by the method of moments in a straightforward manner. Since the equation does not involve any derivative operation on the unknown (as usual, for scatterers containing perfect conductors with TM incidence the quantity $\partial F/\partial n$ in (12) is treated as an unknown rather than the normal derivative of an unknown), the pulse expansion and point-matching technique [1]-[3] can be easily applied to give accurate results. This is in contrast to the conventional volume integral equations, which contain derivatives operating on unknowns for the general case, and thus pulse functions are inappropriate for use in expanding the unknowns [3]. Hence, the volume integral equation approach requires more effort in selecting expansion functions to obtain accurate results [8].

Since the method of moments is well documented, here we only give the result of discretization. We also only consider the problem illustrated in Figure 1; the problems of Figures 2 and 3 can be treated in a similar manner. Assume the region Ω is divided into N cells and the boundary Γ is divided into M segments. If we use ϕ_i to denote the discretized fields in Ω and ϕ_b the fields on Γ, the application

of the pulse expansion and point-matching technique gives the matrix equation

$$\begin{bmatrix} A & B \\ C & D \end{bmatrix} \begin{bmatrix} \phi_i \\ \phi_b \end{bmatrix} = \begin{bmatrix} \phi_i^{INC} \\ \phi_b^{INC} \end{bmatrix} \tag{22}$$

where A, B, C, and D are submatrices with dimension of $N \times N$, $N \times M$, $M \times N$, and $M \times M$, respectively. The expressions for their elements are given in Appendix II. On the right-hand side of (22) is the discretized incident field. The solution of the problem is obtained by solving (22) for ϕ_i and ϕ_b. Once these discretized fields are found, the far field is calculated using (10) with the large-argument approximation for $G_0(\bar{r}|\bar{r}')$.

We next present two numerical examples. The first one is the bistatic scattering from a homogeneous circular cylinder with a radius of 0.32λ (λ is the free-space wavelength), a relative permittivity of $\epsilon_r = 2.5 - j0.5$, and a relative permeability of $\mu_r = 1.5 - j0.5$. The computed scattering cross sections, σ/λ as defined in [9], are shown in Figure 4, along with the exact eigenfunction solution. In the figure, VSIEM stands for the formulation presented in this paper, i.e., the *Volume-Surface Integral Equation Method.* Note that the two results are almost identical.

The second example is the backscattering from an inhomogeneous rectangular cylinder of size $0.4\lambda \times 0.8\lambda$. Its relative permittivity is a function of position given by $\epsilon_r = [1 + \cos(\pi x/0.4\lambda)][1 + \cos(\pi y/0.8\lambda)]$; and its relative permeability is a constant, $\mu_r = 1.5$. The results are shown in Figure 5, and are compared with those obtained using the Hybrid Finite Element Method (HFEM) [10], [11]. Again excellent agreement is observed.

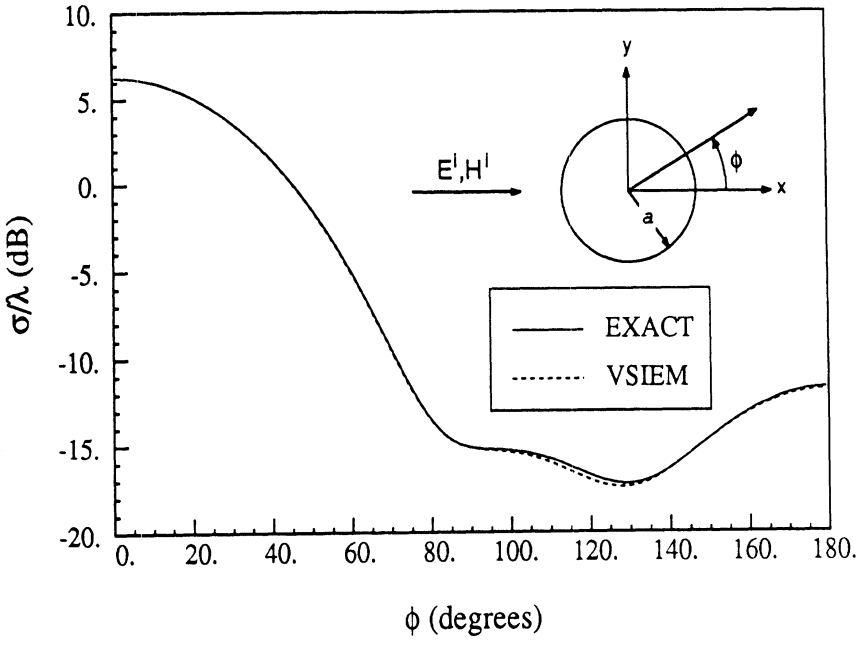

(a)

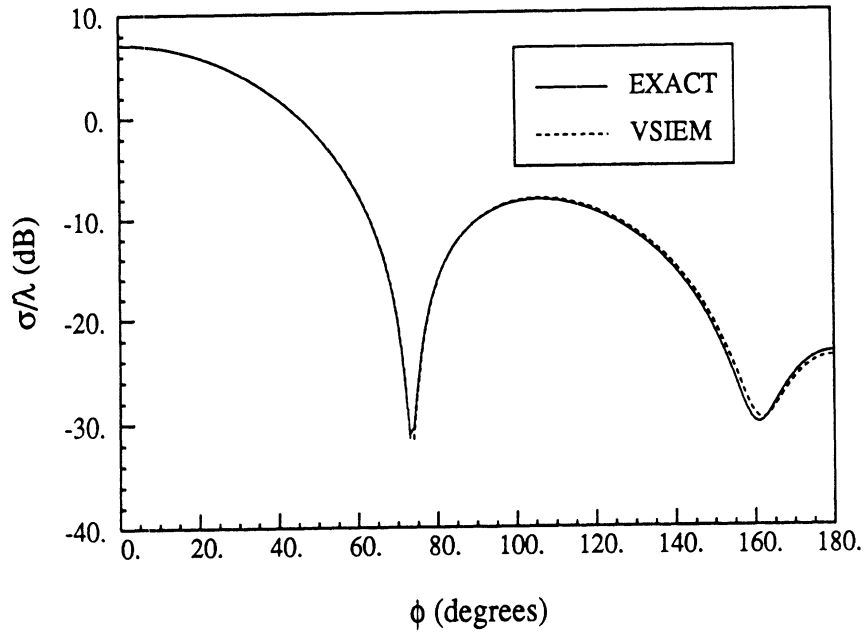

(b)

Figure 4: Bistatic scattering pattern of a homogeneous circular cylinder, $a = 0.32\lambda$, $\epsilon_r = 2.5 - j0.5$, $\mu_r = 1.5 - j0.5$. (a) TE case; (b) TM case.

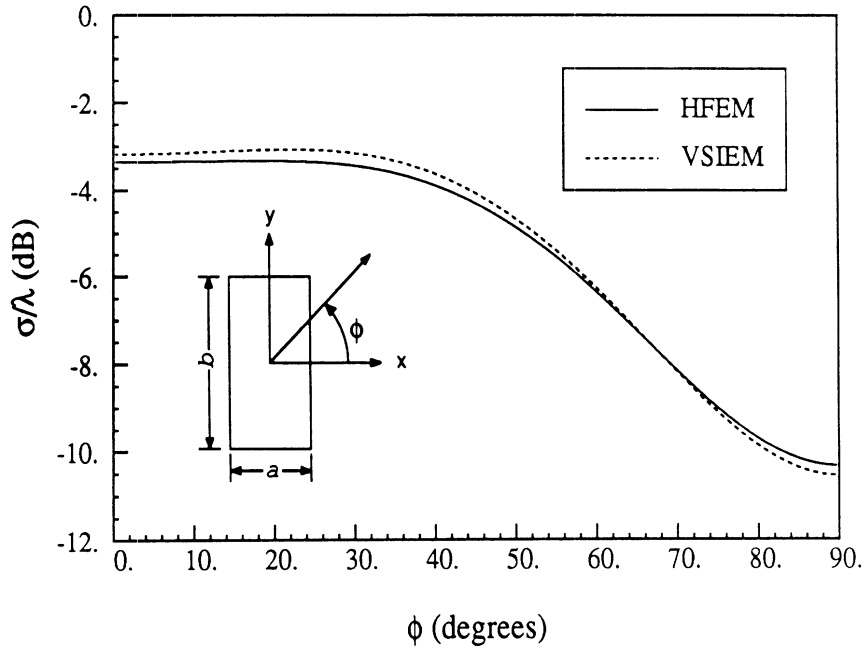

(a)

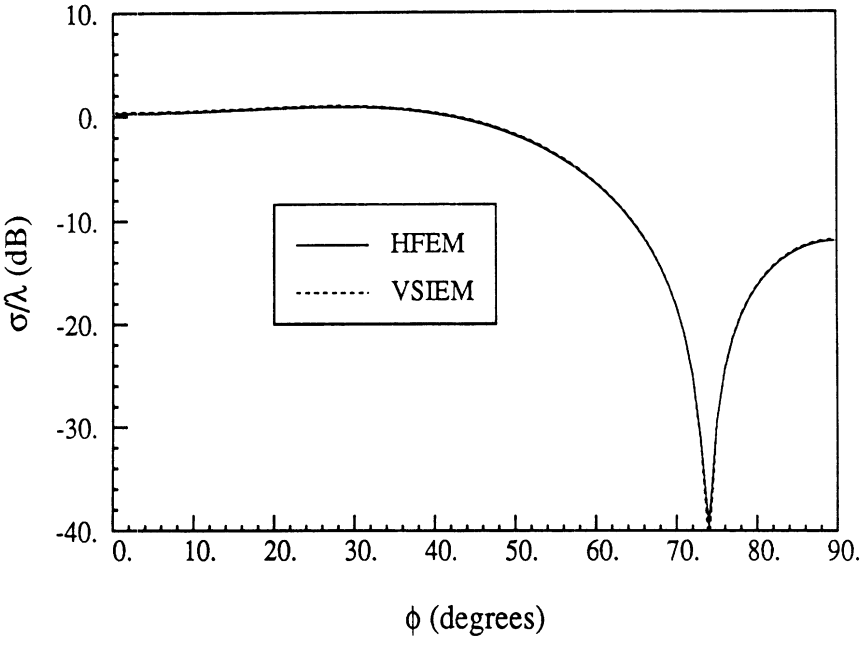

(b)

Figure 5: Backscattering pattern of an inhomogeneous rectangular cylinder, $a = 0.4\lambda$, $b = 0.8\lambda$, $\epsilon_r = [1 + \cos(\pi x/a)][1 + \cos(\pi y/b)]$, $\mu_r = 1.5$. (a) TE case; (b) TM case.

It should be noted that the above VSIEM results were obtained with a sampling criterion of 12 points per material wavelength.

Although the program we developed can be applied to arbitrary two-dimensional geometries and configurations, the above two examples, we believe, are sufficient to demonstrate the validity of equation (10) and the corresponding computer program.

To show the contribution of various terms in (10) to the scattered field, we also made a computation for scattering by an inhomogeneous circular cylinder, whose geometry is the same as that illustrated in Figure 4. The cylinder has a radius of $a = 0.4\lambda$, a relative permittivity of $\epsilon_r = 2 - (r/a)^2$ which is that of a slice through the center of a Luneberg lens, and a relative permeability of $\mu_r = 1.2$. For the TE case, the scattered field is due to an equivalent volume magnetic current (2nd term in (10)) and an equivalent volume magnetic dipole moment (3rd term in (10)). There is no surface dipole moment, since ϵ_r becomes one at the surface of the cylinder, making the 4th term vanish in (10). The results are shown in Figure 6 in terms of the amplitude and phase of the scattered far-field coefficient $P(\phi)$ [9]. For the TM case, the scattered field is due to an equivalent volume electric current (2nd term in (10)) and an equivalent surface electric dipole moment (4th term in (10)). In this case there is no volume dipole moment, since μ_r is a constant. The results are shown in Figure 7. From both Figures 6 and 7, we see that in the forward scatter region the field due to the volume currents is dominant and in-phase with the field that is due to the volume and surface dipoles; while in

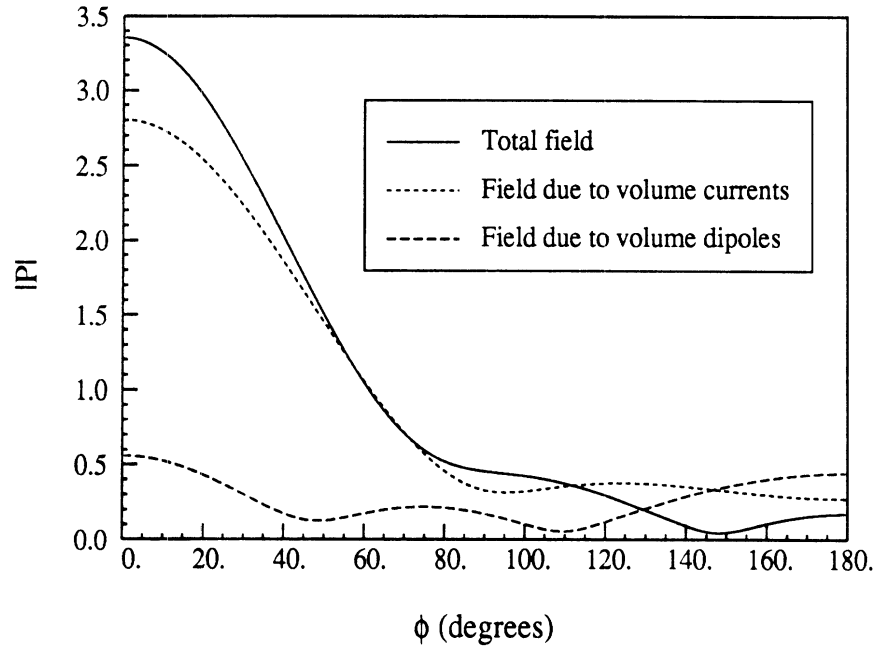

(a)

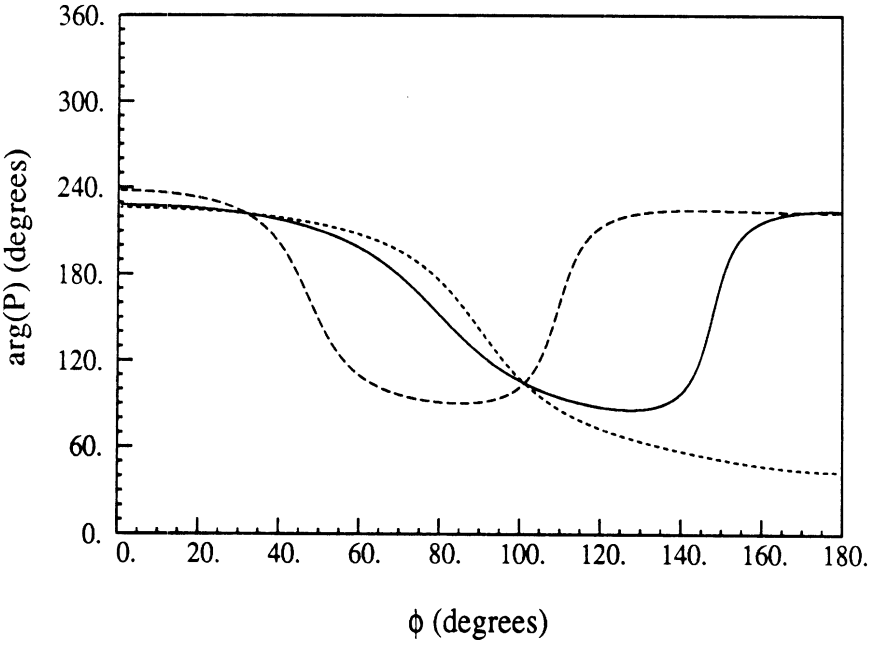

(b)

Figure 6: Bistatic scattered field of an inhomogeneous circular cylinder for the TE case, $a = 0.4\lambda$, $\epsilon_r = 2 - (r/a)^2$, $\mu_r = 1.2$. (a) Amplitude; (b) Phase.

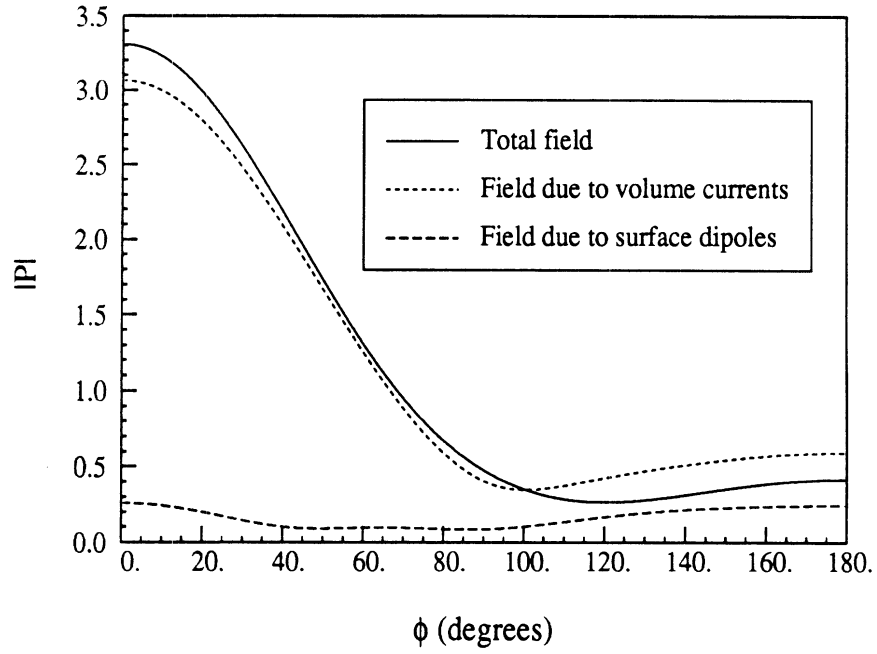

(a)

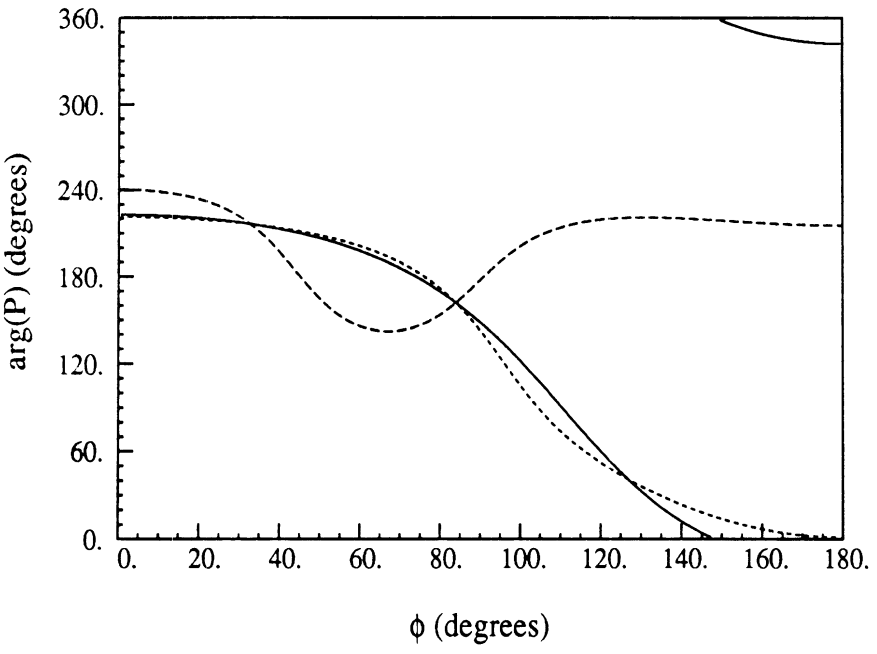

(b)

Figure 7: Bistatic scattered field of an inhomogeneous circular cylinder for the TM case, $a = 0.4\lambda$, $\epsilon_r = 2 - (r/a)^2$, $\mu_r = 1.2$. (a) Amplitude; (b) Phase.

the backscatter region both fields due to currents and dipoles have comparable magnitudes and they are out of phase.

5. Conclusion

In this paper, an integral equation is derived for the analysis of two-dimensional electromagnetic scattering by inhomogeneous cylinders. The equation contains both volume and surface integrals but involves only one field component. From its physical interpretation it is seen that the field scattered by a cylinder is produced by a set of equivalent electric (or magnetic) current and dipole sources for TM (or TE) wave scattering. In regards to numerical analysis, the equation has two advantages: first, the equation contains only one unknown component, and thus is numerically more efficient than the volume integral equation formulation; second, the equation does not contain any derivative operation on the unknown, and hence the simple pulse expansion and point-matching technique can be used without loss of accuracy.

Appendix I

Derivation of (10) using the Method of Equivalent Polarized Currents

In the method of equivalent polarized currents, the scatterer is replaced by an equivalent polarized electric current

$$\overline{J} = j\omega\epsilon_0(\epsilon_r - 1)\overline{E} \tag{23}$$

and an equivalent polarized magnetic current

$$\overline{M} = j\omega\mu_0(\mu_r - 1)\overline{H} \tag{24}$$

where $\overline{E}$ and $\overline{H}$ are the total electric and magnetic fields, which are related by Maxwell's equations

$$\begin{cases} \nabla \times \overline{E} = -j\omega\mu_0\mu_r\overline{H} \\ \nabla \times \overline{H} = j\omega\epsilon_0\epsilon_r\overline{E} \end{cases} \tag{25}$$

Let $\overline{E}_e$ and $\overline{H}_e$ represent the fields produced by $\overline{J}$, and $\overline{E}_m$ and $\overline{H}_m$ the fields produced by $\overline{M}$. They obey the free-space Maxwell's equations

$$\begin{cases} \nabla \times \overline{E}_e = -j\omega\mu_0\overline{H}_e \\ \nabla \times \overline{H}_e = j\omega\epsilon_0\overline{E}_e + \overline{J} \end{cases} \tag{26}$$

and

$$\begin{cases} \nabla \times \overline{E}_m = -j\omega\mu_0\overline{H}_m - \overline{M} \\ \nabla \times \overline{H}_m = j\omega\epsilon_0\overline{E}_m \end{cases} \tag{27}$$

Let us consider TM wave incidence first. For this case, the electric field has only a z-component. The field due to $\overline{J}$ is

$$\begin{aligned} \overline{E}_e(\bar{r}) &= -j\omega\mu_0 \int\int_\Omega \overline{J}(\bar{r}')G_0(\bar{r}|\bar{r}')ds' \\ &= \hat{z}k_0^2 \int\int_\Omega [\epsilon_r(\bar{r}') - 1]E_z(\bar{r}')G_0(\bar{r}|\bar{r}')ds' \end{aligned} \tag{28}$$

and the field due to $\overline{M}$ is

$$\begin{aligned} \overline{E}_m(\bar{r}) &= -\nabla \times \int\int_\Omega \overline{M}(\bar{r}')G_0(\bar{r}|\bar{r}')ds' \\ &= \nabla \times \int\int_\Omega \left[1 - \frac{1}{\mu_r(\bar{r}')}\right] G_0(\bar{r}|\bar{r}')\nabla' \times \overline{E}(\bar{r}')ds' \\ &= \nabla \times \int\int_\Omega \nabla' \times \left\{ \left[1 - \frac{1}{\mu_r(\bar{r}')}\right] G_0(\bar{r}|\bar{r}')\overline{E}(\bar{r}') \right\} ds' \\ &\quad - \nabla \times \int\int_\Omega \left[1 - \frac{1}{\mu_r(\bar{r}')}\right] \nabla' G_0(\bar{r}|\bar{r}') \times \overline{E}(\bar{r}')ds' \\ &\quad + \nabla \times \int\int_\Omega G_0(\bar{r}|\bar{r}')\nabla' \left[\frac{1}{\mu_r(\bar{r}')}\right] \times \overline{E}(\bar{r}')ds' \end{aligned} \tag{29}$$

Noting that $\nabla G_0(\bar{r}|\bar{r}') = -\nabla' G_0(\bar{r}|\bar{r}')$, we can show that (29) can be expressed as

$$\begin{aligned}
\overline{E}_m(\bar{r}) &= \hat{z}\int\int_\Omega \nabla' \cdot \left\{ \left[1 - \frac{1}{\mu_r(\bar{r}')}\right] E_z(\bar{r}')\nabla' G_0(\bar{r}|\bar{r}') \right\} ds' \\
&\quad - \hat{z}\int\int_\Omega \left[1 - \frac{1}{\mu_r(\bar{r}')}\right] E_z(\bar{r}')\nabla'^2 G_0(\bar{r}|\bar{r}') ds' \\
&\quad + \hat{z}\int\int_\Omega \nabla' \left[\frac{1}{\mu_r(\bar{r}')}\right] \cdot [E_z(\bar{r}')\nabla' G_0(\bar{r}|\bar{r}')]\, ds' \qquad (30)
\end{aligned}$$

Using equation (2) and the two-dimensional divergence theorem, we can also write the above equation as

$$\begin{aligned}
\overline{E}_m(\bar{r}) &= \hat{z}\oint_\Gamma \left[1 - \frac{1}{\mu_r(\bar{r}')}\right] E_z(\bar{r}')\frac{\partial G_0(\bar{r}|\bar{r}')}{\partial n'} dl' \\
&\quad + \hat{z}k_0^2\int\int_\Omega \left[1 - \frac{1}{\mu_r(\bar{r}')}\right] E_z(\bar{r}')G_0(\bar{r}|\bar{r}') ds' \\
&\quad + \hat{z}\int\int_\Omega \nabla' \left[\frac{1}{\mu_r(\bar{r}')}\right] \cdot [E_z(\bar{r}')\nabla' G_0(\bar{r}|\bar{r}')]\, ds' \\
&\quad + \begin{cases} \hat{z}\,[1 - 1/\mu_r(\bar{r})]\, E_z(\bar{r}) & \text{for } \bar{r} \in \Omega \\ \hat{z}\frac{1}{2}[1 - 1/\mu_r(\bar{r})]E_z(\bar{r}) & \text{for } \bar{r} \text{ on } \Gamma \\ 0 & \text{for } \bar{r} \in \Omega_\infty \end{cases} \qquad (31)
\end{aligned}$$

The total electric field is the superposition of the incident field, the field due to the electric current $\overline{J}$, and the field due to the magnetic current $\overline{M}$

$$E_z(\bar{r}) = E_z^{INC}(\bar{r}) + \hat{z} \cdot \overline{E}_e(\bar{r}) + \hat{z} \cdot \overline{E}_m(\bar{r}) \qquad (32)$$

Substituting (28) and (31) into the above equation, we thus obtain

$$\begin{aligned}
&E_z^{INC}(\bar{r}) + k_0^2\int\int_\Omega \left[\epsilon_r(\bar{r}') - \frac{1}{\mu_r(\bar{r}')}\right] E_z(\bar{r}')G_0(\bar{r}|\bar{r}') ds' \\
&+ \int\int_\Omega \nabla' \left[\frac{1}{\mu_r(\bar{r}')}\right] \cdot [E_z(\bar{r}')\nabla' G_0(\bar{r}|\bar{r}')]\, ds'
\end{aligned}$$

$$+ \oint_\Gamma \left[1 - \frac{1}{\mu_r(\bar{r}')}\right] E_z(\bar{r}') \frac{\partial G_0(\bar{r}|\bar{r}')}{\partial n'} dl'$$

$$= \begin{cases} [1/\mu_r(\bar{r})] E_z(\bar{r}) & \text{for } \bar{r} \in \Omega \\ \frac{1}{2}[1 + 1/\mu_r(\bar{r})] E_z(\bar{r}) & \text{for } \bar{r} \text{ on } \Gamma \\ E_z(\bar{r}) & \text{for } \bar{r} \in \Omega_\infty \end{cases} \tag{33}$$

This equation is the same as (10) for TM incidence. The derivation for TE incidence is similar. Note that the boundary conditions on Γ are automatically satisfied in this method, while in the derivation of Section 2 they are explicitly enforced.

Appendix II

Matrix Element Expressions for (22)

The element expressions for submatrices A, B, C, and D in equation (22) are given below:

$$A_{ij} = \frac{j}{4} k_0^2 [v(\bar{r}_j^i) - u(\bar{r}_j^i)] H_0^{(2)}(k_0 |\bar{r}_i^i - \bar{r}_j^i|) s_j$$
$$+ \frac{j}{4} k_0 \left[u_x(\bar{r}_j^i) \frac{x_i^i - x_j^i}{|\bar{r}_i^i - \bar{r}_j^i|} + u_y(\bar{r}_j^i) \frac{y_i^i - y_j^i}{|\bar{r}_i^i - \bar{r}_j^i|} \right] H_1^{(2)}(k_0 |\bar{r}_i^i - \bar{r}_j^i|) s_j$$
$$i, j = 1, 2, 3, \cdots, N; \; i \neq j$$

$$A_{ii} = u(\bar{r}_i^i) + \left[v(\bar{r}_i^i) - u(\bar{r}_i^i)\right] \left[1 + j \frac{\pi}{2} k_0 a_i H_1^{(2)}(k_0 a_i)\right]$$
$$i = 1, 2, 3, \cdots, N$$

$$B_{ij} = \frac{j}{4} k_0 [1 - u(\bar{r}_j^i)] \left[n_x(\bar{r}_j^b) \frac{x_i^i - x_j^b}{|\bar{r}_i^i - \bar{r}_j^b|} + n_y(\bar{r}_j^b) \frac{y_i^i - y_j^b}{|\bar{r}_i^i - \bar{r}_j^b|} \right] H_1^{(2)}(k_0 |\bar{r}_i^i - \bar{r}_j^b|) l_j$$
$$i = 1, 2, 3, \cdots, N; \; j = 1, 2, 3, \cdots, M$$

$$C_{ij} = \frac{j}{4} k_0^2 [v(\bar{r}_j^i) - u(\bar{r}_j^i)] H_0^{(2)}(k_0 |\bar{r}_i^b - \bar{r}_j^i|) s_j$$

$$+\frac{j}{4}k_0\left[u_x(\bar{r}_j^i)\frac{x_i^b-x_j^i}{|\bar{r}_i^b-\bar{r}_j^i|}+u_y(\bar{r}_j^b)\frac{y_i^b-y_j^i}{|\bar{r}_i^b-\bar{r}_j^i|}\right]H_1^{(2)}(k_0|\bar{r}_i^b-\bar{r}_j^i|)s_j$$

$$i=1,2,3,\cdots,M;\ j=1,2,3,\cdots,N$$

$$D_{ij} = \frac{j}{4}k_0[1-u(\bar{r}_j^b)]\left[n_x(\bar{r}_j^b)\frac{x_i^b-x_j^b}{|\bar{r}_i^b-\bar{r}_j^b|}+n_y(\bar{r}_j^b)\frac{y_i^b-y_j^b}{|\bar{r}_i^b-\bar{r}_j^b|}\right]H_1^{(2)}(k_0|\bar{r}_i^b-\bar{r}_j^b|)l_j$$

$$i,j=1,2,3,\cdots,M;\ i\neq j$$

$$D_{ii} = \frac{1}{2}[1+u(\bar{r}_i^b)]$$

$$i=1,2,3,\cdots,M$$

The superscripts i and b are used to distinguish those variables in Ω and on Γ, respectively. In the above expressions, s_j denotes the area of the jth cell, l_j the length of the jth segment, $a_i=\sqrt{s_i/\pi}$, u_x and u_y are defined by $\nabla u = u_x\hat{x}+u_y\hat{y}$, and n_x and n_y by $\hat{n}=n_x\hat{x}+n_y\hat{y}$. $H_0^{(2)}$ and $H_1^{(2)}$ are the Hankel functions of the second kind, of the zeroth and first order, respectively.

Acknowledgments

The authors wish to thank Mr. Leland Pierce for his many helpful suggestions, and the JEWA reviewers for their comments.

Part of this work (J.M.J. and C.T.T.) was supported by the National Science Foundation under Grant ECS-8319595.

References

[1] Richmond, J. H., "Scattering by a dielectric cylinder of arbitrary cross-section shape," *IEEE Trans. Antennas Propagat.*, vol. AP-13, pp. 334-341, 1965.

[2] Richmond, J. H., "TE-wave scattering by a dielectric cylinder of arbitrary cross-section shape," *IEEE Trans. Antennas Propagat.*, vol. AP-14, pp. 460-464, 1966.

[3] Harrington, R. F., *Field Computation by Moment Methods.* New York: Macmillan, 1968.

[4] Newman, E. H., "TM and TE scattering by a dielectric/ferrite cylinder in the presence of a half-plane," *IEEE Trans. Antennas Propagat.*, vol. AP-34, pp. 804-813, 1986.

[5] Ricoy, M. A. and J. L. Volakis, "Integral equations with reduced unknowns for the simulation of two-dimensional composite structures," The University of Michigan Radiation Laboratory Report No. 389492-2-T, Nov. 1987.

[6] Tai, C.-T., "A note on the integral equations for the scattering of a plane wave by an electromagnetically permeable body," *Electromagnetics*, vol. 5, pp. 79-88, 1985.

[7] Harrington, R. F., *Time-Harmonic Electromagnetic Fields.* New York: McGraw-Hill, 1961.

[8] Hill, S. C., C. H. Durney, and D. A. Christensen, "Numerical calculations of low-frequency TE fields in arbitrarily shaped inhomogeneous lossy dielectric cylinders," *Radio Science*, vol. 18, pp. 328-336, 1983.

[9] Bowman, J. J., T. B. A. Senior, and P. L. E. Uslenghi ed., *Electromagnetic and*

Acoustic Scattering by Simple Shapes. North-Holland Publishing Company-Amsterdam, pp. 6-7, 1969. A revised printing is published by Hemisphere Publishing Corporation, New York, 1987.

[10] Jin, J.-M. and V. V. Liepa, "Application of hybrid finite element method to electromagnetic scattering from coated cylinders," *IEEE Trans. Antennas Propagat.*, vol. AP-36, pp. 50-54, 1988.

[11] Jin, J.-M. and V. V. Liepa, "A note on hybrid finite element method for solving scattering problems," *IEEE Trans. Antennas Propagat.*, vol. AP-36, pp. 1486-1490, 1988.

A SIMPLE MOMENT METHOD PROGRAM FOR COMPUTING SCATTERING FROM COMPLEX CYLINDRICAL OBSTACLES

Jian-Ming Jin and Valdis V. Liepa

Radiation Laboratory

Department of Electrical Engineering and Computer Science

The University of Michigan

Ann Arbor, Michigan 48109

(accepted for publication in *Proc. Inst. Elec. Eng., part H*, 1989)

ABSTRACT

This paper describes a moment method program for computing electromagnetic scattering (for both E- and H-polarization) from multiple perfectly conducting and penetrable inhomogeneous cylinders (The latter can be lossy and have both permittivity and permeability different from their free-space values). The program is a numerical implementation of a recently derived volume-surface integral equation and uses the pulse expansion and point-matching technique. The main feature of this program is its simplicity in generating the model and transforming the integral equation into a linear system of equations. Using this program, we explore and

demonstrate the usefulness as well as the limitations of the volume-surface integral equation formulation.

I. Introduction

In the frequency domain the problem of open region electromagnetic scattering is usually treated using integral equation methods (see e.g., [1]-[4]), partial differential equation methods (see e.g., [5]), and hybrid techniques which combine the partial differential equation methods with a surface integral equation or an eigenfunction expansion (see e.g., [6]-[9]). The integral equation methods have the advantages of simple numerical implementation and minimum discretization region, since the formulations incorporate the radiation condition by means of the free-space Green's function. However, they have the disadvantage of rather difficult formulation for complex media and result in full matrices which are costly to solve when they are very large. The partial differential equation methods have the advantages of simple formulation even for complex media and simple numerical implementation, and produce sparse matrices which are much easier to solve. Their major disadvantage, however, is the need of extending the discretization region to the far field region in order to enforce the radiation condition, which usually leads to an extremely large number of unknowns[1]. The hybrid techniques represent a synthesis of these two methods: their advantages remain while their disadvantages are eliminated. As a result, they are more powerful especially for treating large scatterers. However, the formulations and especially the numerical implementation

[1]Currently, much attention is aimed at employing more complicated radiation conditions to reduce the discretization region.

of the hybrid techniques usually require more effort.

This paper deals with two-dimensional electromagnetic scattering via the integral equation approach. The purpose of this paper is to describe a simple moment method program which is based on the formulation of a recently derived volume-surface integral equation (VSIE) [10]. Using this program, we will explore and demonstrate the usefulness as well as the limitations of the VSIE, and answer some questions raised about this new formulation and its applications.

Electromagnetic scattering from and interaction with complex cylindrical obstacles of arbitrary cross section has recently attracted much attention from researchers due to its applications such as the control of radar cross section and the design of microwave devices. A surface integral equation solution has been presented by Arvas *et al.* for multiple perfectly conducting and homogeneous, lossy dielectric cylinders for transverse magnetic (TM) wave scattering [11]. A similar solution has also been presented recently by Yuan *et al.* for a homogeneous dielectric cylinder partially covered by conductors for both TM and TE (transverse electric) wave scattering [12]. Earlier, Newman treated a special case involving TM and TE scattering from a dielectric cylinder in the presence of a perfectly conducting half-plane using a volume integral equation with the half-plane Green's function as its kernel [13]. We will show that the formulation and its numerical implementation presented in this paper can effectively handle the most general case — TM and TE scattering from multiple cylinders which include perfectly conducting cylinders and lossy inhomogeneous penetrable cylinders with both permittivity

and permeability different from their free-space values.

In Section II, the VSIE is presented for both E-polarization (TM) and H-polarization (TE) fields in such a way that the physical meaning of the terms in the equation is more obvious. The application of the method of moments with pulse basis functions and point-matching to the VSIE is described in detail in Section III. Section IV gives some numerical examples to demonstrate the validity and versatility of the computer program. Following this is Section V discussing the limitations of the VSIE and the program. It is the authors' intent that with the description given in this paper the interested reader can easily develop his/her own program and further explore the VSIE application from different perspectives.

II. Volume-Surface Integral Equation

The volume-surface integral equation (VSIE) is an integral equation governing two-dimensional electromagnetic radiation and scattering phenomena. This equation has been recently derived by Jin, Liepa, and Tai [10]. It differs from the conventional integral equations in that: (i) the VSIE contains both line and area integrals while the conventional integral equations usually contain only area integrals for inhomogeneous obstacles [2], [3] or line integrals for homogeneous obstacles [4]; (ii) the VSIE has only one scalar unknown variable regardless of the material properties of the obstacles and the polarization of the fields, while the conventional volume integral equations have one or two or three scalar unknown variables depending on the permittivity and permeability of the obstacles and the polarization of the fields (see Table 1); and more importantly (iii) the VSIE does

Table 1. Numbers of Scalar Variables in the Volume Integral Equations (VIE) and Volume-Surface Integral Equation (VSIE)

Material	$\epsilon \neq \epsilon_0$, $\mu = \mu_0$		$\epsilon = \epsilon_0$, $\mu \neq \mu_0$		$\epsilon \neq \epsilon_0$, $\mu \neq \mu_0$	
Field	E-pol.	H-pol.	E-pol.	H-pol.	E-pol.	H-pol.
VIE	1	2	2	1	3	3
VSIE	1	1	1	1	1	1

not involve any derivative operation on the unknown while the conventional volume integral equations have derivatives operating on the unknowns for the general case. The second and third differences give the VSIE a notable advantage over the conventional volume integral equations. In this section, we will present, without derivation, the VSIE while the detailed formulation can be found in [10].

The problem under consideration is illustrated in Figure 1, where a source excites an electromagnetic field in the presence of some obstacles which consist of inhomogeneous dielectrics[2] and perfect conductors. The source and the obstacles are of infinite extent in the z-direction, and have no variation of any kind with respect to the z-coordinate. Thus, the resultant field under such circumstances has no variation with respect to the z-coordinate.

In the two-dimensional case which we consider here, an arbitrary electromagnetic field can be expressed as the sum of an E-polarized field which has only a z-

[2]By the word *dielectric*, in this paper we refer to the general penetrable material rather than a kind of particular material with $\mu_r = 1$.

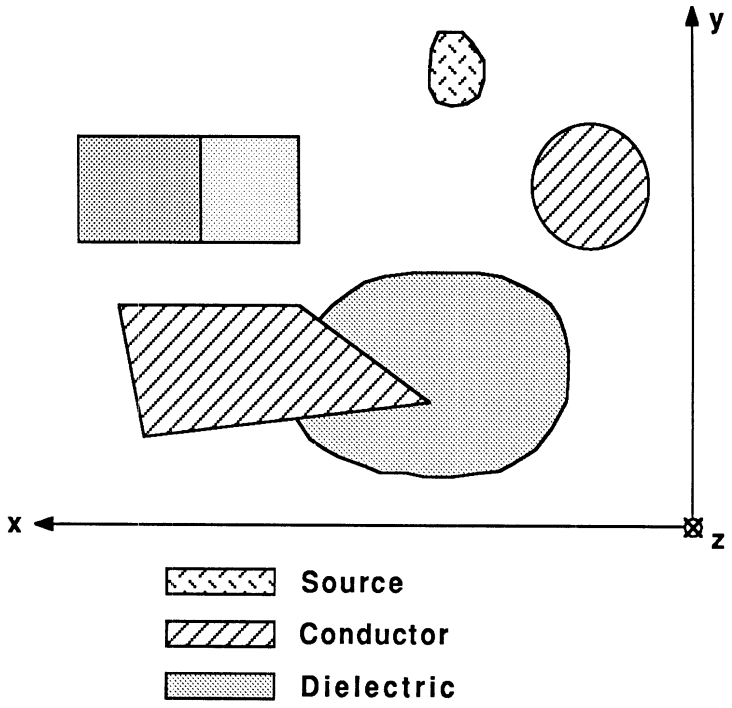

Figure 1: An illustration of the problem under consideration.

component of electric field and an H-polarized field which has only a z-component of magnetic field. Therefore, we can solve the problem by treating the E-polarized and H-polarized fields separately. In the following, we state the VSIE for these two fields separately. A unified presentation of the VSIE for the two fields is possible if appropriate notations are used [10].

E-polarization (TM)

The total z-directed electric field, E_z, is a superposition of the incident field, E_z^i, due to the excitation and the scattered field, E_z^s, due to the presence of the obstacles:

$$E_z(\bar{r}) = E_z^i(\bar{r}) + E_z^s(\bar{r}). \tag{1}$$

For the problem under consideration, the scattered field consists of five parts due to five different sources:

$$E_z^s(\bar{r}) = \sum_{i=1}^{5} E_z^{s(i)}(\bar{r}). \tag{2}$$

1. The first source is a volume electric current due to the non-unity of the permittivity in the region, Ω, occupied by the dielectric obstacles:

$$J_z(\bar{r}') = j\omega\epsilon_0[\epsilon_r(\bar{r}') - 1]E_z(\bar{r}'). \tag{3}$$

The Green's function[3] applied to this source is

$$G(\bar{r}|\bar{r}') = -j\omega\mu_0 G_0(\bar{r}|\bar{r}') \tag{4}$$

[3]By the phrase *Green's function*, here we mean the electric field produced by a unit source.

where $G_0(\bar{r}|\bar{r}') = -(j/4)H_0^{(2)}(k_0|\bar{r}-\bar{r}'|)$. Thus, the source produces a field

$$E_z^{s(1)}(\bar{r}) = k_0^2 \int\int_\Omega [\epsilon_r(\bar{r}') - 1] E_z(\bar{r}') G_0(\bar{r}|\bar{r}') ds'. \tag{5}$$

2. The second source is also a volume electric current; but, it is due to the non-unity of the permeability:

$$J_z(\bar{r}') = j\omega\epsilon_0 \left[1 - \frac{1}{\mu_r(\bar{r}')}\right] E_z(\bar{r}'). \tag{6}$$

The Green's function applied to this source is

$$G(\bar{r}|\bar{r}') = -j\omega\mu_0 \left[\frac{\delta(\bar{r}-\bar{r}')}{k_0^2} + G_0(\bar{r}|\bar{r}')\right] \tag{7}$$

and the field produced by the source is then

$$E_z^{s(2)}(\bar{r}) = \left[1 - \frac{1}{\mu_r(\bar{r})}\right] E_z(\bar{r}) + k_0^2 \int\int_\Omega \left[1 - \frac{1}{\mu_r(\bar{r}')}\right] E_z(\bar{r}') G_0(\bar{r}|\bar{r}') ds'. \tag{8}$$

3. The third source is a volume electric dipole moment due to the continuous variation of the permeability:

$$\bar{p}_v(\bar{r}') = \frac{j}{\omega\mu_0} E_z(\bar{r}') \nabla' \left[\frac{1}{\mu_r(\bar{r}')}\right] \tag{9}$$

which is a transverse vector. Its Green's function is also a transverse vector:

$$\bar{G}(\bar{r}|\bar{r}') = -j\omega\mu_0 \nabla' G_0(\bar{r}|\bar{r}') \tag{10}$$

and gives

$$E_z^{s(3)}(\bar{r}) = \int\int_\Omega E_z(\bar{r}') \nabla' \left[\frac{1}{\mu_r(\bar{r}')}\right] \cdot \nabla' G_0(\bar{r}|\bar{r}') ds'. \tag{11}$$

4. The fourth source is a surface electric dipole moment induced on the interfaces denoted by Γ_d where the permeability changes abruptly (including the air-dielectric interface):

$$\bar{p}_s(\bar{r}') = \frac{j}{\omega\mu_0}\left[\frac{1}{\mu_r(\bar{r}'_+)} - \frac{1}{\mu_r(\bar{r}'_-)}\right] E_z(\bar{r}')\hat{n}'_d \tag{12}$$

where $\hat{n}'_d$ is a unit vector normal to Γ_d and pointing from the "$-$" side to the "$+$" side. The Green's function for this source is the same as (10). Thus, the source produces a field

$$E_z^{s(4)}(\bar{r}) = \int_{\Gamma_d}\left[\frac{1}{\mu_r(\bar{r}'_+)} - \frac{1}{\mu_r(\bar{r}'_-)}\right] E_z(\bar{r}')\hat{n}'_d \cdot \nabla' G_0(\bar{r}|\bar{r}')dl'. \tag{13}$$

5. The last source is a surface electric current induced on the conductors' surfaces denoted by Γ_c:

$$K_z(\bar{r}') = \frac{1}{j\omega\mu_0\mu_r(\bar{r}')}\hat{n}'_c \cdot \nabla' E_z(\bar{r}') \tag{14}$$

where $\hat{n}'_c$ is the outward unit vector normal to Γ_c. This current produces a field

$$E_z^{s(5)}(\bar{r}) = -\int_{\Gamma_c}\frac{1}{\mu_r(\bar{r}')}G_0(\bar{r}|\bar{r}')\hat{n}'_c \cdot \nabla' E_z(\bar{r}')dl'. \tag{15}$$

Note that in this case (E-polarization) the variation (either continuous or abrupt) of the permittivity does not induce any kind of dipole source.

When all the above sources are combined, the VSIE for the E-polarization case becomes

$$k_0^2\int\int_\Omega\left[\epsilon_r(\bar{r}') - \frac{1}{\mu_r(\bar{r}')}\right] E_z(\bar{r}')G_0(\bar{r}|\bar{r}')ds' + \int\int_\Omega E_z(\bar{r}')\nabla'\left[\frac{1}{\mu_r(\bar{r}')}\right]\cdot\nabla' G_0(\bar{r}|\bar{r}')ds'$$

$$+\int_{\Gamma_d}\left[\frac{1}{\mu_r(\bar{r}'_+)}-\frac{1}{\mu_r(\bar{r}'_-)}\right]E_z(\bar{r}')\frac{\partial G_0(\bar{r}|\bar{r}')}{\partial n'_d}dl'-\int_{\Gamma_c}\frac{1}{\mu_r(\bar{r}')}G_0(\bar{r}|\bar{r}')\frac{\partial E_z(\bar{r}')}{\partial n'_c}dl'$$

$$+E_z^i(\bar{r})=\begin{cases}[1/\mu_r(\bar{r})]\,E_z(\bar{r}) & \text{for } \bar{r} \text{ in dielectrics}\\ 0 & \text{for } \bar{r} \text{ in conductors}\\ E_z(\bar{r}) & \text{for } \bar{r} \text{ everywhere else.}\end{cases} \tag{16}$$

H-polarization (TE)

The formulation for the H-polarization case is dual to the above for the E-polarization case. For brevity, we only give the equations:

$$H_z(\bar{r})=H_z^i(\bar{r})+H_z^s(\bar{r}) \tag{17}$$

where

$$H_z^s(\bar{r})=\sum_{i=1}^{5}H_z^{s(i)}(\bar{r}) \tag{18}$$

with

$$H_z^{s(1)}(\bar{r})=k_0^2\int\int_\Omega[\mu_r(\bar{r}')-1]H_z(\bar{r}')G_0(\bar{r}|\bar{r}')ds' \tag{19}$$

(volume magnetic current contribution)

$$H_z^{s(2)}(\bar{r})=\left[1-\frac{1}{\epsilon_r(\bar{r})}\right]H_z(\bar{r})+k_0^2\int\int_\Omega\left[1-\frac{1}{\epsilon_r(\bar{r}')}\right]H_z(\bar{r}')G_0(\bar{r}|\bar{r}')ds' \tag{20}$$

(volume magnetic current contribution)

$$H_z^{s(3)}(\bar{r})=\int\int_\Omega H_z(\bar{r}')\nabla'\left[\frac{1}{\epsilon_r(\bar{r}')}\right]\cdot\nabla'G_0(\bar{r}|\bar{r}')ds' \tag{21}$$

(volume magnetic dipole contribution)

$$H_z^{s(4)}(\bar{r}) = \int_{\Gamma_d} \left[\frac{1}{\epsilon_r(\bar{r}'_+)} - \frac{1}{\epsilon_r(\bar{r}'_-)} \right] H_z(\bar{r}') \hat{n}'_d \cdot \nabla' G_0(\bar{r}|\bar{r}') dl' \tag{22}$$

(surface magnetic dipole contribution)

$$H_z^{s(5)}(\bar{r}) = \int_{\Gamma_c} \frac{1}{\epsilon_r(\bar{r}')} H_z(\bar{r}') \hat{n}'_c \cdot \nabla G_0(\bar{r}|\bar{r}') dl' \tag{23}$$

(surface electric current contribution).

In contrast to the E-polarization case, here the variation of the permeability does not introduce any kind of dipole source.

The VSIE for the H-polarization case can then be written as

$$k_0^2 \int\int_{\Omega} \left[\mu_r(\bar{r}') - \frac{1}{\epsilon_r(\bar{r}')} \right] H_z(\bar{r}') G_0(\bar{r}|\bar{r}') ds' + \int\int_{\Omega} H_z(\bar{r}') \nabla' \left[\frac{1}{\epsilon_r(\bar{r}')} \right] \cdot \nabla' G_0(\bar{r}|\bar{r}') ds'$$
$$+ \int_{\Gamma_d} \left[\frac{1}{\epsilon_r(\bar{r}'_+)} - \frac{1}{\epsilon_r(\bar{r}'_-)} \right] H_z(\bar{r}') \frac{\partial G_0(\bar{r}|\bar{r}')}{\partial n'_d} dl' + \int_{\Gamma_c} \frac{1}{\epsilon_r(\bar{r}')} H_z(\bar{r}') \frac{\partial G_0(\bar{r}|\bar{r}')}{\partial n'_c} dl'$$
$$+ H_z^i(\bar{r}) = \begin{cases} [1/\epsilon_r(\bar{r})] H_z(\bar{r}) & \text{for } \bar{r} \text{ in dielectrics} \\ 0 & \text{for } \bar{r} \text{ in conductors} \\ H_z(\bar{r}) & \text{for } \bar{r} \text{ everywhere else.} \end{cases} \tag{24}$$

III. Application of the Method of Moments

The VSIE of (16) for E-polarization and (24) for H-polarization can be numerically solved using the method of moments (MM) [14]. To ensure an easy generation of the model, we adopt the simple pulse expansion (basis) functions and delta testing (weighting) functions (point matching) for the MM solution. In this section, we will describe the procedure of applying this pulse expansion and point matching technique to the VSIE.

Discretization of Obstacles

The first step of the application is to discretize the obstacles, *i.e.*, to divide the obstacles into a set of cells and segments. Such is illustrated through an example shown in Figure 2.

Figure 2(a) shows an obstacle consisting of a half-circular dielectric cylinder and a rectangular dielectric cylinder with a smaller rectangular conducting cylinder embedded inside. At the interface between the half-circular cylinder and the rectangular cylinder, there exists a step discontinuity in both permittivity and permeability.

Figure 2(b) shows a discretization model of the obstacle. The region Ω, occupied by the dielectrics, is divided into a set of triangular and quadrilateral cells, and the interface of discontinuity Γ_d and the conductor's surface Γ_c are divided into a set of line segments.

The number of discrete points determines the number of the discretized unknowns in the final system of equations. Assume the number of cells in Ω is N, the number of segments on Γ_d is M, and the number of segments on Γ_c is L. The total number of discretized unknowns is given in Table 2 for different properties of the materials and different polarizations of the incident fields.

The above discretization model is easy to generate. Since, as we will show later, the discretization of the VSIE only needs the area and the center-point position of each cell, one does not have to be concerned with the shape of the cell. This substantially simplifies the generation of models.

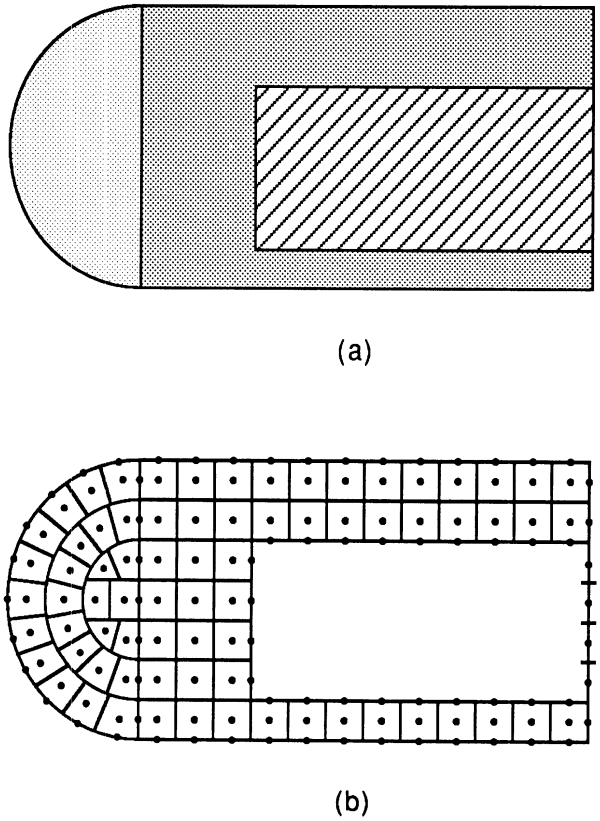

Figure 2: (a) An original problem; (b) Its discretization model.

Table 2. Number of Discretized Unknowns in the System Matrix Equation

Material	$\epsilon \neq \epsilon_0$, $\mu = \mu_0$		$\epsilon = \epsilon_0$, $\mu \neq \mu_0$		$\epsilon \neq \epsilon_0$, $\mu \neq \mu_0$	
Field	E-pol.	H-pol.	E-pol.	H-pol.	E-pol.	H-pol.
Unknowns	$N+L$	$N+M+L$	$N+M+L$	$N+L$	$N+M+L$	$N+M+L$

N — Number of cells in the regions (Ω) occupied by dielectrics

M — Number of segments on the interfaces (Γ_d) between dielectrics

L — Number of segments on the surfaces (Γ_c) of conductors

To generate the points on the interfaces and the conductors' surfaces, we first break the curves of the interfaces and the surfaces into several arcs with straight lines as a special case. We then input the end-point coordinates of and the angle subtended by each arc, and the number of segments we wish to put on the arc. The program generates the length, the mid-point coordinates, and the normal sine and cosine of each segment. To generate the points inside the dielectrics, we first divide the cross-sections of the dielectrics into a number of curved or planar strips each of which has a constant thickness. Then we input the thickness of each strip, the end-point coordinates of and the angle subtended by the center-line of the strip, and the number of cells we wish to use. The program will generate the area and the center-point coordinates of each cell. Such a model generation can be accomplished by a rather small program.

We found that the above input format is very convenient, and with care we can generate a quite accurate model for an arbitrary geometry. This is one of the reasons for our choice of pulse expansion and point matching. Other expansions

such as linear expansion requires generating more complicated models such as the triangular patch model. Such models are usually difficult to generate, since they need detailed information about the shape of each cell. Though there are some methods which are capable of doing such a job, they usually require quite large program packages.

Discretization of the VSIE

The second step of applying the MM is to discretize the VSIE of (16) for E-polarization and (24) for H-polarization. For brevity, we only consider the E-polarization case here. The discretization of (24) for the H-polarization case is similar.

Let us consider the formulation for the discretization model shown in Figure 2(b). We first approximate the continuous unknown field in terms of a set of pulse functions. For the field in Ω, we have

$$E_z(\bar{r}') = \sum_{i=1}^{N} \alpha_i P_i \tag{25}$$

where P_i is a pulse function which equals 1 in cell s_i and equals 0 everywhere else, and α_i is an unknown coefficient. For the field on Γ_d, we have

$$E_z(\bar{r}') = \sum_{j=1}^{M} \beta_j P_j \tag{26}$$

where P_j is a pulse function which equals 1 on segment l_j and equals 0 everywhere else, and β_j is an unknown coefficient. Similarly, for the field on Γ_c, we have

$$\frac{1}{\mu_r(\bar{r}')} \frac{\partial E_z(\bar{r}')}{\partial n_c'} = \sum_{k=1}^{L} \gamma_k P_k \tag{27}$$

where P_k is a pulse function which equals 1 on segment c_k and equals 0 everywhere else, and γ_k is an unknown coefficient.

Substituting (25)-(27) into (16), we have

$$\begin{aligned}
&\sum_{i=1}^{N}\alpha_i \int\int_{s_i}\left\{k_0^2\left[\epsilon_r(\bar{r}')-\frac{1}{\mu_r(\bar{r}')}\right]G_0(\bar{r}|\bar{r}')+\nabla'\left[\frac{1}{\mu_r(\bar{r}')}\right]\cdot\nabla' G_0(\bar{r}|\bar{r}')\right\}ds' \\
&+\sum_{j=1}^{M}\beta_j \fint_{l_j}\left[\frac{1}{\mu_r(\bar{r}'_+)}-\frac{1}{\mu_r(\bar{r}'_-)}\right]\frac{\partial G_0(\bar{r}|\bar{r}')}{\partial n'_d}dl' - \sum_{k=1}^{L}\gamma_k\int_{c_k} G_0(\bar{r}|\bar{r}')dl' \\
&+E_z^i(\bar{r}) = \begin{cases} [1/\mu_r(\bar{r})]\sum_{i=1}^{N}\alpha_i P_i & \text{for } \bar{r} \text{ in } \Omega \\ (1/2)\,[1/\mu_r(\bar{r}_+)+1/\mu_r(\bar{r}_-)]\sum_{j=1}^{M}\beta_j P_j & \text{for } \bar{r} \text{ on } \Gamma_d \\ 0 & \text{for } \bar{r} \text{ on } \Gamma_c \end{cases} \qquad (28)
\end{aligned}$$

where $\fint$ denotes the Cauchy principle value integral with singularities removed.

By satisfying (28) at each center-point of N cells and mid-point of M and L segments, we obtain $N+M+L$ linear algebraic equations whose solution gives values for the $N+M+L$ unknown cofficients. The scattered far field coefficient, $P(\phi)$ defined in [15], is then obtained by

$$\begin{aligned}
P(\phi) \;=\; &\sum_{i=1}^{N}\alpha_i S_i\left\{-\frac{j}{4}k_0^2\left[\epsilon_r(\bar{r}_i)-\frac{1}{\mu_r(\bar{r}_i)}\right]+\frac{k_0}{4}\left[\frac{\partial}{\partial x}\frac{1}{\mu_r(\bar{r})}\bigg|_{\bar{r}=\bar{r}_i}\cos\phi\right.\right. \\
&\left.\left.+\frac{\partial}{\partial y}\frac{1}{\mu_r(\bar{r})}\bigg|_{\bar{r}=\bar{r}_i}\sin\phi\right]\right\}\mathrm{e}^{jk_0(x_i\cos\phi+y_i\sin\phi)} \\
&+\sum_{j=1}^{M}\beta_j L_j\frac{k_0}{4}\left[\frac{1}{\mu_r(\bar{r}_{j+})}-\frac{1}{\mu_r(\bar{r}_{j-})}\right](\cos\theta_d\cos\phi+\sin\theta_d\sin\phi) \\
&\cdot\mathrm{e}^{jk_0(x_j\cos\phi+y_j\sin\phi)}+\sum_{k=1}^{L}\gamma_k C_k\frac{j}{4}\mathrm{e}^{jk_0(x_k\cos\phi+y_k\sin\phi)} \qquad (29)
\end{aligned}$$

where ϕ is the observation angle, S_i is the area of cell s_i, L_j is the length of segment l_j, C_k is the length of the segment c_k, and θ_d is defined by $\hat{n}_d = \hat{x}\cos\theta_d + \hat{y}\sin\theta_d$.

For a two dimensional geometry the radar cross section (RCS) per wavelength is

$$\frac{\sigma(\phi)}{\lambda} = \frac{2}{\pi}|P(\phi)|^2 \tag{30}$$

with λ being the free-space wavelength.

Before we close this section, we would like to address the evaluation of some of the integrals. To cast (28) into the final system matrix equation form, one needs to evaluate the following integrals

$$I_1 = \int\int_{s_i} k_0^2 \left[\epsilon_r(\bar{r}') - \frac{1}{\mu_r(\bar{r}')}\right] G_0(\bar{r}_m|\bar{r}')ds' \tag{31}$$

$$I_2 = \int\int_{s_i} \nabla' \left[\frac{1}{\mu_r(\bar{r}')}\right] \cdot \nabla' G_0(\bar{r}_m|\bar{r}')ds' \tag{32}$$

$$I_3 = \oint_{l_j} \left[\frac{1}{\mu_r(\bar{r}'_+)} - \frac{1}{\mu_r(\bar{r}'_-)}\right] \frac{\partial G_0(\bar{r}_m|\bar{r}')}{\partial n'_d} dl' \tag{33}$$

$$I_4 = \int_{c_k} G_0(\bar{r}_m|\bar{r}')dl' \tag{34}$$

where $\bar{r}_m = \bar{r}_i$ $(i = 1, 2, \cdots, N)$, or $\bar{r}_m = \bar{r}_j$ $(j = 1, 2, \cdots, M)$, or $\bar{r}_m = \bar{r}_k$ $(k = 1, 2, \cdots, L)$.

For evaluating the area integrals I_1 and I_2, if $\bar{r}_i \neq \bar{r}_m$, we use the approximation

$$I_1 = k_0^2 \left[\epsilon_r(\bar{r}_i) - \frac{1}{\mu_r(\bar{r}_i)}\right] G_0(\bar{r}_m|\bar{r}_i) \cdot S_i \tag{35}$$

$$I_2 = \left\{\nabla \left[\frac{1}{\mu_r(\bar{r})}\right] \cdot \nabla G_0(\bar{r}_m|\bar{r})\right\}_{\bar{r}=\bar{r}_i} \cdot S_i. \tag{36}$$

If $\bar{r}_i = \bar{r}_m$, we first approximate cell s_i as a circular cell of an area equal to that of the original cell and then evaluate the integrals analytically. The results are

$$I_1 = -\left[\epsilon_r(\bar{r}_i) - \frac{1}{\mu_r(\bar{r}_i)}\right] \left[1 + j\frac{\pi}{2} k_0 a_i H_1^{(2)}(k_0 a_i)\right] \tag{37}$$

$$I_2 = 0 \tag{38}$$

where $a_i = (S_i/\pi)^{1/2}$. It may be worth pointing out that (35) and (36) are approximate from the perspective of the pulse function expansion. However, if we use the delta function expansion

$$E_z(\bar{r}) = \sum_{i=1}^{N} \alpha_i S_i \delta(\bar{r} - \bar{r}_i) \tag{39}$$

for the non-self or off-diagonal elements, (35) and (36) become exact. Therefore, to be more precise, the expansion we use is a pulse function expansion for the diagonals ($\bar{r}_i = \bar{r}_m$) and a delta function expansion for the off-diagonals ($\bar{r}_i \neq \bar{r}_m$).

The line integrals I_3 and I_4 can be approximately evaluated as

$$I_3 = \begin{cases} [1/\mu_r(\bar{r}_{j+}) - 1/\mu_r(\bar{r}_{j-})]\, \partial G_0(\bar{r}_m|\bar{r})/\partial n_d|_{\bar{r}=\bar{r}_j} \cdot L_j & \text{for } \bar{r}_j \neq \bar{r}_m \\ 0 \quad \text{for } \bar{r}_j = \bar{r}_m \end{cases} \tag{40}$$

$$I_4 = \begin{cases} G_0(\bar{r}_m|\bar{r}_k) \cdot C_k & \text{for } \bar{r}_k \neq \bar{r}_m \\ (-j/4)\left[1 - j\frac{2}{\pi}\log(\gamma k_0 C_k/4e)\right] \cdot C_k & \text{for } \bar{r}_k = \bar{r}_m \end{cases} \tag{41}$$

where $\gamma = 1.781$ and $e = 2.718$.

It should be pointed out that the above integral evaluation is a crude approximation. However, it has the advantage of resulting in simple analytical expressions, and more importantly, the evaluation of I_1 and I_2 needs only the central point coordinates and the area of each cell, rather than detailed information about the shape of the cell. As pointed out earlier, such an approach substantially simplifies the work of the discretization of the obstacles.

The discretization of (24) for H-polarization is similar to that described above, since (24) is dual to (16), except for the last integral which is along the conductors'

surfaces. This integral requires the evaluation of

$$I_5 = \int_{c_k} \frac{\partial G_0(\bar{r}_m|\bar{r}')}{\partial n_c'} dl' \tag{42}$$

and the result is

$$I_5 = \begin{cases} \partial G_0(\bar{r}_m|\bar{r})/\partial n_c|_{\bar{r}=\bar{r}_k} \cdot C_k & \text{for } \bar{r}_k \neq \bar{r}_m \\ -\frac{1}{2} & \text{for } \bar{r}_k = \bar{r}_m. \end{cases} \tag{43}$$

IV. Numerical Results

In this section, we present some numerical results computed using the moment method (MM) program based on the formulation and discussion given above. Seven different geometries are considered to demonstrate the validity and versatility of the program.

The first geometry is a coated conducting circular cylinder, which can be solved analytically using an eigenfunction expansion technique. Such an exact solution can then be used to verify our VSIE MM results. In Figure 3 we present both eigenfunction and VSIE MM solutions for the backscattering radar cross section of the cylinder as a function of the coating thickness for three different coatings. Overall, the VSIE MM solutions agree quite well with the eigenfunction solutions.

The second and third geometries are related to radar targets. The second geometry is an inhomogeneous dielectric circular cylinder backed by a conducting strip, as shown in Figure 4(a). The cylinder has the permittivity variation in radius the same as that of a spherical Luneberg lens. The third geometry, as shown in Figure 5(a), is an inhomogeneous dielectric half-circular cylinder backed

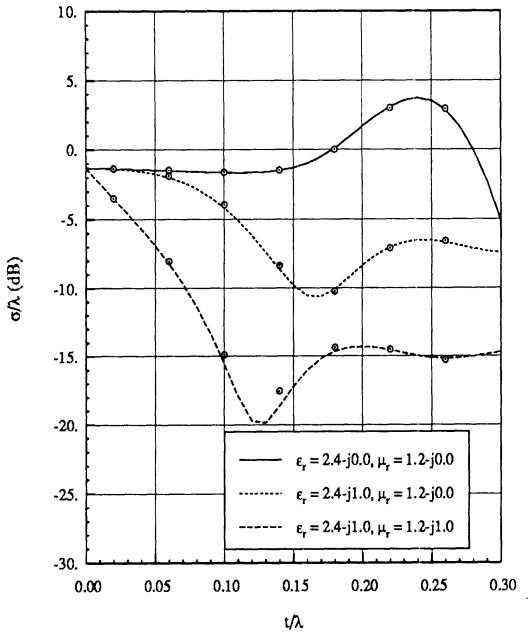

(a)

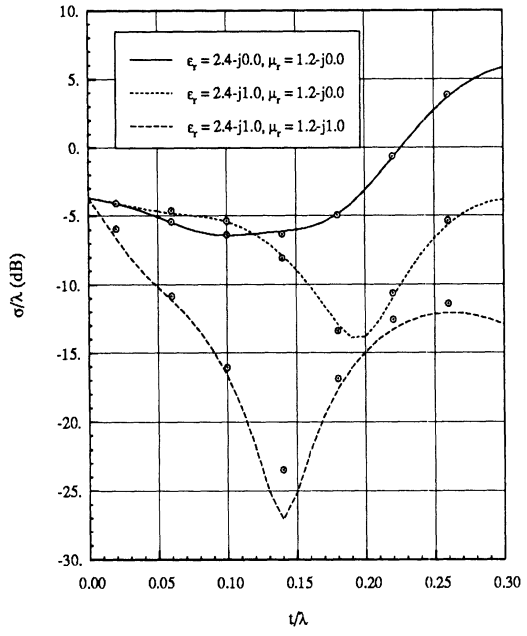

(b)

Figure 3: Backscattering cross section (σ) of a coated conducting circular cylinder vs coating thickness (t). The radius of the conducting cylinder equals 0.2λ. The lines represent the eigenfunction expansion solutions. The circles respresent the VSIE MM solutions. (a) E-polarization; (b) H-polarization.

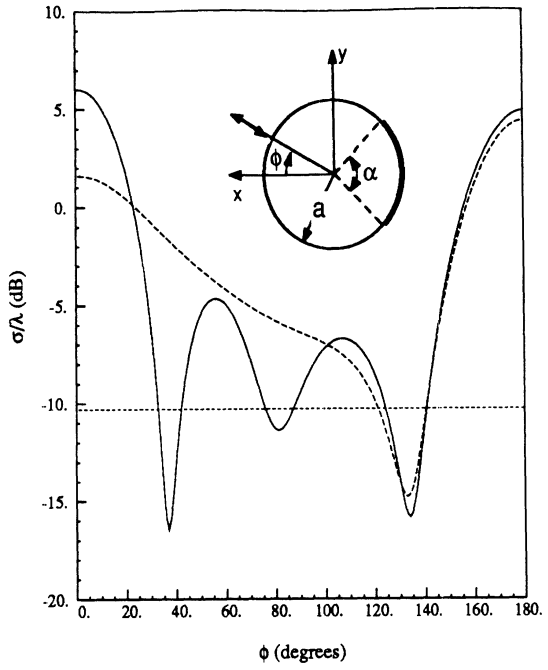

(a)

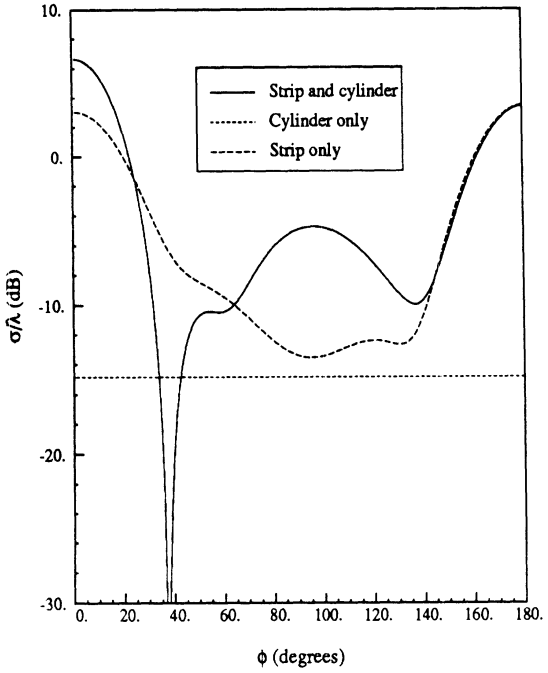

(b)

Figure 4: Backscattering pattern of a cylindrical Luneberg lens backed by a conducting strip. $a = 0.4\lambda$, $\alpha = 90^o$, $\epsilon_r = 2 - (r/a)^2$, $\mu_r = 1$. (a) E-polarization; (b) H-polarization.

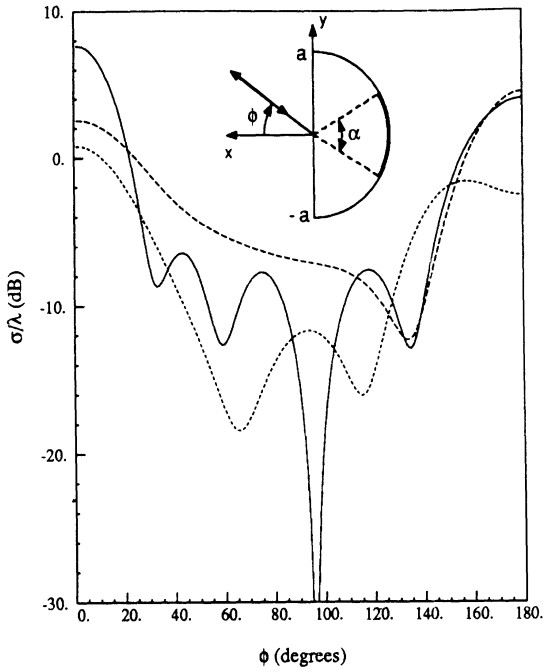

(a)

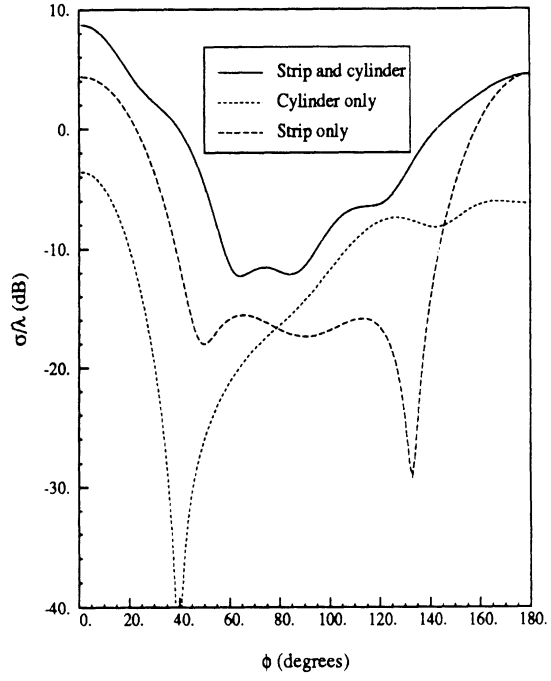

(b)

Figure 5: Backscattering pattern of a half cylindrical Maxwell fish eye backed by a conducting strip. $a = 0.6\lambda$, $\alpha = 60^{o}$, $\epsilon_r = 4/[1 + (r/a)^2]^2$, $\mu_r = 1$. (a) E-polarization; (b) H-polarization.

by a conducting strip. This cylinder has the permittivity variation in radius same as that of a Maxwell fish eye. In the figures we show the computed backscattering radar cross sections of the dielectric cylinder, conducting strip and the combined structure.

The fourth geometry, shown in Figure 6(a), is a 3λ wide conducting strip having its edges loaded with dielectric circular cylinders. The results presented are the backscattering radar cross section of the strip with and without loadings.

We should note that for the E-polarization computations shown in Figures 4(a), 5(a) and 6(a) the conducting strips are infinitely thin, while for the H-polarization computations of Figures 4(b), 5(b) and 6(b) the strips are assumed to have a finite thickness of 0.06λ in order to allievate the difficulty encountered in the H-polarization formulation for thin strips of zero thickness.

We should also note that the problem of electromagnetic scattering from microstrip structures, such as those treated in [11] and [12], is similar to that of Figures 4 and 5, and thus can be treated in the same manner.

The last three geometries concern the application of the program to the calculation of the scattering from arbitrarily shaped conducting cylinders coated with dielectrics. The geometries are shown in Figures 7(a), 8(a) and 9(a), and they are coated square, ogival and wedge cylinders, respectively. The results shown are the backscattering radar cross sections of the cylinders for different coating thicknesses and for different permittivities and permeabilities of the coatings. Also given in Figures 7 and 8 are the results obtained using the hybrid finite element method

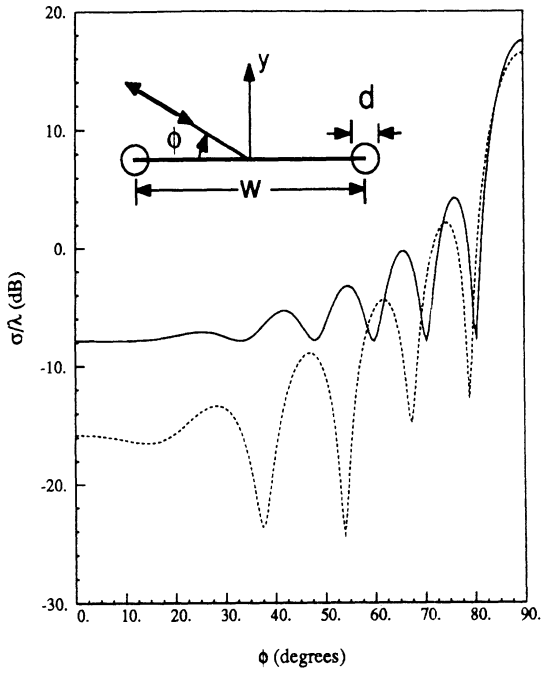

(a)

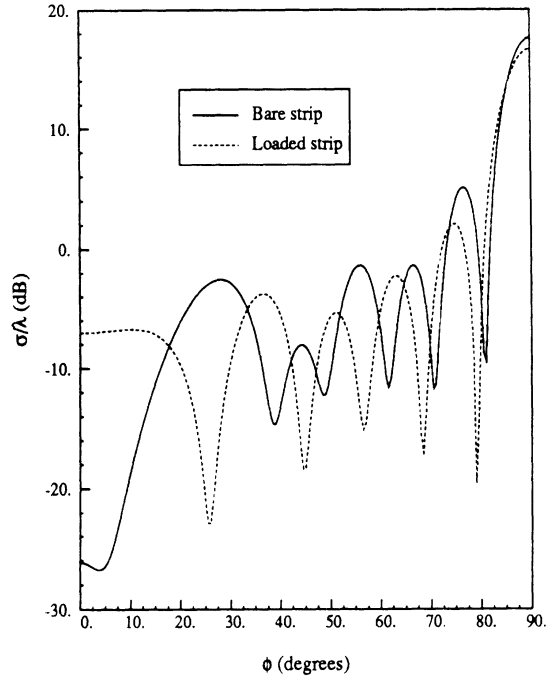

(b)

Figure 6: Backscattering pattern of an edge-loaded conducting strip. $w = 3.0\lambda$, $d = 0.3\lambda$, $\epsilon_r = 4.0 - j4.0$, $\mu_r = 2.0 - j2.0$. (a) E-polarization; (b) H-polarization.

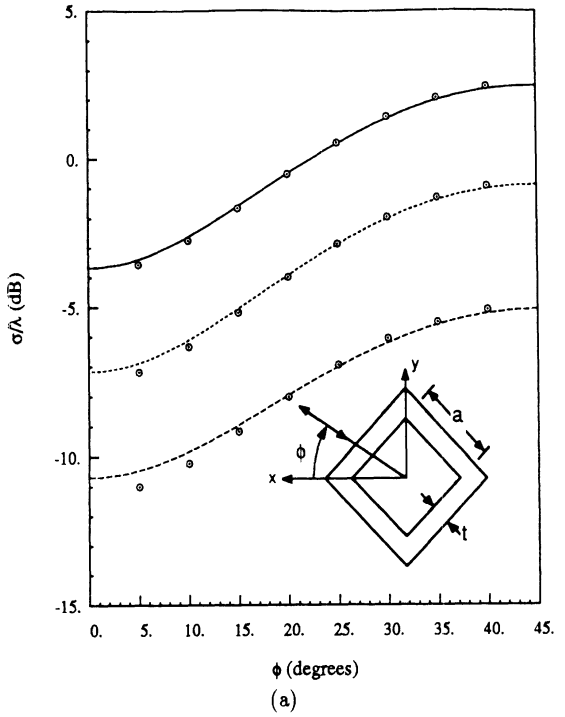

(a)

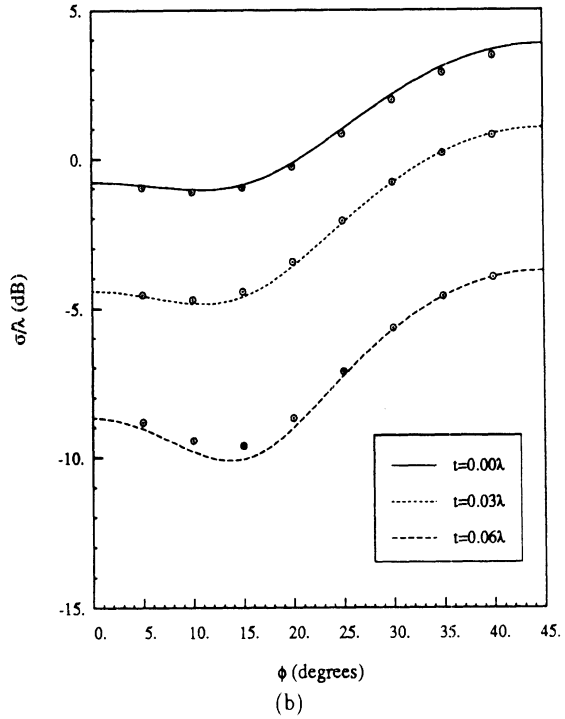

(b)

Figure 7: Backscattering pattern of a coated square cylinder. $a = 0.5\lambda$, $\epsilon_r = 2 - j2, \mu_r = 2 - j2$. The lines represent the VSIE MM solutions. The circles represent the HFEM solutions. (a) E-polarization; (b) H-polarization.

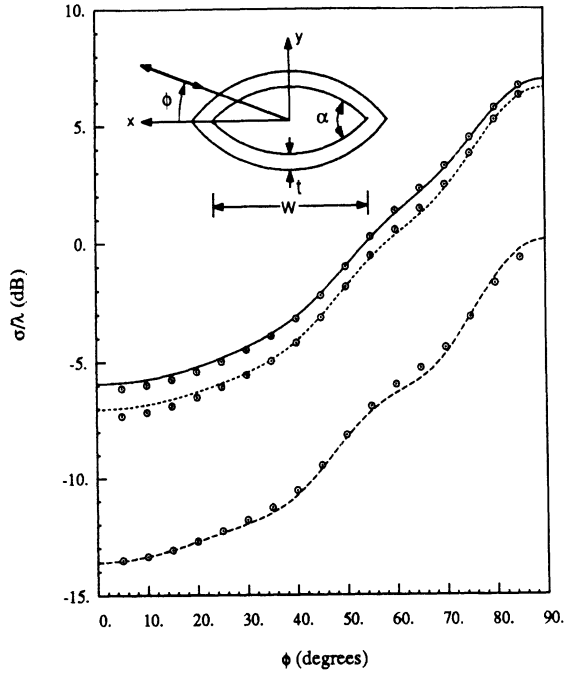

(a)

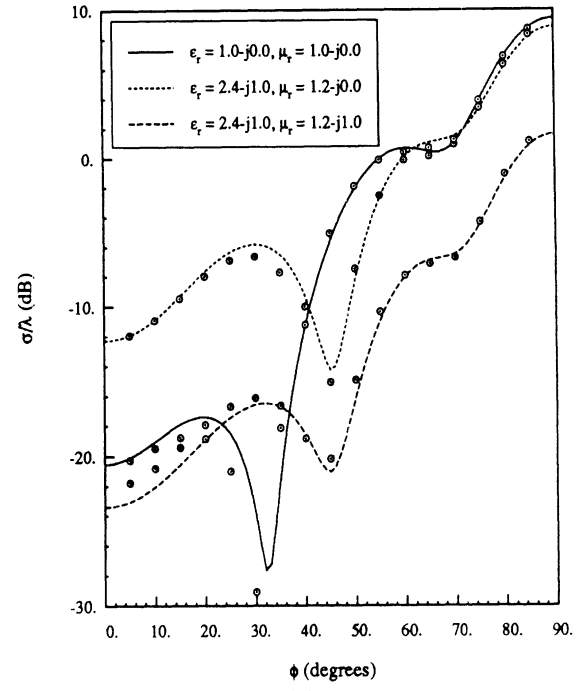

(b)

Figure 8: Backscattering pattern of a coated ogival cylinder. $w = 1.2\lambda$, $\alpha = 60^o$, $t = 0.06\lambda$. The lines represent the VSIE MM solutions. The circles represent the HFEM solutions. (a) E-polarization; (b) H-polarization.

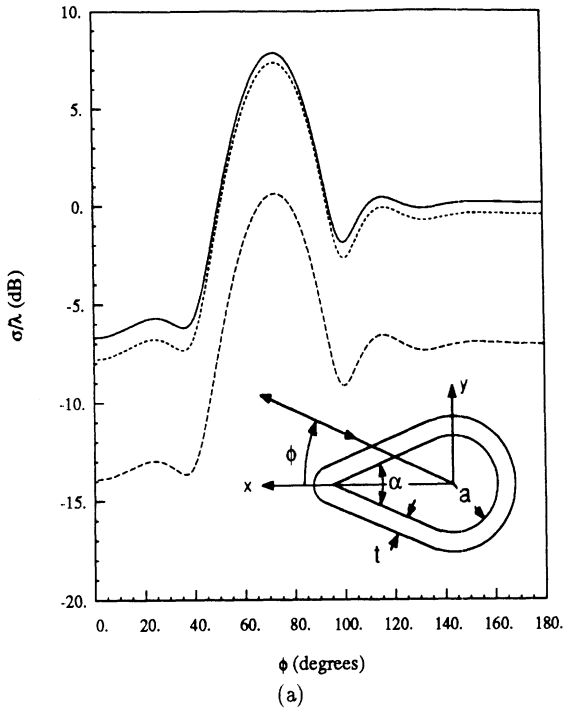

(a)

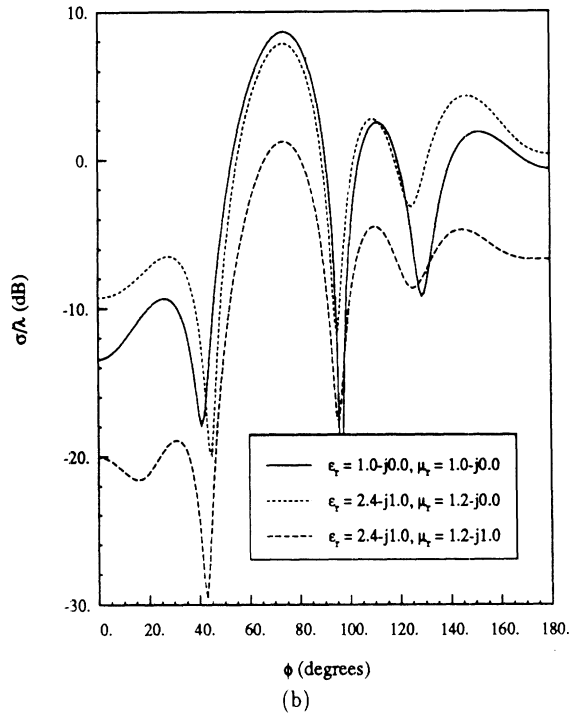

(b)

Figure 9: Backscattering pattern of a coated wedge cylinder. $a = 0.3\lambda$, $\alpha = 40^o$, $t = 0.06\lambda$. (a) E-polarization; (b) H-polarization.

(HFEM) [9]. A generally good agreement between the VSIE MM and HFEM solutions is observed.

Before closing this section, we would like to point out that though we have not encountered any major problem in obtaining the above results, we found that for the H-polarization computations of thinly coated structures the number of discrete points or cells needed to produce a given accuracy is usually larger than that for the E-polarization computations for the same accuracy. This fact is due to the existence of surface waves for the H-polarization case which may produce a complicated field distribution along the circumference of the cylinder. As an example, for a coated circular cylinder with a coating thickness of 0.03λ, a coating permittivity of $\epsilon_r = 2$ and permeability of $\mu_r = 2$, computations show that for the E-polarization case a sampling rate of 12 points per free-space wavelength along the circumference is enough to obtain the backscattered far field with an accuracy of 0.1dB in magnitude and 1 degree in phase, while for the H-polarization case one would increase the sampling rate to 22 points per free-space wavelength to achieve the same accuracy.

V. Some Limitations

Like any other integral equation and numerical method, the VSIE and the program described in this paper also have some limitations. Regarding the main limitations, we note the following four points.

• For using the VSIE, one needs to specify the gradient of permeability for E-polarization and the gradient of permittivity for H-polarization. For some prob-

lems where such a specification is difficult or impossible, the VSIE cannot be used. For such a case, one would turn to the volume integral equation method where only the values of permittivity and permeability are required.

• Because of the presence of the line integral in the VSIE, the resulting linear system of equations does not inherit the convolutional form; hence, the conjugate gradient-fast Fourier transform method, which is an efficient means of solving the pulse expansion-moment method linear system, may not be applied easily.

• The discretization model used here requires calculating the field values on the interfaces of all discontinuities as unknowns. For cylinders containing many internal step discontinuities, the number of unknowns will increase significantly.

• The program is not suited for the calculation of internal fields of cylinders with large values of permittivity for the TE or H-polarization case, though it is very efficient for the TM or E-polarization case.

Of the above four points, the first and second and partly the fourth result from the integral equation itself. The third would not be a drawback if one uses patch models where unknowns are assigned on the patch boundaries. The fourth could be possibly removed if one adopts more accurate models and evaluates the integrals more accurately. More work needs to be done for such cases.

VI. Conclusion

In this paper, a moment method program is described for computing electromagnetic scattering from multiple perfectly conducting and penetrable inhomogeneous cylinders for both TM and TE wave incidence. The program is based on the

formulation of the volume-surface integral equation, and has the advantages of easy generation of the model and simple discretization of the integral equation. These two advantages result from the employment of the pulse and delta expansion and point-matching technique. The pulse and delta functions are in the domain of the VSIE operator, while they are not in the domain of the volume integral equation operator for the general case. The program is useful for solving the complicated two-dimensional scattering problems involving perfect conductors and lossy inhomogeneous materials, and may find applications in the areas of scattering control, radar identification and remote sensing.

Concerning the three-dimensional case, we note that a similar equation has been formulated by Tai for scattering by homogeneous, electrically and magnetically permeable bodies and inhomogeneous bodies with $\mu_r = 1$ [16]. It would be beneficial if one would derive a similar VSIE for the general three-dimensional case.

Acknowledgments

The authors wish to thank Drs. D. G. Dudley, C. H. Durney and E. H. Newman for their valuable comments on this work, and Mr. Leland Pierce for many helpful discussions.

References

[1] Mei, K. K. and J. Van Bladel, "Scattering by perfectly conducting rectangular cylinder," *IEEE Trans. Antennas Propagat.*, vol. AP-11, pp. 185-192, 1963.

[2] Richmond, J. H., "Scattering by a dielectric cylinder of arbitrary cross-section shape," *IEEE Trans. Antennas Propagat.*, vol. AP-13, pp. 334-341, 1965.

[3] Richmond, J. H., "TE-wave scattering by a dielectric cylinder of arbitrary cross-section shape," *IEEE Trans. Antennas Propagat.*, vol. AP-14, pp. 460-464, 1966.

[4] Wu, T. K. and L. L. Tsai, "Scattering by arbitrarily cross sectioned layered lossy dielectric cylinders," *IEEE Trans. Antennas Propagat.*, vol. AP-25, pp. 518-524, 1977.

[5] Mason, J. L., "Finite element solution for electromagnetic scattering from two-dimensional bodies," Ph.D. dissertation, The University of Michigan, Ann Arbor, 1982.

[6] Chang, S. K. and K. K. Mei, "Application of the unimoment method to electromagnetic scattering of dielectric cylinders," *IEEE Trans. Antennas Propagat.*, vol. AP-24, pp. 35-42, 1976.

[7] Marin, S. P., "Computing scattering amplitudes for arbitrary cylinders under incident plane waves," *IEEE Trans. Antennas Propagat.*, vol. AP-30, pp. 1045-1049, 1982.

[8] Jeng, S. K. and C. H. Chen, "On variational electromagnetics: theory and application," *IEEE Trans. Antennas Propagat.*, vol. AP-32, pp. 902-907, 1984.

[9] Jin, J. M. and V. V. Liepa, "Application of hybrid finite element method to electromagnetic scattering from coated cylinders," *IEEE Trans. Antennas Propagat.*, vol. AP-36, pp. 50-54, 1988.

[10] Jin, J. M., V. V. Liepa, and C. T. Tai, "A volume-surface integral equation for electromagnetic scattering by inhomogeneous cylinders," *Journal of Electromagnetic Waves and Applications*, vol. 2, no. 5/6, pp. 573-588, 1988.

[11] Arvas, E., S. M. Rao, and T. K. Sarkar, "E-field solution of TM-scattering from multiple perfectly conducting and lossy dielectric cylinders of arbitrary cross-section," *IEE proc. H, Microwaves, Antennas and Propagation*, vol. 133, pp. 115-121, 1986.

[12] Yuan, X., R. F. Harrington, and S. S. Lee, "Electromagnetic scattering by a dielectric cylinder partially covered by conductors," *Journal of Electromagnetic Waves and Applications*, vol. 2, no. 1, pp. 21-44, 1988.

[13] Newman, E. H., "TM and TE scattering by a dielectric/ferrite cylinder in the presence of a half-plane," *IEEE Trans. Antennas Propagat.*, vol. AP-34, pp. 804-813, 1986.

[14] Harrington, R. F., *Field Computation by Moment Methods.* New York: Macmillan, 1968.

[15] Bowman, J. J., T. B. A. Senior, and P. L. E. Uslenghi ed., *Electromagnetic and Acoustic Scattering by Simple Shapes.* North-Holland Publishing Company-

Amsterdam, 1969. A revised printing is published by Hemisphere Publishing Corporation, New York, 1987.

[16] Tai, C. T., "A note on the integral equations for the scattering of a plane wave by an electromagnetically permeable body," *Electromagnetics*, vol. 5, pp. 79-88, 1985.

A MOMENT METHOD SOLUTION OF A VOLUME-SURFACE INTEGRAL EQUATION USING ISOPARAMETRIC ELEMENTS AND POINT-MATCHING

Jian-Ming Jin, John L. Volakis, and Valdis V. Liepa

Radiation Laboratory

Department of Electrical Engineering and Computer Science

The University of Michigan

Ann Arbor, Michigan 48109

(submitted to *IEEE Trans. Microwave Theory Tech.* for publication)

ABSTRACT

It is shown that traditional subdomain elements such as rectangles and triangles with pulse expansion basis could lead to considerable inaccuracies when simulating biological scatterers having high permittivities. In this paper, isoparametric elements are used in a moment method implementation to remove modelling inaccuracies of fields and boundaries associated with traditional elements. Numerical results are also given that show the improvement achieved in the scattering solution for high contrast circular cylinders.

1. Introduction

A Volume-Surface Integral Equation (VSIE) was recently presented [1], [2] for electromagnetic scattering by inhomogeneous cylinders. A moment method implementation of the VSIE was also considered using rectangular and/or triangular subdomains (elements) with pulse expansion basis functions and point-matching. Recently, however, we observed that such a moment method solution becomes inaccurate in the case of scatterers having high permittivity with transverse electric (TE) incidence or high permeability with transverse magnetic (TM) incidence. This is primarily true for cylindrical scatterers associated with curved boundaries such as those encountered in biological models. Under these circumstances, the simple rectangular and/or triangular elements with pulse expansion basis do not render an accurate modelling of the internal fields and the scatterers' boundaries. This model inaccuracy is generally forgiving in the case of scatterers with nominal values of refractive indices but it will be shown to be too compromising when the refractive index becomes large as is usually the case with biological scatterers. Alternative discretization elements are therefore required to improve the scatterer's modelling accuracy. The isoparametric elements [3] are found to be capable of serving this purpose and in this paper we present a numerical solution of the VSIE by employing such elements.

The isoparametric elements were first introduced in finite element analysis [3] and refer to discretization elements of the geometry having the same order (shape) as the field representation within them. That is, the field expansion/basis over a

quadratic line element, for example, is also quadratic. The main advantage of using isoparametric elements is to allow an accurate modelling in the case of curved arbitrarily shaped geometries. However, it appears that only recently [4] they have been employed in applications related to solutions of integral equations for electromagnetics. Below we first discuss the inaccuracy associated with traditional solutions of integral equations for penetrable scatterers having high refractive indices. This is followed by the introduction of the isoparametric elements and the presentation of a moment method solution of the VSIE using such elements. Results are subsequently presented which reveal the stability of the solution in the case of cylindrical geometries associated with high refractive indices.

2. Discussion of Integral Equations for TE Scattering

In this section we examine the three integral equations for the computation of the internal fields in a dielectric cylinder for the TE incidence. Assume that the cylinder has its infinite dimension along the z-axis. The VSIE for this case is [1]

$$\begin{aligned} & H_z^{INC}(\bar{r}) + k_0^2 \int\int_\Omega \left[1 - \frac{1}{\epsilon_r(\bar{r}')}\right] H_z(\bar{r}') G_0(\bar{r}|\bar{r}') ds' + \int\int_\Omega \nabla' \left[\frac{1}{\epsilon_r(\bar{r}')}\right] \\ & \cdot [H_z(\bar{r}') \nabla' G_0(\bar{r}|\bar{r}')] ds' + \oint_\Gamma \left[\frac{1}{\epsilon_r(\bar{r}'_+)} - \frac{1}{\epsilon_r(\bar{r}'_-)}\right] H_z(\bar{r}') \frac{\partial G_0(\bar{r}|\bar{r}')}{\partial n'} dl' \\ = & \begin{cases} [1/\epsilon_r(\bar{r})] H_z(\bar{r}) & \text{for } \bar{r} \text{ not on } \Gamma \\ (1/2)\left[1/\epsilon_r(\bar{r}'_+) - 1/\epsilon_r(\bar{r}'_-)\right] H_z(\bar{r}) & \text{for } \bar{r} \text{ on } \Gamma \end{cases} \end{aligned} \tag{1}$$

where H_z^{INC} denotes the z-component of the incident magnetic field, H_z represents the z-component of the total magnetic field, ϵ_r denotes the relative permittivity of the scatterer and $G_0(\bar{r}|\bar{r}')$ is the two-dimensional free-space Green's function. In addition, Ω denotes the region occupied by the cylinder, Γ denotes the interface

where $\epsilon_r(\bar{r})$ has a step discontinuity, $\hat{n}$ is the unit vector normal to Γ pointing from the "$-$" side to the "$+$" side and $\oint$ denotes the Cauchy principle value integral.

Alternative integral equations for this problem were also given by Borup *et al.* [5] as

$$\overline{E}_t(\bar{r}) = \overline{E}_t^{INC}(\bar{r}) + k_0^2 \int\int [\epsilon_r(\bar{r}') - 1]\,\overline{E}_t(\bar{r}')G_0(\bar{r}|\bar{r}')ds' - \int\int \nabla' \cdot \left[(\epsilon_r(\bar{r}') - 1)\overline{E}_t(\bar{r}')\right] \nabla' G_0(\bar{r}|\bar{r}')ds' \tag{2}$$

and recently by Peterson and Klock [6] as

$$H_z(\bar{r}) = H_z^{INC}(\bar{r}) + \int\int [\hat{z} \cdot \nabla' \times \overline{J}(\bar{r}')]G_0(\bar{r}|\bar{r}')ds' \tag{3}$$

with

$$\overline{J}(\bar{r}) = \left[1 - \frac{1}{\epsilon_r(\bar{r})}\right] \nabla \times [\hat{z}H_z(\bar{r})]$$

and $\overline{E}_t$ denoting the electric field transverse to the z-axis. As usual, $\overline{E}_t^{INC}$ represents the incident electric field transverse to the z-axis.

Let us now examine the numerical implications which may arise when either of the three integral equations are implemented in the case of large $|\epsilon_r|$. Referring first to (1), we may assume without loss of generality that the incident wave, H_z^{INC}, has unity amplitude. As a result the total internal field, H_z, will also have an amplitude around unity and thus the value of the right hand side of (1) will be about $1/|\epsilon_r|$ for a field point inside the cylinder. For large $|\epsilon_r|$ this implies that the integrals over Ω and Γ must together give a value nearly equal to and negative of H_z^{INC}. That is, if $|\epsilon_r| = 100$ and we demand a 1% solution accuracy for the internal

fields, the integrals must be computed with a corresponding accuracy of 0.01%. In general, the presence of $|\epsilon_r|$ acts as an error amplifier and we may conclude that for a solution accuracy of $\delta\%$ the integral must be evaluated with a corresponding accuracy of $\delta/|\epsilon_r|$ percent. This statement has been experimentally verified and, clearly, for large $|\epsilon_r|$ a crude discretization of the scatterer is unlikely to produce the accuracy demanded here.

A similar examination of (2) also reveals that for a desired solution accuracy of $\delta\%$, the integral must be evaluated with a corresponding accuracy of δ/m percent, where $m = |\overline{E}_t^{INC}|/|\overline{E}_t| \approx 1/\sqrt{\epsilon_r}$. Thus, even though (2) is slightly less demanding in accuracy, it is still unstable for scatterers with large refractive indices. This exposition satisfactorily explains the difficulties encountered in [5] as well as the success of their modified approach. Also, the results given by Boyes and Kennedy [7] can be explained in this manner.

At first glance, (3) appears to be the most attractive of all three integral equations. It is certainly more stable than (1) and (2); however, it involves a second derivative of the unknown field quantity and as a result demands higher order basis functions than (1) and (2). In particular, (1) can be implemented with pulse basis and (2) with linear basis but (3) requires quadratic basis[1]. Since the introduction of quadratic basis in (1) and (2) will improve their accuracy, there is no clear choice which of the three is more attractive for numerical implementation. Each is certainly associated with its own advantages and disadvantages for large refractive

[1]If ϵ_r is uniform within each element, the corresponding basis functions can be one order lower.

indices but for nominal values of ϵ_r the VSIE given in (1) is generally superior over the others.

In the next section we consider an implementation of the VSIE using isoparametric elements. As stated in the introduction these provide a more accurate geometrical simulation of the scatterer and representation of its interior field distribution. They are, therefore, expected to provide the required accuracy for the simulation of high contrast dielectrics.

3. Formulation of Isoparametric Elements and Point-Matching Technique

In this section we describe a numerical solution of the VSIE using isoparametric elements with point-matching. Let us consider both TE and TM wave scattering by an inhomogeneous cylinder having non-unity permittivity and permeability. From [1], the field satisfies the general VSIE

$$\begin{aligned} & F^{INC}(\bar{r}) + k_0^2 \int\int_\Omega [v(\bar{r}') - u(\bar{r}')]F(\bar{r}')G_0(\bar{r}|\bar{r}')ds' \\ & + \int\int_\Omega \nabla' u(\bar{r}') \cdot [F(\bar{r}')\nabla' G_0(\bar{r}|\bar{r}')]ds' + \oint_\Gamma \left[u(\bar{r}'_+) - u(\bar{r}'_-)\right] F(\bar{r}') \frac{\partial G_0(\bar{r}|\bar{r}')}{\partial n'} dl' \\ = & \begin{cases} u(\bar{r})F(\bar{r}) & \text{for } \bar{r} \text{ not on } \Gamma \\ \frac{1}{2}[u(\bar{r}_+) + u(\bar{r}_-)]F(\bar{r}) & \text{for } \bar{r} \text{ on } \Gamma \end{cases} \end{aligned} \tag{4}$$

where

$$F(\bar{r}) = E_z(\bar{r}), \quad u(\bar{r}) = \frac{1}{\mu_r(\bar{r})}, \quad v(\bar{r}) = \epsilon_r(\bar{r}),$$

for TM incidence and

$$F(\bar{r}) = H_z(\bar{r}), \quad u(\bar{r}) = \frac{1}{\epsilon_r(\bar{r})}, \quad v(\bar{r}) = \mu_r(\bar{r}).$$

for TE incidence, in which E_z represents the z-component of the electric field and μ_r denotes the relative permeability of the scatterer as usual. For convenience, we can write (4) as

$$\begin{aligned} & F^{INC}(\bar{r}) + \int\int_{\Omega} A(\bar{r}|\bar{r}')F(\bar{r}')ds' + \oint_{\Gamma} B(\bar{r}|\bar{r}')F(\bar{r}')dl' \\ = & \begin{cases} u(\bar{r})F(\bar{r}) & \text{for } \bar{r} \text{ not on } \Gamma \\ \frac{1}{2}[u(\bar{r}_+) + u(\bar{r}_-)]F(\bar{r}) & \text{for } \bar{r} \text{ on } \Gamma \end{cases} \end{aligned} \tag{5}$$

where the expressions for $A(\bar{r}|\bar{r}')$ and $B(\bar{r}|\bar{r}')$ are determined by direct comparison with (4).

In a numerical solution of (4) or (5) using isoparametric elements, the two-dimensional region Ω is broken up into a number of quadrilaterals whose sides can be curved, as shown, for example, in Figure 1. A usual rule for this subdivision is that the interface Γ coincides the with boundries of the quadrilaterals. Assuming now that the discretization results in $M2$ quadrilaterals and that $M1$ curved segments make up the contour(s) Γ, equation (5) becomes

$$\begin{aligned} & F^{INC}(\bar{r}) + \sum_{e=1}^{M2}\sum_{i=1}^{n2} \phi_i^e \int\int_{\Omega^e} A(\bar{r}|\bar{r}')V_i^e(\bar{r}')ds' + \sum_{s=1}^{M1}\sum_{i=1}^{n1} \phi_i^s \oint_{\Gamma^s} B(\bar{r}|\bar{r}')U_i^s(\bar{r}')dl' \\ = & \begin{cases} u(\bar{r})F(\bar{r}) & \text{for } \bar{r} \text{ not on } \Gamma \\ \frac{1}{2}[u(\bar{r}_+) + u(\bar{r}_-)]F(\bar{r}) & \text{for } \bar{r} \text{ on } \Gamma. \end{cases} \end{aligned} \tag{6}$$

In (6), the field in the eth quadrilateral has been expanded as

$$F^e(\bar{r}) = \sum_{i=1}^{n2} V_i^e(\bar{r})\phi_i^e \tag{7}$$

where $V_i^e(\bar{r})$ $(i = 1, 2, ..., n2)$ are a set of known expansion basis functions and ϕ_i^e $(i = 1, 2, ..., n2)$ are the corresponding unknown coefficients. Similarly, the field in

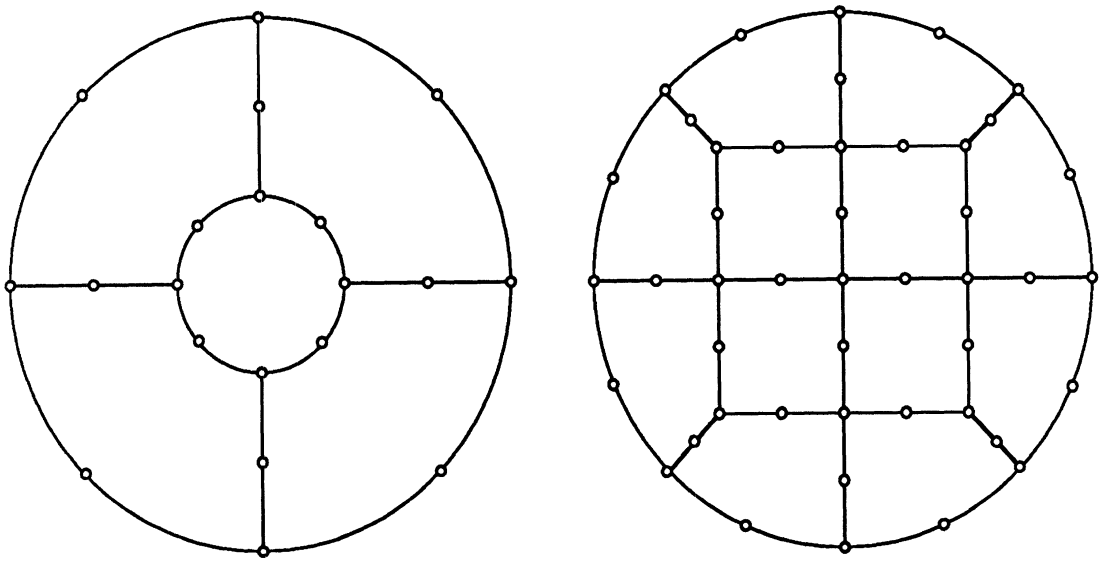

(a) (b)

Figure 1: Two examples for breaking a circular region. (a) A 5 quadrilateral element model with 20 nodes. (b) A 12 quadrilateral element model with 45 nodes.

the sth segment was expanded as

$$F^s(\bar{r}) = \sum_{i=1}^{n1} U_i^s(\bar{r})\phi_i^s \tag{8}$$

where $U_i^s(\bar{r})$ $(i = 1, 2, ..., n1)$ represent the known expansion basis functions and ϕ_i^s $(i = 1, 2, ..., n1)$ are the unknown constants.

Before proceeding with a solution of (6) it is first necessary to choose the basis functions $V_i^e(\bar{r})$ and $U_i^s(\bar{r})$ in accordance with the definition of the isoparametric elements. A possible method of constructing U_i^s and V_i^e is to choose them so that ϕ_i^s $(i = 1, 2, ..., n1)$ represent the field values at $n1$ nodes on the sth segment and likewise ϕ_i^e $(i = 1, 2, ..., n2)$ represent the field values at $n2$ nodes of the eth quadrilateral. A point-matching procedure applied to (6) will then lead to a matrix equation for the solution of the nodal field values.

To find U_i^s as described above it is convenient to introduce the transformation

$$x = \sum_{i=1}^{3} L_i^s(\xi)x_i, \quad y = \sum_{i=1}^{3} L_i^s(\xi)y_i \tag{9}$$

allowing a linearization of a quadratically curved segment as shown in Figure 2. In (9), L_i^s $(i = 1, 2, 3)$ are the shape functions which take the well-known form [3]

$$L_1^s = -\frac{1}{2}(1 - \xi)\xi, \quad L_2^s = \frac{1}{2}(1 + \xi)\xi, \quad L_3^s = 1 - \xi^2.$$

In addition, (9) implies the relation

$$dl = \sqrt{\left(\frac{\partial x}{\partial \xi}\right)^2 + \left(\frac{\partial y}{\partial \xi}\right)^2}\, d\xi = |J^s| d\xi \tag{10}$$

and the unit vector $\hat{n}$ is now given by

$$\hat{n} = \left(\hat{x}\frac{\partial y}{\partial \xi} - \hat{y}\frac{\partial x}{\partial \xi}\right)|J^s|^{-1}. \tag{11}$$

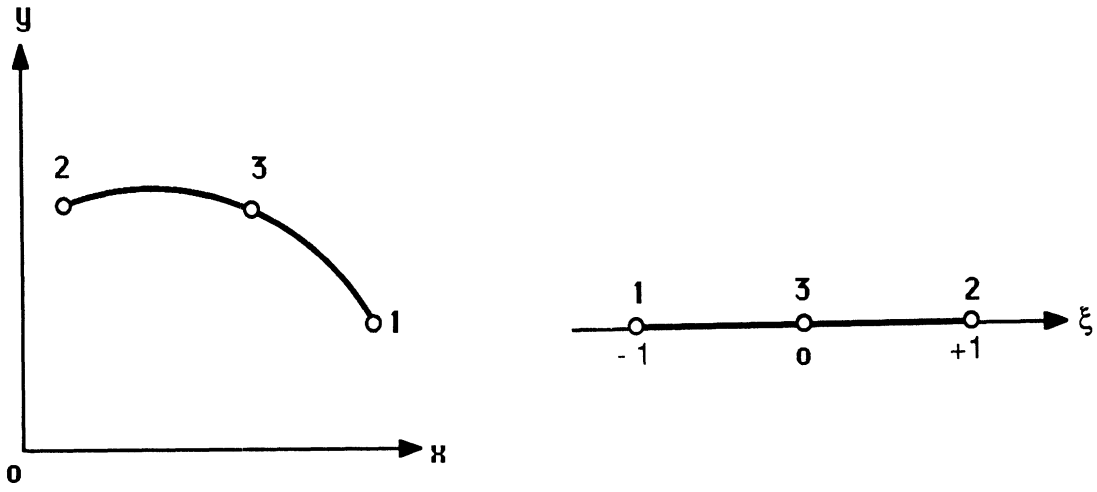

(a) (b)

Figure 2: A quadratically curved segment in the xy-plane (a) can be transformed into a straight segment lying on the ξ-axis (b).

It is observed that $L_i^s(\xi)$ is unity at the ith node and thus by choosing $U_i^s = L_i^s$, ϕ_i^s will coincide with the nodal values of the field $F^s(\bar{r})$. This actually is the definition of the isoparametric elements since L_i^s describe the geometrical shape of the discrete elements. When this expansion is substituted in (6), it leads to integrals of the form

$$I^s = \int_{\Gamma^s} B(\bar{r}|\bar{r}')L_i^s(\xi')dl' = \int_{-1}^{1} B(\bar{r}|\bar{r}')L_i^s(\xi')|J^s(\xi')|d\xi' \tag{12}$$

and these can be evaluated via a four point Gaussian integration formula giving

$$I^s = \sum_{j=1}^{4} W_j B(\bar{r}|\bar{r}_j')L_i^s(\xi_j)|J^s(\xi_j)| \tag{13}$$

where $\xi_1 = -0.8611363116$, $\xi_2 = -0.3399810436$, $\xi_3 = 0.3399810436$, $\xi_4 = 0.8611363116$, $W_1 = W_4 = 0.3478548451$, $W_2 = W_3 = 0.6521451549$, and $\bar{r}_j' = x(\xi_j)\hat{x} + y(\xi_j)\hat{y}$ in which $x(\xi_j)$ and $y(\xi_j)$ are given by (9).

The treatment of the area integral over Ω follows a similar procedure. We can again introduce the transformation

$$x = \sum_{i=1}^{8} N_i^e(\xi,\eta)x_i, \quad y = \sum_{i=1}^{8} N_i^e(\xi,\eta)y_i \tag{14}$$

allowing the representation of an arbitrarily shaped quadrilateral with quadratically curved sides in the xy-plane to a square in the $\xi\eta$-plane as shown in Figure 3. The shape functions are now N_i^e $(i = 1, 2, ..., 8)$ and they take the known form [3]

$$N_1^e = -\frac{1}{4}(1-\xi)(1-\eta)(\xi+\eta+1), \quad N_2^e = \frac{1}{4}(1+\xi)(1-\eta)(\xi-\eta-1),$$
$$N_3^e = \frac{1}{4}(1+\xi)(1+\eta)(\xi+\eta-1), \quad N_4^e = \frac{1}{4}(1-\xi)(1+\eta)(-\xi+\eta-1),$$

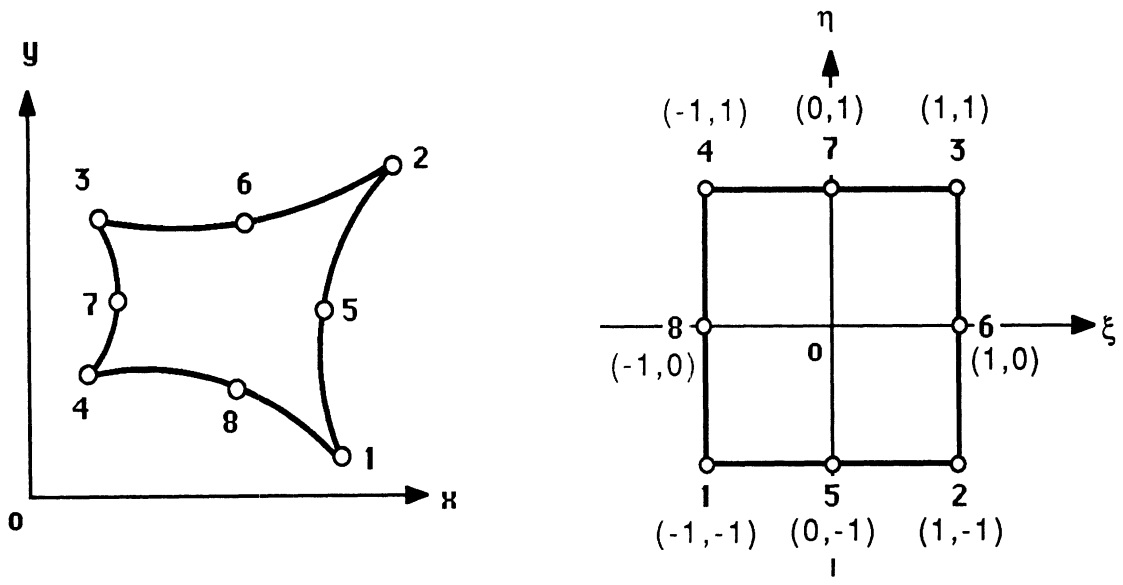

(a) (b)

Figure 3: A quadrilateral element with quadratically curved sides in the xy-plane (a) can be transformed into a square in the local $\xi\eta$-plane (b).

$$N_5^e = \frac{1}{2}(1-\xi^2)(1-\eta), \quad N_6^e = \frac{1}{2}(1+\xi)(1-\eta^2),$$
$$N_7^e = \frac{1}{2}(1-\xi^2)(1+\eta), \quad N_8^e = \frac{1}{2}(1-\xi)(1-\eta^2).$$

With this transformation the area element ds can be expressed as

$$ds = |J^e| d\xi d\eta \tag{15}$$

in which

$$|J^e| = \frac{\partial x}{\partial \xi}\frac{\partial y}{\partial \eta} - \frac{\partial x}{\partial \eta}\frac{\partial y}{\partial \xi}.$$

is the determinant of the Jacobian transformation matrix. Similarly to the one dimensional case, the shape function $N_i^e(\xi,\eta)$ is unity when $\xi = \xi_i$ and $\eta = \eta_i$. Thus, in accordance with the definition of the isoparametric elements we choose $V_i^e = N_i^e$ and as such the coefficients ϕ_i^e will coincide with the nodal values of the field $F^e(\bar{r})$. When this expansion is substituted in (6) we obtain integrals of the form

$$I^e = \int\int_{\Omega^e} A(\bar{r}|\bar{r}')N_i^e(\bar{r}')ds' = \int_{-1}^{1}\int_{-1}^{1} A(\bar{r}|\bar{r}')N_i^e(\xi',\eta')|J^e(\xi',\eta')|d\xi' d\eta' \tag{16}$$

and by using a nine point Gaussian integration formula, I^e can be written as

$$I^e = \sum_{j=1}^{3}\sum_{k=1}^{3} W_j W_k A(\bar{r}|\bar{r}'_{jk})N_i^e(\xi_j,\eta_k)|J^e(\xi_j,\eta_k)|, \tag{17}$$

where $\xi_1 = \eta_1 = -0.7745966692$, $\xi_2 = \eta_2 = 0.0$, $\xi_3 = \eta_3 = 0.7745966692$, $W_1 = W_3 = 0.5555555556$, $W_2 = 0.8888888889$, and $\bar{r}'_{jk} = x(\xi_j,\eta_k)\hat{x} + y(\xi_j,\eta_k)\hat{y}$ with $x(\xi_j,\eta_k)$ and $y(\xi_j,\eta_k)$ as given in (14).

We remark that the above formulation overcomes difficulties associated with singularities in the integrand. The numerical implementation is also rather straightforward and substantially simpler than those employed in traditional formulations. Most importantly the accuracy of the solution will be seen to be remarkable and to render accurate results for the internal fields for a scatterer having a large value of u.

4. Numerical Results

To validate the above moment method formulation and show its usefulness, we performed a few numerical experiments. For the results shown below, the incident field is assumed to be a plane wave propagating in the x-direction and the axis of the cylinder is coincident with the z-axis.

We first consider the problem of plane wave scattering by a dielectric circular cylinder with a radius 0.05λ (free-space wavelength) and relative permittivity as high as $\epsilon_r = 72.0 - j162.0$ corresponding to a muscle cylinder at 100 MHz. Figures 4 and 5 show, respectively, the electric and magnetic fields inside the cylinder for the TM and TE cases. Also, Table 1 gives the bistatic radar cross section, all compared with the exact eigenfunction solutions. As seen, there is an excellent agreement when the element size is chosen sufficiently small. We note that our previous moment method codes [1] ,[2] employing rectangular and triangular elements with pulse basis functions are unable to predict the correct TE result shown in Figure 5. A similar conclusion was also reached by Peterson and Klock [6] when they examined Richmond's [8] formulation where pulse basis functions were employed

Table 1. Bistatic Radar Cross Section (σ/λ) for a Homogeneous Dielectric Circular Cylinder with Radius Equal to 0.05λ and Relative Permittivity $72.0 - j162.0$

	TM case			TE case		
Angle (deg.)	20 unk	45 unk	Exact	45 unk	76 unk	Exact
0	-4.03	-3.96	-3.95	-20.44	-20.46	-20.54
30	-4.19	-4.12	-4.11	-22.23	-22.49	-22.26
60	-4.63	-4.56	-4.55	-30.28	-28.93	-28.99
90	-5.25	-5.19	-5.18	-28.35	-26.92	-26.73
120	-5.89	-5.83	-5.82	-19.99	-19.72	-19.65
150	-6.38	-6.31	-6.31	-16.77	-16.64	-16.60
180	-6.56	-6.49	-6.49	-15.85	-15.75	-15.71

for the solution of the electric field integral equation.

In [6], Peterson and Klock presented an improved magnetic field integral equation formulation by employing triangular elements with linear basis functions in the TE case. Here we compare our results with those in [6] for a dielectric cylinder with a radius 0.05λ having a relative permittivity $\epsilon_r = 4.0 - j100.0$. The results are shown in Figure 6 and as seen the isoparametric elements provide a higher accuracy.

In addition to the extreme situation described above, we also compared results obtained using isoparametric elements with those attributed to pulse expansion

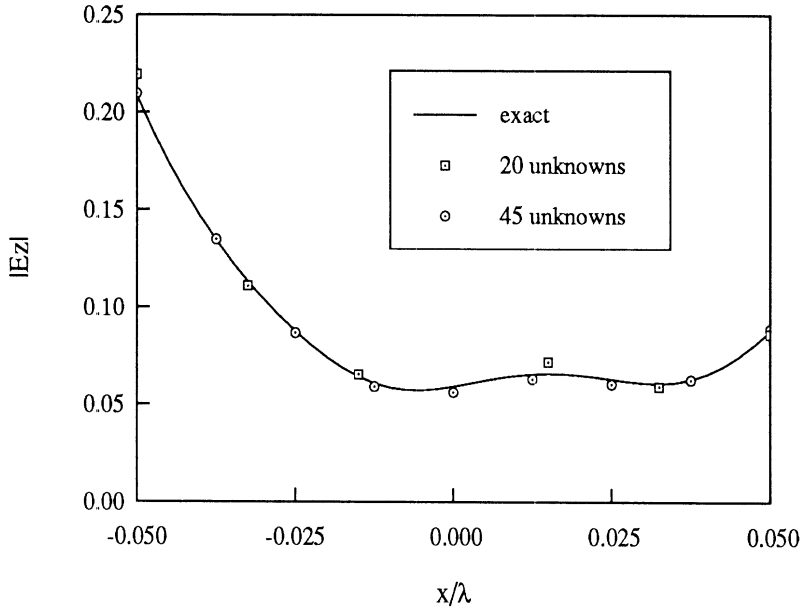

(a)

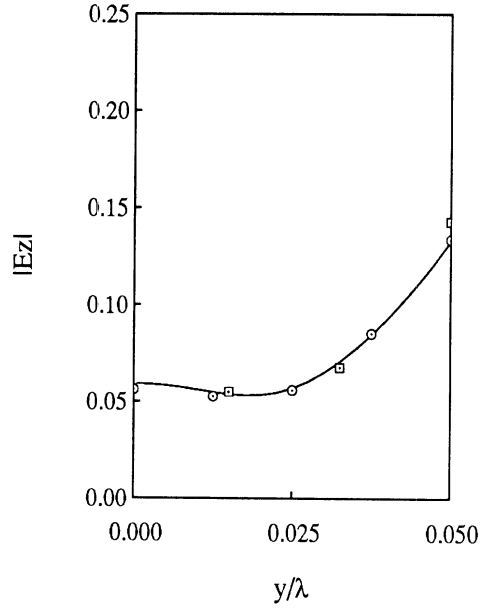

(b)

Figure 4: The electric field along (a) the x-axis and (b) y-axis inside a homogeneous dielectric circular cylinder of radius $a = 0.05\lambda$ and $\epsilon_r = 72.0 - j162.0$ for TM wave incidence.

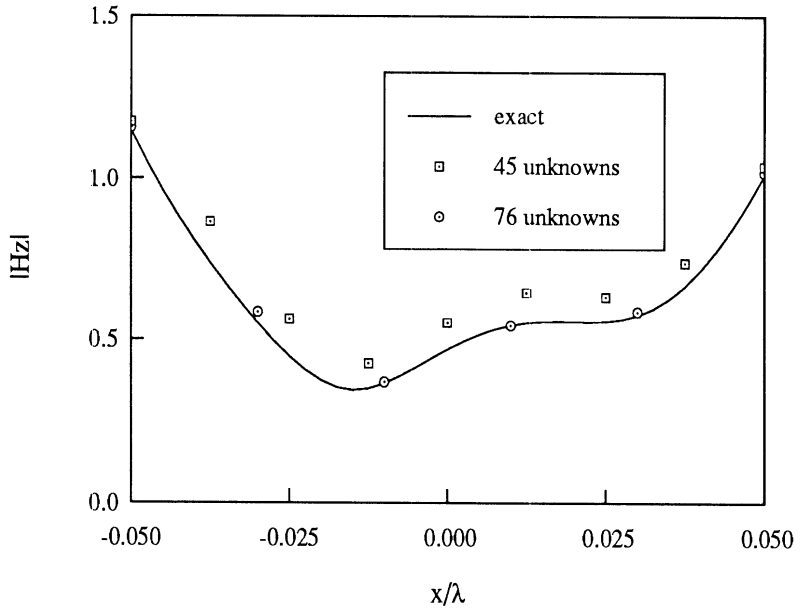

(a)

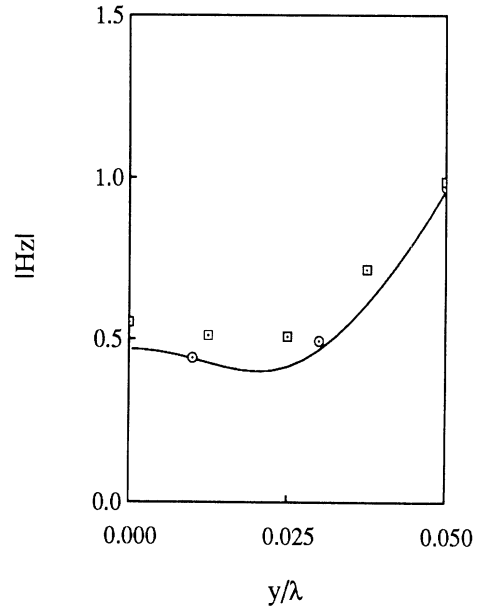

(b)

Figure 5: The magnetic field along (a) the x-axis and (b) y-axis inside a homogeneous dielectric circular cylinder of radius $a = 0.05\lambda$ and $\epsilon_r = 72.0 - j162.0$ for TE wave incidence.

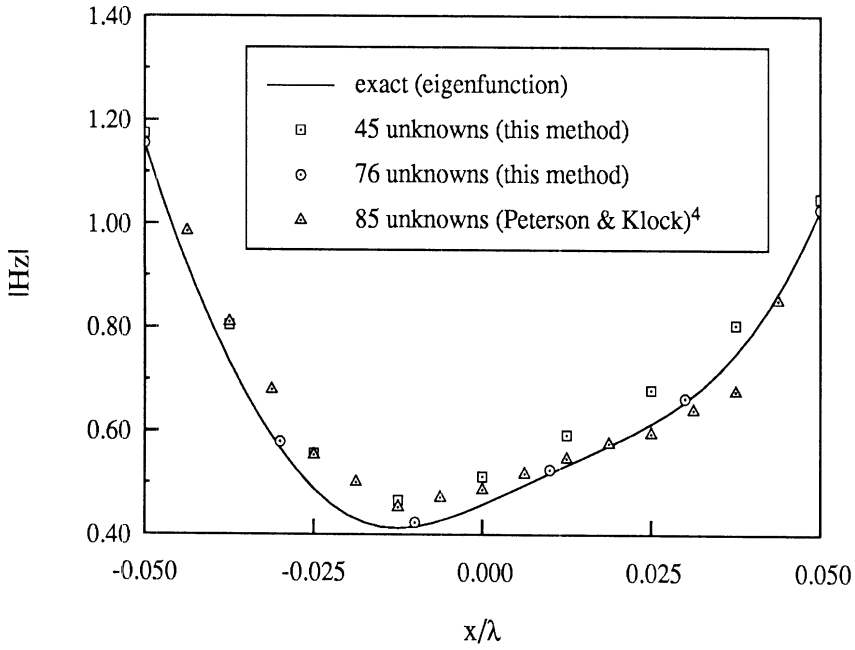

Figure 6: The magnetic field along the x-axis inside a homogeneous dielectric circular cylinder of radius $a = 0.05\lambda$ and $\epsilon_r = 4.0 - j100.0$ for TE wave incidence. A comparison with exact data and those given in [6].

functions for the case of nominal refractive indices. Overall, it was observed that the solution with isoparametric elements is more accurate and efficient than those employing pulse expansion basis. The improvement in these cases, though, is not as pronounced.

5. Conclusion

In this paper, we examined three integral equations for TE scattering by dielectric cylinders having large values of permittivity. A moment method solution of the volume-surface integral equation was then developed by employing isoparametric elements and point-matching. Differing from the traditional solutions using pulse basis, the one presented here was shown to be more accurate and stable, particularly in the case of scatterers having large refractive indices.

References

[1] Jin, J. M., V. V. Liepa, and C. T. Tai, "A volume-surface integral equation for electromagnetic scattering by inhomogeneous cylinders," *The Journal of Electromagnetic Waves and Applications*, vol. 2, pp. 573-588, 1988.

[2] Ricoy, M. A., S. Kilberg, and J. L. Volakis, "A simple set of integral equations for two-dimensional scattering with further reduction on unknowns," submitted to *Proc. Inst. Elec. Eng., part H.*

[3] Zienkiewicz, O. C., *The Finite Element Method,* 3rd ed. New York: McGraw-Hill, 1977.

[4] Graglia, R. D., "The use of parametric elements in the moment method solution of static and dynamic volume integral equations," *IEEE Trans. Antennas Propagat.*, vol. AP-36, pp. 636-646, 1988.

[5] Borup, D. T., D. M. Sullivan, and O. P. Gandhi, "Comparison of the FFT conjugate gradient method and the finite-difference time-domain method for the 2-D absorption problem," *IEEE Trans. Microwave Theory Tech.*, vol. MTT-35, pp. 383-395, 1987.

[6] Peterson, A. F. and P. W. Klock, "An improved MFIE formulation for TE-scattering from lossy, inhomogeneous dielectric cylinders," *IEEE Trans. Antennas Propagat.*, vol. AP-36, pp. 45-49, 1988.

[7] Boyse, W. E. and W. D. Kennedy, "A study of two-dimensional cylinders illuminated by TE polarized microwaves using the k-space algorithm," *1988 IEEE AP-S International Symposium Digest*, vol. 1, pp. 84-87, Syracuse, NY, June 1988.

[8] Richmond, J. H., "TE-wave scattering by a dielectric cylinder of arbitrary cross-section shape," *IEEE Trans. Antennas Propagat.*, vol. AP-14, pp. 460-464, 1966.

DESCRIPTION AND LIST OF CODE **VSIEM**

Jian-Ming Jin

Radiation Laboratory

Department of Electrical Engineering and Computer Science

The University of Michigan

Ann Arbor, Michigan 48109

ABSTRACT

A FORTRAN program named as **VSIEM** and developed by the author is described briefly and listed thereafter.

1. Objective of VSIEM

VSIEM is a computer code written in FORTRAN language and developed for computing electromagnetic scattering from perfectly conducting and inhomogeneous penetrable cylinders for both TE and TM incidence.

VSIEM uses the pulse expansion functions and point-matching technique to solve the volume-surface integral equation (VSIE). For the formulation of VSIE, please read the first paper in this report. For the description of the numerical implementation, please read the second paper. **VSIEM** was used to generate the data presented in the two papers.

2. Input Data

All input data are provided by file **INPUT** except for relative permittivity and permeability and their derivatives which are specified by subroutines **EMFUN** and **DRFUN**. A detailed description of the input data is given in the main program. A sample file of **INPUT** is listed below.

```
COATED CIRCULAR CYLINDER
 0   2.
 1  0   0.      180.       30.       0.
   10  -0.4       0.0       0.4       0.0     180.
   10   0.4       0.0      -0.4       0.0     180.
    0
   10  -0.44      0.0       0.44      0.0     180.
   10   0.44      0.0      -0.44      0.0     180.
    0
   10  -0.42      0.0       0.42      0.0     180.        0.04
   10   0.42      0.0      -0.42      0.0     180.        0.04
    0
```

3. Output Data

The output data are written in file **OUTPUT**. The data contain the geometry and discretization information and the computed result. Following is a sample output.

```
 COATED CIRCULAR CYLINDER


 SEG   NUM          ENDPOINTS OF THE SEGMENT              SEGMENT PARAMETERS
 NUM  CELLS      XA        YA        XB        YB       ANGLE  RADIUS  LENGTH
  1    10    -0.40000   0.00000   0.40000   0.00000   180.00   0.400  1.2566
  2    10     0.40000   0.00000  -0.40000   0.00000   180.00   0.400  1.2566


 SEG   NUM          ENDPOINTS OF THE SEGMENT              SEGMENT PARAMETERS
 NUM  CELLS      XA        YA        XB        YB       ANGLE  RADIUS  LENGTH
  1    10    -0.44000   0.00000   0.44000   0.00000   180.00   0.440  1.3823
  2    10     0.44000   0.00000  -0.44000   0.00000   180.00   0.440  1.3823


 LAY   NUM          ENDPOINTS OF THE LAYER                LAYER PARAMETERS
 NUM  CELLS      XA        YA        XB        YB       ANGLE  RADIUS  LENGTH
  1    10    -0.42000   0.00000   0.42000   0.00000   180.00   0.420  1.3195
  2    10     0.42000   0.00000  -0.42000   0.00000   180.00   0.420  1.3195
```

KEY PARAMETERS

INCIDENT POLARIZATION	E
NUMBER OF POINTS ON SURFACE(C)	20
NUMBER OF POINTS ON SURFACE(D)	20
NUMBER OF POINTS INSIDE DIELE	20
NUMBER OF INCIDENT FIELD DIRECTIONS	1
NUMBER OF BISTATIC DIRECTIONS	7
WAVELENGTH	2.00000

BISTATIC SCATTERING CROSS SECTION
FOR INCIDENT FIELD DIRECTION= 0.00

THETA	10*LOG(SIGMA/LAMBDA)	PHASE
0.00	-1.33	-93.0
30.00	-1.39	-98.1
60.00	-1.63	-114.1
90.00	-1.70	-143.6
120.00	0.15	-179.9
150.00	2.91	158.0
180.00	4.05	151.7

4. Program Description

Following is a brief description of the main program and subroutines developed for **VSIEM**. All others not described here are standard subroutines.

VSIEM - Main program acting as a driver for subroutines.

EMFUM - Specifies ϵ_r and μ_r at a given point (x, y).

DRFUN - Specifies $\nabla\epsilon_r$ and $\nabla\mu_r$ at a given point (x, y).

GEOMS - Discretizes the surfaces of conducting and dielectric cylinders.

GEOMI - Discretizes the cross section of the dielectric cylinder.

MATX1 - Generates the system matrix for E-polarization.

MATX2 - Generates the system matrix for H-polarization.

FARF1 - Computes the far field and RCS for E-polarization.

FARF2 - Computes the far field and RCS for H-polarization.

```
C*********************************************************************C
                          PROGRAM VSIEM
C*********************************************************************C
C  INPUT FORMAT FOR PROGRAM VSIEM----VERSION OF JAN 21, 1988          C
C  MODIFIED JAN 21, 1988                                              C
C  THIS IS A GENERALIZED VERSION OF VSIEM EXTENDED TO TREAT CONDUCTING C
C  SURFACE.  --- APRIL 23, 1988                                       C
C*********************************************************************C
C  CARD 1  FORMAT (18A4)          TITLE CARD; USE UP TO 72 COLUMNS    C
C*********************************************************************C
C  CARD 2  FORMAT (I2,F10.5)   KODE,WAVE                              C
C          KODE=0       COMPUTES BISTATIC SCATTERING PATTERN          C
C          KODE=1       COMPUTES BACKSCATTERING PATTERN               C
C          WAVE         WAVELENGTH                                    C
C*********************************************************************C
C  CARD 3  FORMAT (I2,I3,4F10.5)  IPP,IOPT,FIRST,LAST,INK,CANG        C
C          IPP=1        E-POLARIZATION                                C
C          IPP=2        H-POLARIZATION                                C
C          IOPT=0       PARAMETERS NOT PRINTED                        C
C          IOPT=1       PARAMETERS PRINTED                            C
C          FIRST        INITIAL SCATTERING AND INCIDENCE ANGLE        C
C          LAST         FINAL ANGLE                                   C
C          INK          ANGULAR INCREMENT                             C
C          CANG         ANGLE FOR BISTATIC COMPUTATION                C
C*********************************************************************C
C          FORMAT FOR INPUT CONDUCTING SURFACE                         C
C*********************************************************************C
C  CARD 4  FORMAT (I5,5F10.5)  N,XA,YA,XB,YB,ANGLE                    C
C          N            NUMBER OF SAMPLING POINTS ON THIS SEGMENT     C
C          XA,YA,XB,YB  SEGMENT ENDPOINTS                             C
C          ANGLE        ANGLE SUBTENDED BY THE SEGMENT                C
C*********************************************************************C
C          REPEAT CARD 4 FOR EACH SEGMENT                              C
C*********************************************************************C
C  CARD 5  FORMAT (I2)            INTEGER ZERO IN COLUMN 5;  SHUTS    C
C                                 OFF READING OF SEGMENT PARAMETERS   C
C*********************************************************************C
C          FORMAT FOR INPUT DIELECTRIC SURFACE                         C
C*********************************************************************C
C  CARD 6  FORMAT (I5,5F10.5)  N,XA,YA,XB,YB,ANGLE                    C
C          N            NUMBER OF SAMPLING POINTS ON THIS SEGMENT     C
C          XA,YA,XB,YB  SEGMENT ENDPOINTS                             C
C          ANGLE        ANGLE SUBTENDED BY THE SEGMENT                C
C*********************************************************************C
C          REPEAT CARD 6 FOR EACH SEGMENT                              C
C*********************************************************************C
C  CARD 7  FORMAT (I2)            INTEGER ZERO IN COLUMN 5;  SHUTS    C
C                                 OFF READING OF SEGMENT PARAMETERS   C
C*********************************************************************C
C          FORMAT FOR INPUT DIELECTRIC LAYERS                          C
C*********************************************************************C
C  CARD 8  FORMAT (I2,6F10.5)  N,XA,YA,XB,YB,ANGLE,DL                 C
C          N            NUMBER OF SAMPLING POINTS ON THIS LAYER       C
C          XA,YA,XB,YB  LAYER ENDPOINTS                               C
C          ANGLE        ANGLE SUBTENDED BY THE LAYER                  C
C          DL           THICKNESS OF THE LAYER                        C
C*********************************************************************C
```

```
C          REPEAT CARD 8 FOR EACH LAYER                                  C
C*************************************************************************C
C  CARD 9  FORMAT (I2)            INTEGER ZERO IN COLUMN 5;  SHUTS       C
C                                 OFF READING OF LAYER PARAMETERS        C
C*************************************************************************C
C*************************************************************************C
      COMPLEX A(500,500),FINC(500)
      COMPLEX EPS(100),MU(100),EPSI(300),MUI(300)
      COMPLEX DXEPS(300),DYEPS(300),DXMU(300),DYMU(300)
      REAL LAST,INK
      DIMENSION XC(100),YC(100),XNC(100),YNC(100),SC(100),DSQC(100),
     &          ANGC(100)
      DIMENSION XS(100),YS(100),XN(100),YN(100),S(100),DSQ(100),ANG(100)
      DIMENSION XI(300),YI(300),SI(300),DSQI(300),ANGI(300)
      DIMENSION ID(18),LUMPC(100,2),LUMPS(100,2),LUMPI(300,2),IPOL(2)
      DIMENSION THEA(361),SCATA(361),FASEA(361),KPVT(500)
      DATA RED,DIG,PIF,IPOL/0.01745329,57.29578,0.07957747151,
     &4HEEEE,4HHHHH/
      OPEN(UNIT=5,FILE='INPUT')
      OPEN(UNIT=6,FILE='OUTPUT')
C.....READ INPUT DATA AND GENERATE BODY PROFILE
    5 READ (5,100) ID
      READ (5,125) KODE,WAVE
      READ (5,200) IPP,IOPT,FIRST,LAST,INK,CANG
      WRITE (6,150) ID
      WRITE (6,300)
      CALL GEOMS(LUMPC,XC,YC,XNC,YNC,SC,DSQC,ANGC,EPS,MU,MC,LLC)
      IF(IOPT.EQ.0) GOTO 8
      WRITE (6,500)
      DO 6 I=1,MC
    6 WRITE(6,250)(LUMPC(I,J),J=1,2),XC(I),YC(I),XNC(I),YNC(I),
     &SC(I),DSQC(I)
    8 WRITE (6,300)
      CALL GEOMS(LUMPS,XS,YS,XN,YN,S,DSQ,ANG,EPS,MU,MS,LLS)
      IF(IOPT.EQ.0) GOTO 20
      WRITE (6,500)
      DO 10 I=1,MS
   10 WRITE(6,250)(LUMPS(I,J),J=1,2),XS(I),YS(I),XN(I),YN(I),
     &S(I),DSQ(I),EPS(I),MU(I)
   20 WRITE (6,310)
      CALL GEOMI(LUMPI,XI,YI,SI,DSQI,ANGI,EPSI,MUI,DXEPS,DYEPS,
     &DXMU,DYMU,MI,LLI)
      IF(IOPT.EQ.0) GOTO 40
      WRITE (6,510)
      DO 30 I=1,MI
   30 WRITE(6,260)(LUMPI(I,J),J=1,2),XI(I),YI(I),S(I),DSQI(I),
     &EPSI(I),MUI(I)
   40 CONTINUE
C.....GENERATE SYSTEM MATRIX
      XK=6.283185/WAVE
      IF(IPP.EQ.2) GOTO 50
      CALL MATX1(A,MC,MS,MI,XC,YC,XS,YS,XN,YN,XI,YI,DSQC,DSQ,DSQI,
     &EPS,MU,EPSI,MUI,DXMU,DYMU,XK)
      GOTO 60
   50 CALL MATX2(A,MC,MS,MI,XC,YC,XS,YS,XNC,YNC,XN,YN,XI,YI,DSQC,
     &DSQ,DSQI,MU,EPS,MUI,EPSI,DXEPS,DYEPS,XK)
   60 CONTINUE
      N=MC+MS+MI
      CALL CGECO(A,500,N,KPVT,RC,FINC)
      IF (KODE.NE.0) GO TO 70
```

```
      NINC=1
      NBIT=1+IFIX((LAST-FIRST)/INK)
      GO TO 80
   70 NBIT=0
      NINC=1+IFIX((LAST-FIRST)/INK)
   80 WRITE (6,400) IPOL(IPP),MC,MS,MI,NINC,NBIT,WAVE
      IF(KODE.EQ.1) WRITE(6,600)
      IF(KODE.EQ.1) CANG=FIRST
C.....COMPUTE INCIDENT FIELD
   82 TETA=RED*CANG
      CT=COS(TETA)
      ST=SIN(TETA)
      DO 84 I=1,MI
      HOLD=XK*(CT*XI(I)+ST*YI(I))
   84 FINC(I)=CMPLX(COS(HOLD),SIN(HOLD))
      DO 85 I=1,MS
      HOLD=XK*(CT*XS(I)+ST*YS(I))
   85 FINC(I+MI)=CMPLX(COS(HOLD),SIN(HOLD))
      DO 851 I=1,MC
      HOLD=XK*(CT*XC(I)+ST*YC(I))
  851 FINC(I+MI+MS)=CMPLX(COS(HOLD),SIN(HOLD))
C.....COMPUTE NEAR FIELD (NODAL FIELD VALUES)
      CALL CGESL(A,500,N,KPVT,FINC,0)
C      DO 98 I=1,N
C   98 WRITE(6,99) I,FINC(I),CABS(FINC(I))
C   99 FORMAT(5X,I5,10X,2E16.6,10X,F16.8)
C.....CALL SUBROUTINE TO COMPUTE FAR FIELD
      IF(KODE.EQ.0) GOTO 88
      IF(IPP.EQ.2) GOTO 86
      CALL FARF1(FINC,MC,MS,MI,XC,YC,XS,YS,XN,YN,XI,YI,DSQC,DSQ,DSQI,
     &EPS,MU,EPSI,MUI,DXMU,DYMU,XK,CANG,CANG,1)
      GOTO 87
   86 CALL FARF2(FINC,MC,MS,MI,XC,YC,XS,YS,XNC,YNC,XN,YN,XI,YI,DSQC,
     &DSQ,DSQI,MU,EPS,MUI,EPSI,DXEPS,DYEPS,XK,CANG,CANG,1)
   87 CANG=CANG+INK
      IF(CANG.LE.LAST) GOTO 82
      GOTO 1000
   88 WRITE(6,610) CANG
      IF(IPP.EQ.2) GOTO 90
      CALL FARF1(FINC,MC,MS,MI,XC,YC,XS,YS,XN,YN,XI,YI,DSQC,DSQ,DSQI,
     &EPS,MU,EPSI,MUI,DXMU,DYMU,XK,FIRST,INK,NBIT)
      GOTO 1000
   90 CALL FARF2(FINC,MC,MS,MI,XC,YC,XS,YS,XNC,YNC,XN,YN,XI,YI,DSQC,
     &DSQ,DSQI,MU,EPS,MUI,EPSI,DXEPS,DYEPS,XK,FIRST,INK,NBIT)

  100 FORMAT (18A4)
  125 FORMAT(I2,F10.5)
  150 FORMAT (1X,18A4)
  200 FORMAT (I2,I3,4F10.5)
  250 FORMAT (2I5,10F10.5)
  260 FORMAT (2I5, 8F10.5)
  300 FORMAT (/,/10H SEG   NUM,11X,24HENDPOINTS OF THE SEGMENT,11X,
     &' SEGMENT PARAMETERS '/11H NUM  CELLS,6X,2HXA,8X,2HYA,8X,2HXB,8X,
     &2HYB,6X,21HANGLE  RADIUS  LENGTH)
  310 FORMAT (/,/10H LAY   NUM,11X,24HENDPOINTS OF THE LAYER  ,11X,
     &'  LAYER PARAMETERS  '/11H NUM  CELLS,6X,2HXA,8X,2HYA,8X,2HXB,8X,
     &2HYB,6X,21HANGLE  RADIUS  LENGTH)
  400 FORMAT (//25X,14HKEY PARAMETERS//
     &10X,21HINCIDENT POLARIZATION,22X,1A1/
     &10X,34HNUMBER OF POINTS ON SURFACE(C)    ,I10/
```

```
     &10X,34HNUMBER OF POINTS ON SURFACE(D)     ,I10/
     &10X,34HNUMBER OF POINTS INSIDE DIELE     ,I10/
     &10X,35HNUMBER OF INCIDENT FIELD DIRECTIONS,I9/
     &10X,29HNUMBER OF BISTATIC DIRECTIONS,I15/
     &10X,10HWAVELENGTH,F34.5)

 500  FORMAT (/,/11H    I   SEG,4X,4HX(I),6X,4HY(I),5X,5HXN(I),
     &5X,5HYN(I),6X,4HS(I),5X,6HDSQ(I),3X,7HEPSR(I),3X,7HEPSI(I),
     &4X,6HMUR(I),4X,6HMUI(I))
 510  FORMAT (/,/11H    I   SEG,4X,4HX(I),6X,4HY(I),6X,4HS(I),4X,
     &7HAREA(I),3X,7HEPSR(I),3X,7HEPSI(I),4X,6HMUR(I),4X,6HMUI(I))
 600  FORMAT (///,20X,28HBACKSCATTERING CROSS SECTION/17X,
     &36HTHETA   10*LOG(SIGMA/LAMBDA)   PHASE/)
 610  FORMAT (///,19X,33HBISTATIC SCATTERING CROSS SECTION/18X,
     &29HFOR INCIDENT FIELD DIRECTION=,F7.2/17X,
     &36HTHETA   10*LOG(SIGMA/LAMBDA)   PHASE/)
 700  FORMAT(///,18X,35HFIELD DISTRIBUTION INSIDE SCATTERER/15X,
     &53HPONIT NUM          COMPLEX FIELD          MAG(FIELD)/)
 710  FORMAT(15X,I6,5X,E11.4,4X,E11.4,5X,F9.4)
1000  STOP
      END
```

```
      SUBROUTINE EMFUN(X,Y,EPS,MU)
      COMPLEX EPS,MU
C.....SPECIFY PERMITTIVITY AND PERMEABILITY
      EPS=(2.4,0.0)
      MU=(1.2,0.0)
cc      EPS=2.-(X*X+Y*Y)/(.4*.4)
cc      EPS=4./(1+(X*X+Y*Y)/(0.36))**2
      RETURN
      END



      SUBROUTINE DRFUN(X,Y,DXEPS,DYEPS,DXMU,DYMU)
      COMPLEX DXEPS,DYEPS,DXMU,DYMU
C.....SPECIFY THE DERIVATIVES OF PERMITTIVITY AND PERMEABILITY
      DXEPS=(0.,0.)
      DYEPS=(0.,0.)
cc      DXEPS=-2.*X/(0.4*0.4)
cc      DYEPS=-2.*Y/(0.4*0.4)
cc      DXEPS=-16./((1+(X*X+Y*Y)/(0.36))**3)*X/0.36
cc      DYEPS=-16./((1+(X*X+Y*Y)/(0.36))**3)*Y/0.36
      DXMU=(0.,0.)
      DYMU=(0.,0.)
      RETURN
      END
```

```
C*********************************************************************C
C     TTHIS SUBROUTINE READS DATA AND GENERATE POINTS ON THE SURFACE   C
C     OF THE CYLINDER                                                  C
C*********************************************************************C
      SUBROUTINE GEOMS(LUMP,X,Y,XN,YN,S,DSQ,ANG,EPS,MU,M,LL)
      COMPLEX EPS(100),MU(100)
      DIMENSION X(100),Y(100),XN(100),YN(100),DSQ(100),S(100),ANG(100)
      DIMENSION LUMP(100,2)
      DATA RED/0.01745329/
      I=0
      L=0
C.....READ INPUT PARAMETERS AND PREPARE TO GENERATE SAMPLING POINTS
  10  READ (5,200) N,XA,YA,XB,YB,ANGLE
      IF (N.EQ.0) GO TO 120
      LIM=2*N-1
      TX=XB-XA
      TY=YB-YA
      D=SQRT(TX*TX+TY*TY)
      IF (ANGLE.EQ.0.0) GO TO 20
      T=0.5*RED*ANGLE
      TRX=TX+TY/TAN(T)
      TRY=TY-TX/TAN(T)
      RAD=0.5*D/SIN(T)
      ARC=2.0*RAD*T
      ALF=T/N
      DID=2.0*RAD*ALF
      GO TO 30
  20  RAD=999.999
      ARC=D
      DID=D/N
C.....START GENERATING
  30  CONTINUE
      L=L+1
      DO 100 J=1,LIM,2
      I=I+1
      LUMP(I,1)=I
      LUMP(I,2)=L
      IF (ANGLE.EQ.0.0) GO TO 40
      SINQ=SIN(J*ALF)
      COSQ=COS(J*ALF)
      X(I)=XA+0.5*(TRX*(1.0-COSQ)-TRY*SINQ)
      Y(I)=YA+0.5*(TRX*SINQ+TRY*(1.0-COSQ))
      XN(I)=-0.5*(TRX*COSQ+TRY*SINQ)/RAD
      YN(I)= 0.5*(TRX*SINQ-TRY*COSQ)/RAD
      ANG(I)=(ANGLE/N)*RED
      GO TO 50
  40  X(I)=XA+0.5*J*TX/N
      Y(I)=YA+0.5*J*TY/N
      XN(I)=-TY/D
      YN(I)= TX/D
      ANG(I)=(ANGLE/N)*RED
  50  S(I)=0.5*J*DID
C.....COMPUTE THE PERMITTIVITY AND PERMEABILITY
      CALL EMFUN(X(I),Y(I),EPS(I),MU(I))
 100  DSQ(I)=DID
      WRITE (6,300) L,N,XA,YA,XB,YB,ANGLE,RAD,ARC
      GO TO 10
 120  M=I
      LL=L
```

```
200  FORMAT (I5,5F10.5)
250  FORMAT (5X,5F10.5)
300  FORMAT (I3,I6,3X,4F10.5,F8.2,F8.3,F8.4)
     RETURN
     END
```

```
C*********************************************************************C
C     TTHIS SUBROUTINE READS DATA AND GENERATE POINTS INSIDE THE      C
C     CYLINDER                                                        C
C*********************************************************************C
      SUBROUTINE GEOMI(LUMP,X,Y,S,DSQ,ANG,EPS,MU,DXEPS,DYEPS,
     &DXMU,DYMU,M,LL)
      COMPLEX EPS(300),MU(300),DXEPS(300),DYEPS(300),DXMU(300),DYMU(300)
      DIMENSION X(300),Y(300),DSQ(300),S(100),ANG(100)
      DIMENSION LUMP(300,2)
      DATA RED/0.01745329/
      I=0
      L=0
C.....READ INPUT PARAMETERS AND PREPARE TO GENERATE SAMPLING POINTS
  10  READ (5,200) N,XA,YA,XB,YB,ANGLE,THICK
      IF (N.EQ.0) GO TO 120
      LIM=2*N-1
      TX=XB-XA
      TY=YB-YA
      D=SQRT(TX*TX+TY*TY)
      IF (ANGLE.EQ.0.0) GO TO 20
      T=0.5*RED*ANGLE
      TRX=TX+TY/TAN(T)
      TRY=TY-TX/TAN(T)
      RAD=0.5*D/SIN(T)
      ARC=2.0*RAD*T
      ALF=T/N
      DID=2.0*RAD*ALF
      GO TO 30
  20  RAD=999.999
      ARC=D
      DID=D/N
C.....START GENERATING
  30  CONTINUE
      L=L+1
      DO 100 J=1,LIM,2
      I=I+1
      LUMP(I,1)=I
      LUMP(I,2)=L
      IF (ANGLE.EQ.0.0) GO TO 40
      SINQ=SIN(J*ALF)
      COSQ=COS(J*ALF)
      X(I)=XA+0.5*(TRX*(1.0-COSQ)-TRY*SINQ)
      Y(I)=YA+0.5*(TRX*SINQ+TRY*(1.0-COSQ))
      ANG(I)=(ANGLE/N)*RED
      GO TO 50
  40  X(I)=XA+0.5*J*TX/N
      Y(I)=YA+0.5*J*TY/N
      ANG(I)=(ANGLE/N)*RED
  50  S(I)=0.5*J*DID
C.....COMPUTE THE PERMITTIVITY AND PERMEABILITY
      CALL EMFUN(X(I),Y(I),EPS(I),MU(I))
      CALL DRFUN(X(I),Y(I),DXEPS(I),DYEPS(I),DXMU(I),DYMU(I))
 100  DSQ(I)=DID*THICK
      WRITE (6,300) L,N,XA,YA,XB,YB,ANGLE,RAD,ARC
      GO TO 10
 120  M=I
      LL=L
 200  FORMAT (I5,6F10.5)
 250  FORMAT (5X,5F10.5)
```

```
300  FORMAT (I3,I6,3X,4F10.5,F8.2,F8.3,F8.4)
     RETURN
     END
```

```
C*********************************************************************C
C     SUBROUTINE FORMS SYSTEM MATRIX [A] FOR E-POLARIZATION;          C
C     FOR H-POLARIZATION, USE MATX2.                                  C
C*********************************************************************C
      SUBROUTINE MATX1(A,MC,MS,MI,XC,YC,XS,YS,XN,YN,XI,YI,DSQC,DSQ,DSQI,
     &EPS,MU,EPSI,MUI,DXMU,DYMU,XK)
      COMPLEX A(500,500),EPS(100),MU(100),EPSI(300),MUI(300),DXMU(300),
     &DYMU(300),HZERO,HONE
      DIMENSION XC(100),YC(100),XS(100),YS(100),XN(100),YN(100),XI(300),
     &YI(300),DSQC(100),DSQ(100),DSQI(300)
      PI=3.141592654
      DO 20 I=1,MI
      DO 20 J=1,MI
      IF(I.EQ.J) GOTO 10
      XJI=XI(J)-XI(I)
      YJI=YI(J)-YI(I)
      RJI=SQRT(XJI*XJI+YJI*YJI)
      RKO=XK*RJI
      CALL HANKZ2(RKO,2,HZERO,HONE)
      A(I,J)=(XK*XK*(EPSI(J)-1./MUI(J))*HZERO+(DXMU(J)*XJI/RJI+
     &DYMU(J)*YJI/RJI)/(MUI(J)*MUI(J))*XK*HONE)*CMPLX(0.,0.25)*DSQI(J)
      GOTO 20
 10   RKA=SQRT(DSQI(J)/PI)*XK
      CALL HANKZ2(RKA,1,HZERO,HONE)
      A(I,I)=1./MUI(I)+0.5*(EPSI(I)-1./MUI(I))*(2.+CMPLX(0.,1.)
     &*PI*RKA*HONE)
 20   CONTINUE
      DO 30 I=1,MI
      DO 30 J=1,MS
      XJI=XS(J)-XI(I)
      YJI=YS(J)-YI(I)
      RJI=SQRT(XJI*XJI+YJI*YJI)
      RKO=XK*RJI
      CALL HANKZ2(RKO,1,HZERO,HONE)
 30   A(I,J+MI)=(1./MU(J)-1.)*(XJI/RJI*XN(J)+YJI/RJI*YN(J))
     &*CMPLX(0.,0.25)*XK*HONE*DSQ(J)
      DO 40 I=1,MS
      DO 40 J=1,MI
      XJI=XI(J)-XS(I)
      YJI=YI(J)-YS(I)
      RJI=SQRT(XJI*XJI+YJI*YJI)
      RKO=XK*RJI
      CALL HANKZ2(RKO,2,HZERO,HONE)
 40   A(I+MI,J)=(XK*XK*(EPSI(J)-1./MUI(J))*HZERO+(DXMU(J)*XJI/RJI+
     &DYMU(J)*YJI/RJI)/(MUI(J)*MUI(J))*XK*HONE)*CMPLX(0.,0.25)*DSQI(J)
      DO 60 I=1,MS
      DO 60 J=1,MS
      IF(I.EQ.J) GOTO 50
      XJI=XS(J)-XS(I)
      YJI=YS(J)-YS(I)
      RJI=SQRT(XJI*XJI+YJI*YJI)
      RKO=XK*RJI
      CALL HANKZ2(RKO,1,HZERO,HONE)
      A(I+MI,J+MI)=(1./MU(J)-1.)*(XJI/RJI*XN(J)+YJI/RJI*YN(J))
     &*CMPLX(0.,0.25)*XK*HONE*DSQ(J)
      GOTO 60
 50   A(I+MI,J+MI)=0.5*(1.+1./MU(I))
 60   CONTINUE
      DO 70 I=1,MI
```

```
      DO 70 J=1,MC
      XJI=XC(J)-XI(I)
      YJI=YC(J)-YI(I)
      RJI=SQRT(XJI*XJI+YJI*YJI)
      RKO=XK*RJI
      CALL HANKZ2(RKO,0,HZERO,HONE)
   70 A(I,J+MI+MS)=-CMPLX(0.,0.25)*HZERO*DSQC(J)
      DO 80 I=1,MS
      DO 80 J=1,MC
      XJI=XC(J)-XS(I)
      YJI=YC(J)-YS(I)
      RJI=SQRT(XJI*XJI+YJI*YJI)
      RKO=XK*RJI
      CALL HANKZ2(RKO,0,HZERO,HONE)
   80 A(I+MI,J+MI+MS)=-CMPLX(0.,0.25)*HZERO*DSQC(J)
      DO 90 I=1,MC
      DO 90 J=1,MI
      XJI=XI(J)-XC(I)
      YJI=YI(J)-YC(I)
      RJI=SQRT(XJI*XJI+YJI*YJI)
      RKO=XK*RJI
      CALL HANKZ2(RKO,2,HZERO,HONE)
   90 A(I+MI+MS,J)=(XK*XK*(EPSI(J)-1./MUI(J))*HZERO+(DXMU(J)*XJI/RJI+
     &DYMU(J)*YJI/RJI)/(MUI(J)*MUI(J))*XK*HONE)*CMPLX(0.,0.25)*DSQI(J)
      DO 100 I=1,MC
      DO 100 J=1,MS
      XJI=XS(J)-XC(I)
      YJI=YS(J)-YC(I)
      RJI=SQRT(XJI*XJI+YJI*YJI)
      RKO=XK*RJI
      CALL HANKZ2(RKO,1,HZERO,HONE)
  100 A(I+MI+MS,J+MI)=(1./MU(J)-1.)*(XJI/RJI*XN(J)+YJI/RJI*YN(J))
     &*CMPLX(0.,0.25)*XK*HONE*DSQ(J)
      DO 120 I=1,MC
      DO 120 J=1,MC
      IF(I.EQ.J) GOTO 110
      XJI=XC(J)-XC(I)
      YJI=YC(J)-YC(I)
      RJI=SQRT(XJI*XJI+YJI*YJI)
      RKO=XK*RJI
      CALL HANKZ2(RKO,0,HZERO,HONE)
      A(I+MI+MS,J+MI+MS)=-CMPLX(0.,0.25)*HZERO*DSQC(J)
      GOTO 120
  110 A(I+MI+MS,J+MI+MS)=-CMPLX(0.,0.25)*(1.0-CMPLX(0.,2.)/PI*
     &ALOG(0.1638*XK*DSQC(J)))*DSQC(J)
  120 CONTINUE
      RETURN
      END
```

```
C*********************************************************************C
C     SUBROUTINE FORMS SYSTEM MATRIX [A] FOR H-POLARIZATION;          C
C*********************************************************************C
      SUBROUTINE MATX2(A,MC,MS,MI,XC,YC,XS,YS,XNC,YNC,XN,YN,XI,YI,DSQC,
     &DSQ,DSQI,EPS,MU,EPSI,MUI,DXMU,DYMU,XK)
      COMPLEX A(500,500),EPS(100),MU(100),EPSI(300),MUI(300),DXMU(300),
     &DYMU(300),HZERO,HONE
      DIMENSION XC(100),YC(100),XS(100),YS(100),XN(100),YN(100),
     &XNC(100),YNC(100),XI(300),YI(300),DSQC(100),DSQ(100),DSQI(300)
      PI=3.141592654
      DO 20 I=1,MI
      DO 20 J=1,MI
      IF(I.EQ.J) GOTO 10
      XJI=XI(J)-XI(I)
      YJI=YI(J)-YI(I)
      RJI=SQRT(XJI*XJI+YJI*YJI)
      RKO=XK*RJI
      CALL HANKZ2(RKO,2,HZERO,HONE)
      A(I,J)=(XK*XK*(EPSI(J)-1./MUI(J))*HZERO+(DXMU(J)*XJI/RJI+
     &DYMU(J)*YJI/RJI)/(MUI(J)*MUI(J))*XK*HONE)*CMPLX(0.,0.25)*DSQI(J)
      GOTO 20
 10   RKA=SQRT(DSQI(J)/PI)*XK
      CALL HANKZ2(RKA,1,HZERO,HONE)
      A(I,I)=1./MUI(I)+0.5*(EPSI(I)-1./MUI(I))*(2.+CMPLX(0.,1.)
     &*PI*RKA*HONE)
 20   CONTINUE
      DO 30 I=1,MI
      DO 30 J=1,MS
      XJI=XS(J)-XI(I)
      YJI=YS(J)-YI(I)
      RJI=SQRT(XJI*XJI+YJI*YJI)
      RKO=XK*RJI
      CALL HANKZ2(RKO,1,HZERO,HONE)
 30   A(I,J+MI)=(1./MU(J)-1.)*(XJI/RJI*XN(J)+YJI/RJI*YN(J))
     &*CMPLX(0.,0.25)*XK*HONE*DSQ(J)
      DO 40 I=1,MS
      DO 40 J=1,MI
      XJI=XI(J)-XS(I)
      YJI=YI(J)-YS(I)
      RJI=SQRT(XJI*XJI+YJI*YJI)
      RKO=XK*RJI
      CALL HANKZ2(RKO,2,HZERO,HONE)
 40   A(I+MI,J)=(XK*XK*(EPSI(J)-1./MUI(J))*HZERO+(DXMU(J)*XJI/RJI+
     &DYMU(J)*YJI/RJI)/(MUI(J)*MUI(J))*XK*HONE)*CMPLX(0.,0.25)*DSQI(J)
      DO 60 I=1,MS
      DO 60 J=1,MS
      IF(I.EQ.J) GOTO 50
      XJI=XS(J)-XS(I)
      YJI=YS(J)-YS(I)
      RJI=SQRT(XJI*XJI+YJI*YJI)
      RKO=XK*RJI
      CALL HANKZ2(RKO,1,HZERO,HONE)
      A(I+MI,J+MI)=(1./MU(J)-1.)*(XJI/RJI*XN(J)+YJI/RJI*YN(J))
     &*CMPLX(0.,0.25)*XK*HONE*DSQ(J)
      GOTO 60
 50   A(I+MI,J+MI)=0.5*(1.+1./MU(I))
 60   CONTINUE
      DO 70 I=1,MI
      DO 70 J=1,MC
```

```
      XJI=XC(J)-XI(I)
      YJI=YC(J)-YI(I)
      RJI=SQRT(XJI*XJI+YJI*YJI)
      RKO=XK*RJI
      CALL HANKZ2(RKO,1,HZERO,HONE)
   70 A(I,J+MI+MS)=-(XJI/RJI*XNC(J)+YJI/RJI*YNC(J))
     &*CMPLX(0.,0.25)*XK*HONE*DSQC(J)
      DO 80 I=1,MS
      DO 80 J=1,MC
      XJI=XC(J)-XS(I)
      YJI=YC(J)-YS(I)
      RJI=SQRT(XJI*XJI+YJI*YJI)
      RKO=XK*RJI
      CALL HANKZ2(RKO,1,HZERO,HONE)
   80 A(I+MI,J+MI+MS)=-(XJI/RJI*XNC(J)+YJI/RJI*YNC(J))
     &*CMPLX(0.,0.25)*XK*HONE*DSQC(J)
      DO 90 I=1,MC
      DO 90 J=1,MI
      XJI=XI(J)-XC(I)
      YJI=YI(J)-YC(I)
      RJI=SQRT(XJI*XJI+YJI*YJI)
      RKO=XK*RJI
      CALL HANKZ2(RKO,2,HZERO,HONE)
   90 A(I+MI+MS,J)=(XK*XK*(EPSI(J)-1./MUI(J))*HZERO+(DXMU(J)*XJI/RJI+
     &DYMU(J)*YJI/RJI)/(MUI(J)*MUI(J))*XK*HONE)*CMPLX(0.,0.25)*DSQI(J)
      DO 100 I=1,MC
      DO 100 J=1,MS
      XJI=XS(J)-XC(I)
      YJI=YS(J)-YC(I)
      RJI=SQRT(XJI*XJI+YJI*YJI)
      RKO=XK*RJI
      CALL HANKZ2(RKO,1,HZERO,HONE)
  100 A(I+MI+MS,J+MI)=(1./MU(J)-1.)*(XJI/RJI*XN(J)+YJI/RJI*YN(J))
     &*CMPLX(0.,0.25)*XK*HONE*DSQ(J)
      DO 120 I=1,MC
      DO 120 J=1,MC
      IF(I.EQ.J) GOTO 110
      XJI=XC(J)-XC(I)
      YJI=YC(J)-YC(I)
      RJI=SQRT(XJI*XJI+YJI*YJI)
      RKO=XK*RJI
      CALL HANKZ2(RKO,1,HZERO,HONE)
      A(I+MI+MS,J+MI+MS)=-(XJI/RJI*XNC(J)+YJI/RJI*YNC(J))
     &*CMPLX(0.,0.25)*XK*HONE*DSQC(J)
      GOTO 120
  110 A(I+MI+MS,J+MI+MS)=0.5
  120 CONTINUE
      RETURN
      END
```

```
C*********************************************************************C
C     THIS SUBROUTINE CALCULATE FAR FIELD AND RADAR CROSS SECTION     C
C*********************************************************************C
      SUBROUTINE FARF1(FINC,MC,MS,MI,XC,YC,XS,YS,XN,YN,XI,YI,DSQC,DSQ,
     &DSQI,EPS,MU,EPSI,MUI,DXMU,DYMU,XK,FIRST,INK,NBIT)
      COMPLEX FINC(500),EPS(MS),MU(MS),EPSI(MI),MUI(MI)
      COMPLEX PSCAT,HZERO,HONE,DXMU(MI),DYMU(MI)
      REAL INK
      DIMENSION XC(MC),YC(MC),XS(MS),YS(MS),XN(MS),YN(MS),XI(MI),YI(MI),
     &DSQC(MC),DSQ(MS),DSQI(MI)
      PI=3.141592654
      RED=0.01745329
      CANG=FIRST
      DO 100 I=1,NBIT
      PSCAT=CMPLX(0.,0.)
      TETA=RED*CANG
      COT=COS(TETA)
      SIT=SIN(TETA)
      DO 20 J=1,MI
      RP=SQRT(XI(J)*XI(J)+YI(J)*YI(J))
      COP=XI(J)/RP
      SIP=YI(J)/RP
      HOLD=XK*RP*(COT*COP+SIT*SIP)
      HZERO=CMPLX(COS(HOLD),SIN(HOLD))
      HONE=CMPLX(0.,1.)*HZERO
      PSCAT=PSCAT-(XK*XK*(EPSI(J)-1./MUI(J))*HZERO-(DXMU(J)*COT+
     &DYMU(J)*SIT)/(MUI(J)*MUI(J))*XK*HONE)*CMPLX(0.,0.25)*DSQI(J)
     &*FINC(J)
   20 CONTINUE
      DO 30 J=1,MS
      RP=SQRT(XS(J)*XS(J)+YS(J)*YS(J))
      COP=XS(J)/RP
      SIP=YS(J)/RP
      HOLD=XK*RP*(COT*COP+SIT*SIP)
      HZERO=CMPLX(COS(HOLD),SIN(HOLD))
      HONE=CMPLX(0.,1.)*HZERO
   30 PSCAT=PSCAT+(1./MU(J)-1.)*(COT*XN(J)+SIT*YN(J))
     &*CMPLX(0.,0.25)*XK*HONE*DSQ(J)*FINC(MI+J)
      DO 40 J=1,MC
      RP=SQRT(XC(J)*XC(J)+YC(J)*YC(J))
      COP=XC(J)/RP
      SIP=YC(J)/RP
      HOLD=XK*RP*(COT*COP+SIT*SIP)
      HZERO=CMPLX(COS(HOLD),SIN(HOLD))
   40 PSCAT=PSCAT+CMPLX(0.,0.25)*HZERO*DSQC(J)*FINC(MI+MS+J)
      PMAG=CABS(PSCAT)
      PPHS=ATAN2(AIMAG(PSCAT),REAL(PSCAT))*180./PI
      SIGMA=10.*LOG10(2.*PMAG*PMAG/PI)
      WRITE(6,50) CANG,SIGMA,PPHS
   50 FORMAT (9X,F13.2,F15.2,F16.1)
      CANG=CANG+INK
  100 CONTINUE
      RETURN
      END
```

```
C*********************************************************************C
C     THIS SUBROUTINE CALCULATE FAR FIELD AND RADAR CROSS SECTION     C
C*********************************************************************C
      SUBROUTINE FARF2(FINC,MC,MS,MI,XC,YC,XS,YS,XNC,YNC,XN,YN,XI,YI,
     &DSQC,DSQ,DSQI,EPS,MU,EPSI,MUI,DXMU,DYMU,XK,FIRST,INK,NBIT)
      COMPLEX FINC(500),EPS(MS),MU(MS),EPSI(MI),MUI(MI)
      COMPLEX PSCAT,HZERO,HONE,DXMU(MI),DYMU(MI)
      REAL INK
      DIMENSION XC(MC),YC(MC),XS(MS),YS(MS),XN(MS),YN(MS),XI(MI),YI(MI),
     &DSQC(MC),DSQ(MS),DSQI(MI),XNC(MC),YNC(MC)
      PI=3.141592654
      RED=0.01745329
      CANG=FIRST
      DO 100 I=1,NBIT
      PSCAT=CMPLX(0.,0.)
      TETA=RED*CANG
      COT=COS(TETA)
      SIT=SIN(TETA)
      DO 20 J=1,MI
      RP=SQRT(XI(J)*XI(J)+YI(J)*YI(J))
      COP=XI(J)/RP
      SIP=YI(J)/RP
      HOLD=XK*RP*(COT*COP+SIT*SIP)
      HZERO=CMPLX(COS(HOLD),SIN(HOLD))
      HONE=CMPLX(0.,1.)*HZERO
      PSCAT=PSCAT-(XK*XK*(EPSI(J)-1./MUI(J))*HZERO-(DXMU(J)*COT+
     &DYMU(J)*SIT)/(MUI(J)*MUI(J))*XK*HONE)*CMPLX(0.,0.25)*DSQI(J)
     &*FINC(J)
 20   CONTINUE
      DO 30 J=1,MS
      RP=SQRT(XS(J)*XS(J)+YS(J)*YS(J))
      COP=XS(J)/RP
      SIP=YS(J)/RP
      HOLD=XK*RP*(COT*COP+SIT*SIP)
      HZERO=CMPLX(COS(HOLD),SIN(HOLD))
      HONE=CMPLX(0.,1.)*HZERO
 30   PSCAT=PSCAT+(1./MU(J)-1.)*(COT*XN(J)+SIT*YN(J))
     &*CMPLX(0.,0.25)*XK*HONE*DSQ(J)*FINC(MI+J)
      DO 40 J=1,MC
      RP=SQRT(XC(J)*XC(J)+YC(J)*YC(J))
      COP=XC(J)/RP
      SIP=YC(J)/RP
      HOLD=XK*RP*(COT*COP+SIT*SIP)
      HZERO=CMPLX(COS(HOLD),SIN(HOLD))
      HONE=CMPLX(0.,1.)*HZERO
 40   PSCAT=PSCAT-(COT*XNC(J)+SIT*YNC(J))
     &*CMPLX(0.,0.25)*XK*HONE*DSQC(J)*FINC(MI+MS+J)
      PMAG=CABS(PSCAT)
      PPHS=ATAN2(AIMAG(PSCAT),REAL(PSCAT))*180./PI
      SIGMA=10.*LOG10(2.*PMAG*PMAG/PI)
      WRITE(6,50) CANG,SIGMA,PPHS
 50   FORMAT (9X,F13.2,F15.2,F16.1)
      CANG=CANG+INK
100   CONTINUE
      RETURN
      END
```

```
C*****************************************************************C
C                                                                 C
      SUBROUTINE HANKZ2(R,N,HZERO,HONE)
C                                                                 C
C*****************************************************************C
C                                                                 C
C         Called by subroutines MATXE and MATXH to compute Hankle C
C     functions of the second kind for orders one and zero.  The  C
C     argument is variable R and must be positive.                C
C                                                                 C
C.....HANKEL FUNCTIONS ARE OF FIRST KIND--J-iY
C.....   N=0 RETURNS HZERO (H-zero)
C.....   N=1 RETURNS HONE  (H-one)
C.....   N=2 RETURNS HZERO AND HONE
C.....SUBROUTINE REQUIRES R>0
C.....SUBROUTINE ADAM MUST BE SUPPLIED BY USER
      DIMENSION A(7),B(7),C(7),D(7),E(7),F(7),G(7),H(7)
      COMPLEX HZERO,HONE
      DATA A,B,C,D,E,F,G,H/1.0,-2.2499997,1.2656208,-0.3163866,
     &0.0444479,-0.0039444,0.00021,0.36746691,0.60559366,-0.74350384,
     &0.25300117,-0.04261214,0.00427916,-0.00024846,0.5,-0.56249985,
     &0.21093573,-0.03954289,0.00443319,-0.00031761,0.00001109,
     &-0.6366198,0.2212091,2.1682709,-1.3164827,0.3123951,-0.0400976,
     &0.0027873,0.79788456,-0.00000077,-0.0055274,-0.00009512,
     &0.00137237,-0.00072805,0.00014476,-0.78539816,-0.04166397,
     &-0.00003954,0.00262573,-0.00054125,-0.00029333,0.00013558,
     &0.79788456,0.00000156,0.01659667,0.00017105,-0.00249511,
     &0.00113653,-0.00020033,-2.35619449,0.12499612,0.0000565,
     &-0.00637879,0.00074348,0.00079824,-0.00029166/
      IF (R.LE.0.0) GO TO 50
      IF (N.LT.0.OR.N.GT.2) GO TO 50
      IF (R.GT.3.0) GO TO 20
      X=R*R/9.0
      IF (N.EQ.1) GO TO 10
      CALL ADAM(A,X,BJ)
      CALL ADAM(B,X,Y)
      BY=0.6366198*ALOG(0.5*R)*BJ+Y
      HZERO=CMPLX(BJ,-BY)
      IF (N.EQ.0) RETURN
 10   CALL ADAM(C,X,Y)
      BJ=R*Y
      CALL ADAM(D,X,Y)
      BY=0.6366198*ALOG(0.5*R)*BJ+Y/R
      HONE=CMPLX(BJ,-BY)
      RETURN
 20   X=3.0/R
      IF (N.EQ.1) GO TO 30
      CALL ADAM(E,X,Y)
      FOOL=Y/SQRT(R)
      CALL ADAM(F,X,Y)
      T=R+Y
      BJ=FOOL*COS(T)
      BY=FOOL*SIN(T)
      HZERO=CMPLX(BJ,-BY)
      IF (N.EQ.0) RETURN
 30   CALL ADAM(G,X,Y)
      FOOL=Y/SQRT(R)
      CALL ADAM(H,X,Y)
      T=R+Y
```

```
      BJ=FOOL*COS(T)
      BY=FOOL*SIN(T)
      HONE=CMPLX(BJ,-BY)
      RETURN
   50 WRITE(6,90) N,R
   90 FORMAT(32HOSICK DATA IN HANKZ2  *QUIT*  N=,I2,2X,2HR=,E11.3)
      CALL SYSTEM
      END

C*********************************************************************C
C                                                                     C
      SUBROUTINE ADAM(C,X,Y)
C                                                                     C
C*********************************************************************C
C                                                                     C
C     Called by subroutine HANKZ2 to compute the value of a 7th       C
C     order polynomial whose argument is X and coefficients are       C
C     contained in vector C.                                          C
      DIMENSION C(7)
      Y=X*C(7)
         DO 10 I=1,5
         Y=X*(C(7-I)+Y)
   10    CONTINUE
      Y=Y+C(1)
      RETURN
      END
```

```
C*********************************************************************C
C                                                                     C
      SUBROUTINE CGEFA(A,LDA,N,IPVT,INFO)
C                                                                     C
C*********************************************************************C
C                                                                     C
C NAASA  2.1.043 CGEFA  FTN-A 05-02-78  THE UNIV OF MICH COMP CTR  C
C
      INTEGER LDA,N,IPVT(1),INFO
      COMPLEX A(LDA,1)
C
C     CGEFA FACTORS A COMPLEX MATRIX BY GAUSSIAN ELIMINATION.
C
C     CGEFA IS USUALLY CALLED BY CGECO, BUT IT CAN BE CALLED
C     DIRECTLY WITH A SAVING IN TIME IF  RCOND  IS NOT NEEDED.
C     (TIME FOR CGECO) = (1 + 9/N)*(TIME FOR CGEFA) .
C
C     ON ENTRY
C
C        A       COMPLEX(LDA, N)
C                THE MATRIX TO BE FACTORED.
C
C        LDA     INTEGER
C                THE LEADING DIMENSION OF THE ARRAY  A .
C
C        N       INTEGER
C                THE ORDER OF THE MATRIX  A .
C
C     ON RETURN
C
C        A       AN UPPER TRIANGULAR MATRIX AND THE MULTIPLIERS
C                WHICH WERE USED TO OBTAIN IT.
C                THE FACTORIZATION CAN BE WRITTEN  A = L*U  WHERE
C                L  IS A PRODUCT OF PERMUTATION AND UNIT LOWER
C                TRIANGULAR MATRICES AND  U  IS UPPER TRIANGULAR.
C
C        IPVT    INTEGER(N)
C                AN INTEGER VECTOR OF PIVOT INDICES.
C
C        INFO    INTEGER
C                = 0  NORMAL VALUE.
C                = K  IF  U(K,K) .EQ. 0.0 .  THIS IS NOT AN ERROR
C                     CONDITION FOR THIS SUBROUTINE, BUT IT DOES
C                     INDICATE THAT CGESL OR CGEDI WILL DIVIDE BY ZERO
C                     IF CALLED.  USE  RCOND  IN CGECO FOR A RELIABLE
C                     INDICATION OF SINGULARITY.
C
C     LINPACK. THIS VERSION DATED 07/14/77 .
C     CLEVE MOLER, UNIVERSITY OF NEW MEXICO, ARGONNE NATIONAL LABS.
C
C     SUBROUTINES AND FUNCTIONS
C
C     BLAS CAXPY,CSCAL,ICAMAX
C     FORTRAN ABS,AIMAG,CMPLX,REAL
C
C     INTERNAL VARIABLES
C
      COMPLEX T
      INTEGER ICAMAX,J,K,KP1,L,NM1
```

```
C
      COMPLEX ZDUM
      REAL CABS1
      CABS1(ZDUM) = ABS(REAL(ZDUM)) + ABS(AIMAG(ZDUM))
C
CCC   Gaussian elimination with partial pivoting
C
      INFO = 0
      NM1 = N - 1
      IF (NM1 .LT. 1) GO TO 70
      DO 60 K = 1, NM1
         KP1 = K + 1
C
C        FIND L = PIVOT INDEX
C
         L = ICAMAX(N-K+1,A(K,K),1) + K - 1
         IPVT(K) = L
C
CCC      Zero pivot implies this column already triangularized
C
         IF (CABS1(A(L,K)) .EQ. 0.0E0) GO TO 40
C
CCC         Interchange if necessary
C
            IF (L .EQ. K) GO TO 10
               T = A(L,K)
               A(L,K) = A(K,K)
               A(K,K) = T
   10       CONTINUE
C
CCC         Compute multipliers
C
            T = -CMPLX(1.0E0,0.0E0)/A(K,K)
            CALL CSCAL(N-K,T,A(K+1,K),1)
C
CCC         Row elimination with column indexing
C
            DO 30 J = KP1, N
               T = A(L,J)
               IF (L .EQ. K) GO TO 20
                  A(L,J) = A(K,J)
                  A(K,J) = T
   20          CONTINUE
               CALL CAXPY(N-K,T,A(K+1,K),1,A(K+1,J),1)
   30       CONTINUE
         GO TO 50
   40    CONTINUE
            INFO = K
   50    CONTINUE
   60 CONTINUE
   70 CONTINUE
      IPVT(N) = N
      IF (CABS1(A(N,N)) .EQ. 0.0E0) INFO = N
      RETURN
      END
C                                                                      C
C**********************************************************************C
C                                                                      C
      SUBROUTINE CGESL(A,LDA,N,IPVT,B,JOB)
C                                                                      C
```

```
C*****************************************************************C
C                                                                 C
C NAASA  2.1.044 CGESL  FTN-A 05-02-78  THE UNIV OF MICH COMP CTR  C
C
      INTEGER LDA,N,IPVT(1),JOB
      COMPLEX A(LDA,1),B(1)
C
C     CGESL SOLVES THE COMPLEX SYSTEM
C     A * X = B  OR  CTRANS(A) * X = B
C     USING THE FACTORS COMPUTED BY CGECO OR CGEFA.
C
C     ON ENTRY
C
C        A       COMPLEX(LDA, N)
C                THE OUTPUT FROM CGECO OR CGEFA.
C
C        LDA     INTEGER
C                THE LEADING DIMENSION OF THE ARRAY  A .
C
C        N       INTEGER
C                THE ORDER OF THE MATRIX  A .
C
C        IPVT    INTEGER(N)
C                THE PIVOT VECTOR FROM CGECO OR CGEFA.
C
C        B       COMPLEX(N)
C                THE RIGHT HAND SIDE VECTOR.
C
C        JOB     INTEGER
C                = 0         TO SOLVE  A*X = B ,
C                = NONZERO   TO SOLVE  CTRANS(A)*X = B  WHERE
C                            CTRANS(A)  IS THE CONJUGATE TRANSPOSE.
C
C     ON RETURN
C
C        B       THE SOLUTION VECTOR  X .
C
C     ERROR CONDITION
C
C        A DIVISION BY ZERO WILL OCCUR IF THE INPUT FACTOR CONTAINS A
C        ZERO ON THE DIAGONAL.  TECHNICALLY THIS INDICATES SINGULARITY
C        BUT IT IS OFTEN CAUSED BY IMPROPER ARGUMENTS OR IMPROPER
C        SETTING OF LDA .  IT WILL NOT OCCUR IF THE SUBROUTINES ARE
C        CALLED CORRECTLY AND IF CGECO HAS SET RCOND .GT. 0.0
C        OR CGEFA HAS SET INFO .EQ. 0 .
C
C     TO COMPUTE  INVERSE(A) * C  WHERE  C  IS A MATRIX
C     WITH  P  COLUMNS
C           CALL CGECO(A,LDA,N,IPVT,RCOND,Z)
C           IF (RCOND IS TOO SMALL) GO TO ...
C           DO 10 J = 1, P
C              CALL CGESL(A,LDA,N,IPVT,C(1,J),0)
C        10 CONTINUE
C
C     LINPACK. THIS VERSION DATED 07/14/77 .
C     CLEVE MOLER, UNIVERSITY OF NEW MEXICO, ARGONNE NATIONAL LABS.
C
C     SUBROUTINES AND FUNCTIONS
C
C     BLAS CAXPY,CDOTC
```

```
C     FORTRAN CONJG
C
C     INTERNAL VARIABLES
C
      COMPLEX CDOTC,T
      INTEGER K,KB,L,NM1
C
      NM1 = N - 1
      IF (JOB .NE. 0) GO TO 50
C
C        JOB = 0 , SOLVE  A * X = B
C        FIRST SOLVE  L*Y = B
C
         IF (NM1 .LT. 1) GO TO 30
         DO 20 K = 1, NM1
            L = IPVT(K)
            T = B(L)
            IF (L .EQ. K) GO TO 10
               B(L) = B(K)
               B(K) = T
   10       CONTINUE
            CALL CAXPY(N-K,T,A(K+1,K),1,B(K+1),1)
   20    CONTINUE
   30    CONTINUE
C
C        NOW SOLVE  U*X = Y
C
         DO 40 KB = 1, N
            K = N + 1 - KB
            B(K) = B(K)/A(K,K)
            T = -B(K)
            CALL CAXPY(K-1,T,A(1,K),1,B(1),1)
   40    CONTINUE
      GO TO 100
   50 CONTINUE
C
C        JOB = NONZERO, SOLVE  CTRANS(A) * X = B
C        FIRST SOLVE  CTRANS(U)*Y = B
C
         DO 60 K = 1, N
            T = CDOTC(K-1,A(1,K),1,B(1),1)
            B(K) = (B(K) - T)/CONJG(A(K,K))
   60    CONTINUE
C
C        NOW SOLVE CTRANS(L)*X = Y
C
         IF (NM1 .LT. 1) GO TO 90
         DO 80 KB = 1, NM1
            K = N - KB
            B(K) = B(K) + CDOTC(N-K,A(K+1,K),1,B(K+1),1)
            L = IPVT(K)
            IF (L .EQ. K) GO TO 70
               T = B(L)
               B(L) = B(K)
               B(K) = T
   70       CONTINUE
   80    CONTINUE
   90    CONTINUE
  100 CONTINUE
      RETURN
```

```
      END
C                                                                      C
C**********************************************************************C
C                                                                      C
      SUBROUTINE CAXPY(N,CA,CX,INCX,CY,INCY)
C                                                                      C
C**********************************************************************C
C                                                                      C
C NAASA  1.1.014 CAXPY  FTN-A 05-02-78  THE UNIV OF MICH COMP CTR  C
C
C     CONSTANT TIMES A VECTOR PLUS A VECTOR.
C     JACK DONGARRA, LINPACK, 6/17/77.
C
      COMPLEX CX(1),CY(1),CA
      INTEGER I,INCX,INCY,IX,IY,N
C
      IF(N.LE.0)RETURN
      IF (ABS(REAL(CA)) + ABS(AIMAG(CA)) .EQ. 0.0 ) RETURN
      IF(INCX.EQ.1.AND.INCY.EQ.1)GOTO 20
C
CCC      Code for unequal increments or equal increments
CCC      Not equal to 1
C
      IX = 1
      IY = 1
      IF(INCX.LT.0)IX = (-N+1)*INCX + 1
      IF(INCY.LT.0)IY = (-N+1)*INCY + 1
      DO 10 I = 1,N
        CY(IY) = CY(IY) + CA*CX(IX)
        IX = IX + INCX
        IY = IY + INCY
   10 CONTINUE
      RETURN
C
CCC      Code for both increments equal to 1
C
   20 DO 30 I = 1,N
        CY(I) = CY(I) + CA*CX(I)
   30 CONTINUE
      RETURN
      END
C                                                                      C
C**********************************************************************C
      COMPLEX FUNCTION CDOTC(N,CX,INCX,CY,INCY)
C**********************************************************************C
C                                                                      C
C NAASA  1.1.012 CDOTC  FTN-A 05-02-78  THE UNIV OF MICH COMP CTR  C
C
C     FORMS THE DOT PRODUCT OF TWO VECTORS, CONJUGATING THE FIRST
C     VECTOR.
C     JACK DONGARRA, LINPACK,  6/17/77.
C
      COMPLEX CX(1),CY(1),CTEMP
      INTEGER I,INCX,INCY,IX,IY,N
C
      CTEMP = (0.0,0.0)
      CDOTC = (0.0,0.0)
      IF(N.LE.0)RETURN
      IF(INCX.EQ.1.AND.INCY.EQ.1)GOTO 20
C
```

```
CCC      Code for unequal increments or equal increments
CCC      Not equal to 1
C
      IX = 1
      IY = 1
      IF(INCX.LT.0)IX = (-N+1)*INCX + 1
      IF(INCY.LT.0)IY = (-N+1)*INCY + 1
      DO 10 I = 1,N
        CTEMP = CTEMP + CONJG(CX(IX))*CY(IY)
        IX = IX + INCX
        IY = IY + INCY
   10 CONTINUE
      CDOTC = CTEMP
      RETURN
C
CCC      Code for both increments equal to 1
C
   20 DO 30 I = 1,N
        CTEMP = CTEMP + CONJG(CX(I))*CY(I)
   30 CONTINUE
      CDOTC = CTEMP
      RETURN
      END
C                                                                      C
C**********************************************************************C
C                                                                      C
      SUBROUTINE  CSCAL(N,CA,CX,INCX)
C                                                                      C
C**********************************************************************C
C                                                                      C
C NAASA  1.1.019 CSCAL  FTN-A 05-02-78  THE UNIV OF MICH COMP CTR  C
C
C     SCALES A VECTOR BY A CONSTANT.
C     JACK DONGARRA, LINPACK,  6/17/77.
C
      COMPLEX CA,CX(1)
      INTEGER I,INCX,N,NINCX
C
      IF(N.LE.0)RETURN
      IF(INCX.EQ.1)GOTO 20
C
CCC      Code for increment not equal to 1
C
      NINCX = N*INCX
      DO 10 I = 1,NINCX,INCX
        CX(I) = CA*CX(I)
   10 CONTINUE
      RETURN
C
CCC      Code for increment equal to 1
C
   20 DO 30 I = 1,N
        CX(I) = CA*CX(I)
   30 CONTINUE
      RETURN
      END
C                                                                      C
C**********************************************************************C
C                                                                      C
      SUBROUTINE  CSSCAL(N,SA,CX,INCX)
```

```
C                                                                      C
C**********************************************************************C
C                                                                      C
C NAASA  1.1.018 CSSCAL FTN-A 05-02-78  THE UNIV OF MICH COMP CTR  C
C
C     SCALES A COMPLEX VECTOR BY A REAL CONSTANT.
C     JACK DONGARRA, LINPACK, 6/17/77.
C
      COMPLEX CX(1)
      REAL SA
      INTEGER I,INCX,N,NINCX
C
      IF(N.LE.0)RETURN
      IF(INCX.EQ.1)GOTO 20
C
CCC      Code for increment not equal to 1
C
      NINCX = N*INCX
      DO 10 I = 1,NINCX,INCX
        CX(I) = CMPLX(SA*REAL(CX(I)),SA*AIMAG(CX(I)))
   10 CONTINUE
      RETURN
C
CCC      Code for increment equal to 1
C
   20 DO 30 I = 1,N
        CX(I) = CMPLX(SA*REAL(CX(I)),SA*AIMAG(CX(I)))
   30 CONTINUE
      RETURN
      END
C                                                                      C
C**********************************************************************C
      INTEGER FUNCTION ICAMAX(N,CX,INCX)
C**********************************************************************C
C                                                                      C
C NAASA  1.1.021 ICAMAX FTN-A 05-02-78  THE UNIV OF MICH COMP CTR  C
C
C     FINDS THE INDEX OF ELEMENT HAVING MAX. ABSOLUTE VALUE.
C     JACK DONGARRA, LINPACK, 6/17/77.
C
      COMPLEX CX(1)
      REAL SMAX
      INTEGER I,INCX,IX,N
      COMPLEX ZDUM
      REAL CABS1
      CABS1(ZDUM) = ABS(REAL(ZDUM)) + ABS(AIMAG(ZDUM))
C
      ICAMAX = 1
      IF(N.LE.1)RETURN
      IF(INCX.EQ.1)GOTO 20
C
CCC      Code for increment not equal to 1
C
      IX = 1
      SMAX = CABS1(CX(1))
      IX = IX + INCX
      DO 10 I = 2,N
         IF(CABS1(CX(IX)).LE.SMAX) GO TO 5
         ICAMAX = I
         SMAX = CABS1(CX(IX))
```

```
    5    IX = IX + INCX
   10 CONTINUE
      RETURN
C
CCC      Code for increment equal to 1
C
   20 SMAX = CABS1(CX(1))
      DO 30 I = 2,N
         IF(CABS1(CX(I)).LE.SMAX) GO TO 30
         ICAMAX = I
         SMAX = CABS1(CX(I))
   30 CONTINUE
      RETURN
      END
C                                                                      C
C**********************************************************************C
      REAL FUNCTION SCASUM(N,CX,INCX)
C**********************************************************************C
C                                                                      C
C NAASA  1.1.010 SCASUM FTN-A 05-02-78  THE UNIV OF MICH COMP CTR  C
C
C     TAKES THE SUM OF THE ABSOLUTE VALUES OF A COMPLEX VECTOR AND
C     RETURNS A SINGLE PRECISION RESULT.
C     JACK DONGARRA, LINPACK, 6/17/77.
C
      COMPLEX CX(1)
      REAL STEMP
      INTEGER I,INCX,N,NINCX
C
      SCASUM = 0.0E0
      STEMP = 0.0E0
      IF(N.LE.0)RETURN
      IF(INCX.EQ.1)GOTO 20
C
CCC      Code for increment not equal to 1
C
      NINCX = N*INCX
      DO 10 I = 1,NINCX,INCX
        STEMP = STEMP + ABS(REAL(CX(I))) + ABS(AIMAG(CX(I)))
   10 CONTINUE
      SCASUM = STEMP
      RETURN
C
CCC      Code for increment equal to 1
C
   20 DO 30 I = 1,N
        STEMP = STEMP + ABS(REAL(CX(I))) + ABS(AIMAG(CX(I)))
   30 CONTINUE
      SCASUM = STEMP
      RETURN
      END
C**********************************************************************C
C                                                                      C
C     The following subroutines are standard LINPACK routines          C
C     to perform L-U decomposition and back substitution on a          C
C     single precision complex matrix.  See CC-Memo 407 sec 2.1        C
C     for documentation on these routines.                             C
C                                                                      C
C**********************************************************************C
C                                                                      C
```

```
      SUBROUTINE CGECO(A,LDA,N,IPVT,RCOND,Z)
C                                                                       C
C***********************************************************************C
C                                                                       C
C NAASA  2.1.042 CGECO  FTN-A 05-02-78  THE UNIV OF MICH COMP CTR  C
C
      INTEGER LDA,N,IPVT(1)
      COMPLEX A(LDA,1),Z(1)
      REAL RCOND
C
C     CGECO FACTORS A COMPLEX MATRIX BY GAUSSIAN ELIMINATION
C     AND ESTIMATES THE CONDITION OF THE MATRIX.
C
C     IF  RCOND  IS NOT NEEDED, CGEFA IS SLIGHTLY FASTER.
C     TO SOLVE  A*X = B , FOLLOW CGECO BY CGESL.
C     TO COMPUTE  INVERSE(A)*C , FOLLOW CGECO BY CGESL.
C     TO COMPUTE  DETERMINANT(A) , FOLLOW CGECO BY CGEDI.
C     TO COMPUTE  INVERSE(A) , FOLLOW CGECO BY CGEDI.
C
C     ON ENTRY
C
C        A       COMPLEX(LDA, N)
C                THE MATRIX TO BE FACTORED.
C
C        LDA     INTEGER
C                THE LEADING DIMENSION OF THE ARRAY  A .
C
C        N       INTEGER
C                THE ORDER OF THE MATRIX  A .
C
C     ON RETURN
C
C        A       AN UPPER TRIANGULAR MATRIX AND THE MULTIPLIERS
C                WHICH WERE USED TO OBTAIN IT.
C                THE FACTORIZATION CAN BE WRITTEN  A = L*U  WHERE
C                L  IS A PRODUCT OF PERMUTATION AND UNIT LOWER
C                TRIANGULAR MATRICES AND  U  IS UPPER TRIANGULAR.
C
C        IPVT    INTEGER(N)
C                AN INTEGER VECTOR OF PIVOT INDICES.
C
C        RCOND   REAL
C                AN ESTIMATE OF THE RECIPROCAL CONDITION OF  A .
C                FOR THE SYSTEM  A*X = B , RELATIVE PERTURBATIONS
C                IN  A  AND  B  OF SIZE  EPSILON  MAY CAUSE
C                RELATIVE PERTURBATIONS IN  X  OF SIZE  EPSILON/RCOND .
C                IF  RCOND  IS SO SMALL THAT THE LOGICAL EXPRESSION
C                          1.0 + RCOND .EQ. 1.0
C                IS TRUE, THEN  A  MAY BE SINGULAR TO WORKING
C                PRECISION.  IN PARTICULAR,  RCOND  IS ZERO  IF
C                EXACT SINGULARITY IS DETECTED OR THE ESTIMATE
C                UNDERFLOWS.
C
C        Z       COMPLEX(N)
C                A WORK VECTOR WHOSE CONTENTS ARE USUALLY UNIMPORTANT.
C                IF  A  IS CLOSE TO A SINGULAR MATRIX, THEN  Z  IS
C                AN APPROXIMATE NULL VECTOR IN THE SENSE THAT
C                NORM(A*Z) = RCOND*NORM(A)*NORM(Z) .
C
C     LINPACK. THIS VERSION DATED 07/14/77 .
```

```
C     CLEVE MOLER, UNIVERSITY OF NEW MEXICO, ARGONNE NATIONAL LABS.
C
C     SUBROUTINES AND FUNCTIONS
C
C     LINPACK CGEFA
C     BLAS CAXPY,CDOTC,CSSCAL,SCASUM
C     FORTRAN ABS,AIMAG,AMAX1,CMPLX,CONJG,REAL
C
C     INTERNAL VARIABLES
C
      COMPLEX CDOTC,EK,T,WK,WKM
      REAL ANORM,S,SCASUM,SM,YNORM
      INTEGER INFO,J,K,KB,KP1,L
C
      COMPLEX ZDUM,ZDUM1,ZDUM2,CSIGN1
      REAL CABS1
      CABS1(ZDUM) = ABS(REAL(ZDUM)) + ABS(AIMAG(ZDUM))
      CSIGN1(ZDUM1,ZDUM2) = CABS1(ZDUM1)*(ZDUM2/CABS1(ZDUM2))
C
CCC   Compute 1-NORM of A
C
      ANORM = 0.0E0
      DO 10 J = 1, N
      ANORM = AMAX1(ANORM,SCASUM(N,A(1,J),1))
   10 CONTINUE
C
CCC   Factor
C
      CALL CGEFA(A,LDA,N,IPVT,INFO)
C
C     RCOND = 1/(NORM(A)*(ESTIMATE OF NORM(INVERSE(A)))) .
C     ESTIMATE = NORM(Z)/NORM(Y) WHERE  A*Z = Y  AND  CTRANS(A)*Y = E .
C     CTRANS(A)  IS THE CONJUGATE TRANSPOSE OF A .
C     THE COMPONENTS OF  E  ARE CHOSEN TO CAUSE MAXIMUM LOCAL
C     GROWTH IN THE ELEMENTS OF W  WHERE  CTRANS(U)*W = E .
C     THE VECTORS ARE FREQUENTLY RESCALED TO AVOID OVERFLOW.
C
C     SOLVE CTRANS(U)*W = E
C
      EK = CMPLX(1.0E0,0.0E0)
      DO 20 J = 1, N
         Z(J) = CMPLX(0.0E0,0.0E0)
   20 CONTINUE
      DO 100 K = 1, N
         IF (CABS1(Z(K)) .NE. 0.0E0) EK = CSIGN1(EK,-Z(K))
         IF (CABS1(EK-Z(K)) .LE. CABS1(A(K,K))) GO TO 30
            S = CABS1(A(K,K))/CABS1(EK-Z(K))
            CALL CSSCAL(N,S,Z,1)
            EK = CMPLX(S,0.0E0)*EK
   30    CONTINUE
         WK = EK - Z(K)
         WKM = -EK - Z(K)
         S = CABS1(WK)
         SM = CABS1(WKM)
         IF (CABS1(A(K,K)) .EQ. 0.0E0) GO TO 40
            WK = WK/CONJG(A(K,K))
            WKM = WKM/CONJG(A(K,K))
         GO TO 50
   40    CONTINUE
            WK = CMPLX(1.0E0,0.0E0)
```

```
            WKM = CMPLX(1.0E0,0.0E0)
   50     CONTINUE
          KP1 = K + 1
          IF (KP1 .GT. N) GO TO 90
             DO 60 J = KP1, N
                SM = SM + CABS1(Z(J)+WKM*CONJG(A(K,J)))
                Z(J) = Z(J) + WK*CONJG(A(K,J))
                S = S + CABS1(Z(J))
   60        CONTINUE
             IF (S .GE. SM) GO TO 80
                T = WKM - WK
                WK = WKM
                DO 70 J = KP1, N
                   Z(J) = Z(J) + T*CONJG(A(K,J))
   70           CONTINUE
   80        CONTINUE
   90     CONTINUE
          Z(K) = WK
  100  CONTINUE
       S = 1.0E0/SCASUM(N,Z,1)
       CALL CSSCAL(N,S,Z,1)
C
CCC    Solve CTRANS(L)*Y = V
C
       DO 120 KB = 1, N
          K = N + 1 - KB
          IF (K .LT. N) Z(K) = Z(K) + CDOTC(N-K,A(K+1,K),1,Z(K+1),1)
          IF (CABS1(Z(K)) .LE. 1.0E0) GO TO 110
             S = 1.0E0/CABS1(Z(K))
             CALL CSSCAL(N,S,Z,1)
  110     CONTINUE
          L = IPVT(K)
          T = Z(L)
          Z(L) = Z(K)
          Z(K) = T
  120  CONTINUE
       S = 1.0E0/SCASUM(N,Z,1)
       CALL CSSCAL(N,S,Z,1)
C
       YNORM = 1.0E0
C
CCC    Solve L*V = Y
C
       DO 140 K = 1, N
          L = IPVT(K)
          T = Z(L)
          Z(L) = Z(K)
          Z(K) = T
          IF (K .LT. N) CALL CAXPY(N-K,T,A(K+1,K),1,Z(K+1),1)
          IF (CABS1(Z(K)) .LE. 1.0E0) GO TO 130
             S = 1.0E0/CABS1(Z(K))
             CALL CSSCAL(N,S,Z,1)
             YNORM = S*YNORM
  130     CONTINUE
  140  CONTINUE
       S = 1.0E0/SCASUM(N,Z,1)
       CALL CSSCAL(N,S,Z,1)
       YNORM = S*YNORM
C
CCC    Solve U*Z = V
```

```
C
      DO 160 KB = 1, N
         K = N + 1 - KB
         IF (CABS1(Z(K)) .LE. CABS1(A(K,K))) GO TO 150
            S = CABS1(A(K,K))/CABS1(Z(K))
            CALL CSSCAL(N,S,Z,1)
            YNORM = S*YNORM
  150    CONTINUE
         IF (CABS1(A(K,K)) .NE. 0.0E0) Z(K) = Z(K)/A(K,K)
         IF (CABS1(A(K,K)) .EQ. 0.0E0) Z(K) = CMPLX(1.0E0,0.0E0)
         T = -Z(K)
         CALL CAXPY(K-1,T,A(1,K),1,Z(1),1)
  160 CONTINUE
C     MAKE ZNORM = 1.0
      S = 1.0E0/SCASUM(N,Z,1)
      CALL CSSCAL(N,S,Z,1)
      YNORM = S*YNORM
C
      IF (ANORM .NE. 0.0E0) RCOND = YNORM/ANORM
      IF (ANORM .EQ. 0.0E0) RCOND = 0.0E0
      RETURN
      END
```

DESCRIPTION AND LIST OF CODE **VSIE-ISO**

Jian-Ming Jin

Radiation Laboratory

Department of Electrical Engineering and Computer Science

The University of Michigan

Ann Arbor, Michigan 48109

ABSTRACT

A FORTRAN program named as **VSIE-ISO** and developed by the author is described briefly and listed thereafter.

1. Objective of VSIE-ISO

VSIE-ISO is a computer code written in FORTRAN language and developed for computing electromagnetic scattering from an inhomogeneous penetrable cylinder for both TE and TM incidence.

VSIE-ISO uses quadrilateral isoparametric elements and point-matching technique to solve the volume-surface integral equation (VSIE). For the formulation of VSIE, please read the first paper in this report. For the description of the numerical implementation, please read the third paper. **VSIE-ISO** was used to generate the data presented in the third paper.

Due to the success of **VSIE-ISO**, we will extend it to include the treatment of conducting surfaces and discontinous interfaces. The resulting program should be able to treat complex problems as **VSIEM** does, but with a much higher accuracy.

2. Input Data

All input data are provided by file **INPUT** except for relative permittivity and permeability and their derivatives which are specified by subroutines **EMFUN** and **DRFUN**. A detailed description of the input data is given in the main program. A sample file of **INPUT** for the geometry shown in Figure 1 is listed below.

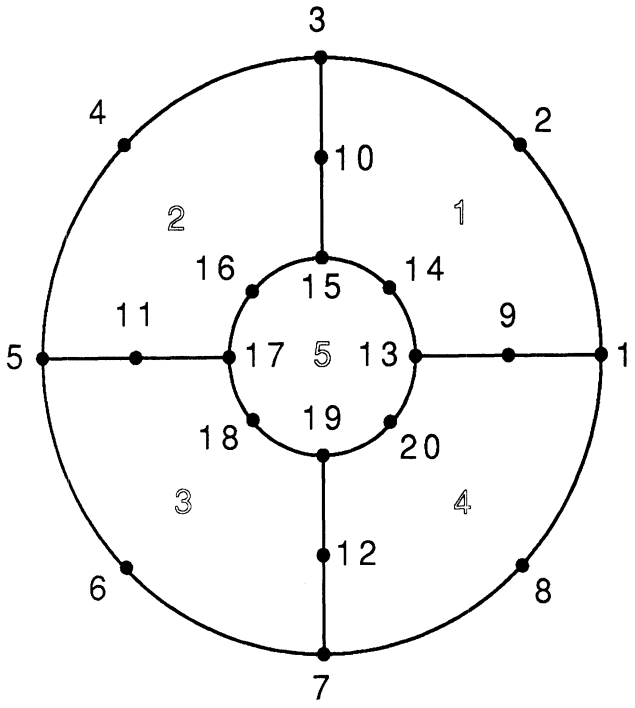

Figure 1: A five quadrilateral element model with 20 nodes for a circular region.

```
DIELECTRIC CIRCULAR CYLINDER
  0  20.0
  1  1   0.      180.       30.      180.
```

```
20  5
 8  4
 1   1.         0.
 2   0.70711    0.70711
 3   0.         1.
 4  -0.70711    0.70711
 5  -1.         0.
 6  -0.70711   -0.70711
 7   0.        -1.
 8   0.70711   -0.70711
 9   0.65       0.
10   0.         0.65
11  -0.65       0.
12   0.        -0.65
13   0.3        0.
14   0.21213    0.21213
15   0.         0.3
16  -0.21213    0.21213
17  -0.3        0.
18  -0.21213   -0.21213
19   0.        -0.3
20   0.21213   -0.21213
 1   15 13  1   3 14  9   2 10
 2   17 15  3   5 16 10   4 11
 3   19 17  5   7 18 11   6 12
 4   13 19  7   1 20 12   8  9
 5   13 15 17 19 14 16 18 20
 1    1  3  2
 2    3  5  4
 3    5  7  6
 4    7  1  8
```

3. Output Data

The output data are written in file **OUTPUT**. The data contain the geometry and discretization information and the computed result. Following is a sample output.

```
DIELECTRIC CIRCULAR CYLINDER
        TOTAL NUMBER OF DISCRETE POINTS      20
         I          X(I)          Y(I)

         1        1.00000        0.00000
         2        0.70711        0.70711
         3        0.00000        1.00000
         4       -0.70711        0.70711
         5       -1.00000        0.00000
         6       -0.70711       -0.70711
         7        0.00000       -1.00000
         8        0.70711       -0.70711
         9        0.65000        0.00000
```

10	0.00000	0.65000
11	-0.65000	0.00000
12	0.00000	-0.65000
13	0.30000	0.00000
14	0.21213	0.21213
15	0.00000	0.30000
16	-0.21213	0.21213
17	-0.30000	0.00000
18	-0.21213	-0.21213
19	0.00000	-0.30000
20	0.21213	-0.21213

TOTAL NUMBER OF AREA ELEMENTS 5

L	N(1,L)	N(2,L)	N(3,L)	N(4,L)	N(5,L)	N(6,L)	N(7,L)	N(8,L)
1	15	13	1	3	14	9	2	10
2	17	15	3	5	16	10	4	11
3	19	17	5	7	18	11	6	12
4	13	19	7	1	20	12	8	9
5	13	15	17	19	14	16	18	20

TOTAL NUMBER OF LINE ELEMENTS 4

L	N(1,L)	N(2,L)	N(3,L)
1	1	3	2
2	3	5	4
3	5	7	6
4	7	1	8

KEY PARAMETERS

INCIDENT POLARIZATION	E
NUMBER OF INCIDENT FIELD DIRECTIONS	1
NUMBER OF BISTATIC DIRECTIONS	7
WAVELENGTH	20.00000

FIELD VALUES AT NODES

NODE	REAL	IMAGINARY	MAGNITUDE
1	0.1071E-01	-0.8549E-01	0.0862
2	0.3847E-01	-0.7804E-01	0.0870
3	0.1417E+00	-0.1951E-01	0.1431
4	0.1945E+00	0.2023E-01	0.1956
5	0.1983E+00	0.9312E-01	0.2191
6	0.1945E+00	0.2023E-01	0.1956
7	0.1417E+00	-0.1951E-01	0.1431
8	0.3847E-01	-0.7804E-01	0.0870
9	-0.5831E-01	-0.9881E-02	0.0591
10	0.1395E-01	-0.6613E-01	0.0676
11	0.7612E-01	-0.8084E-01	0.1110
12	0.1395E-01	-0.6613E-01	0.0676
13	-0.6544E-01	0.2954E-01	0.0718
14	-0.6291E-01	0.1555E-01	0.0648
15	-0.5218E-01	-0.1739E-01	0.0550
16	-0.4194E-01	-0.4392E-01	0.0607
17	-0.3658E-01	-0.5415E-01	0.0653

```
18        -0.4194E-01   -0.4392E-01          0.0607
19        -0.5218E-01   -0.1739E-01          0.0550
20        -0.6291E-01    0.1555E-01          0.0648


      BISTATIC SCATTERING CROSS SECTION
     FOR INCIDENT FIELD DIRECTION= 180.00
    THETA   10*LOG(SIGMA/LAMBDA)   PHASE

     0.00          -4.03          -41.2
    30.00          -4.19          -40.8
    60.00          -4.63          -39.7
    90.00          -5.25          -37.9
   120.00          -5.89          -35.8
   150.00          -6.38          -34.0
   180.00          -6.56          -33.3
```

4. Program Description

Following is a brief description of the main program and subroutines developed for **VSIE-ISO**. All others not described here are standard subroutines and since they are already listed in **VSIEM** they will not be listed here. Note that the equations referenced below are referred to those in the third paper.

VSIE-ISO - Main program acting as a driver for subroutines.

EMFUM - Specifies ϵ_r and μ_r at a given point (x, y).

DRFUN - Specifies $\nabla\epsilon_r$ and $\nabla\mu_r$ at a given point (x, y).

MATRIX1 - Computes the contribution of the area integral to the system matrix.

MATRIX2 - Computes the contribution of the line integral to the system matrix.

FRAF1 - Computes the contribution of the area integral to the far field.

FRAF2 - Computes the contribution of the line integral to the far field.

CALAE - Computes $A(\bar{r}|\bar{r}')$ in (5).

CALAE1 - Computes $A(\bar{r}|\bar{r}')$ in (5) for $\bar{r}$ at infinity.

CALBE - Computes $B(\bar{r}|\bar{r}')$ in (5).

CALBE1 - Computes $B(\bar{r}|\bar{r}')$ in (5) for $\bar{r}$ at infinity.

CALNE - Calculates $N_i^e(\xi,\eta)$ in (14).

CALNEXI - Calculates $\partial N_i^e/\partial\xi$.

CALNETA - Calculates $\partial N_i^e/\partial\eta$.

CALNE1 - Calculates $L_i^s(\xi)$ in (9).

CALNEXI1 - Calculates $\partial L_i^s/\partial\xi$.

```
C*********************************************************************C
C                          PROGRAM VSIE-ISO                           C
C*********************************************************************C
C                                                                     C
C   THIS PROGRAM USES QUADRILATERAL ISOPARAMETRIC ELEMENTS AND POINT- C
C   MATCHING TECHNIQUE TO SOLVE VOLUME-SURFACE INTEGRAL EQUATION FOR  C
C   ELECTROMAGNETIC SCATTERING BY A DIELECTRIC CYLINDER.              C
C                                                                     C
C*********************************************************************C
C*********************************************************************C
C  INPUT FORMAT FOR PROGRAM VSIE-ISO----VERSION OF AUG. 20, 1988      C
C*********************************************************************C
C  CARD 1  FORMAT (18A4)          TITLE CARD; USE UP TO 72 COLUMNS    C
C*********************************************************************C
C  CARD 2  FORMAT (I3,F10.5)   KODE,WAVE                              C
C          KODE=0       COMPUTES BISTATIC SCATTERING PATTERN          C
C          KODE=1       COMPUTES BACKSCATTERING PATTERN               C
C          WAVE         WAVELENGTH                                    C
C*********************************************************************C
C  CARD 3  FORMAT (I3,I3,4F10.5)  IPP,IOPT,FIRST,LAST,INK,CANG        C
C          IPP=1        E-POLARIZATION                                C
C          IPP=2        H-POLARIZATION                                C
C          IOPT=0       INTERIOR FIELDS NOT PRINTED                   C
C          IOPT=1       INTERIOR FIELDS PRINTED                       C
C          FIRST        INITIAL SCATTERING AND INCIDENCE ANGLE        C
C          LAST         FINAL ANGLE                                   C
C          INK          ANGULAR INCREMENT                             C
C          CANG         ANGLE FOR BISTATIC COMPUTATION                C
C*********************************************************************C
C          FORMAT FOR INPUT NUMBER OF NODES AND ELEMENTS              C
C*********************************************************************C
C  CARD 4  FORMAT (2I3)  N,M                                          C
C          N            NUMBER OF NODES                               C
C          M            NUMBER OF QUADRILATERAL ELEMENTS              C
C*********************************************************************C
C          FORMAT FOR INPUT NUMBER OF SURFACE NODES AND SEGMENTS      C
C*********************************************************************C
C  CARD 5  FORMAT (2I3)  N1,M1                                        C
C          N1           NUMBER OF NODES ON THE SURFACE                C
C          M1           NUMBER OF QUADRATIC SEGMENTS ON THE SURFACE   C
C*********************************************************************C
C          DO I=1,N TO READ THE NODE POSITION                         C
C*********************************************************************C
C  CARD 6  FORMAT (I3,2F10.5) I,X(I),Y(I)                             C
C          I            NODE NUMBER                                   C
C          X(I)         NODE X-COORDINATE                             C
C          Y(I)         NODE Y-COORDINATE                             C
C*********************************************************************C
C          REPEAT CARD 6 FOR EACH NODE                                C
C*********************************************************************C
C          DO I=1,M TO READ THE NODE-ELEMENT RELATION                 C
C*********************************************************************C
C  CARD 7  FORMAT (I3,2X,8I3) I,(NUM(J,I),J=1,8)                      C
C          I            ELEMENT NUMBER                                C
C          NUM(J,I)     GLOBAL NUMBER OF NODE J IN ELEMENT I          C
C*********************************************************************C
C          REPEAT CARD 7 FOR EACH ELEMENT                             C
C*********************************************************************C
C          DO I=1,M1 TO READ THE NODE-SEGMENT RELATION                C
```

```
C*********************************************************************C
C  CARD 8  FORMAT (I3,2X,3I3) I,(NUM1(J,I),J=1,3)                     C
C          I            SEGMENT NUMBER                                C
C          NUM1(J,I)    GLOBAL NUMBER OF NODE J AT SEGMENT I          C
C*********************************************************************C
C          REPEAT CARD 8 FOR EACH SEGMENT                             C
C*********************************************************************C
       COMPLEX A(100,100),FINC(100),FAR(91)
       REAL X(100),Y(100),LAST,INK
       INTEGER NUM(8,50),NUM1(3,50),KPVT(100)
       DIMENSION ID(18),IPOL(2)
       DATA RED,IPOL/0.01745329,4HEEEE,4HHHHH/
       OPEN(UNIT=5,FILE='INPUT')
C       OPEN(UNIT=6,FILE='OUTPUT')
       READ(5,1000) ID
       WRITE(6,1005) ID
       READ(5,1010) KODE,WAVE
       READ(5,1020) IPP,IOPT,FIRST,LAST,INK,CANG
       READ(5,1030) N,M
       READ(5,1030) N1,M1
       DO I=1,N
       READ(5,1040) X(I),Y(I)
       END DO
       DO I=1,M
       READ(5,1050) (NUM(J,I),J=1,8)
       END DO
       DO I=1,M1
       READ(5,1050) (NUM1(J,I),J=1,3)
       END DO
C......PRINT INPUT DATA
       WRITE(6,1060) N
       WRITE(6,10) (I,X(I),Y(I),I=1,N)
   10  FORMAT(9X,I3,5X,F10.5,5XF10.5)
       WRITE(6,1070) M
       DO 20 L=1,M
   20  WRITE(6,30) L,(NUM(I,L),I=1,8)
   30  FORMAT(10X,I2,3X,8(3X,I3,2X))
       WRITE(6,1080) M1
       DO 40 L=1,M1
   40  WRITE(6,50) L,(NUM1(I,L),I=1,3)
   50  FORMAT(10X,I2,3X,3(3X,I3,2X))
C......CALL SUBROUTINES TO FORM SYSTEM MATRIX
       CALL MATRIX1(A,N,M,X,Y,NUM,WAVE,IPP)
       CALL MATRIX2(A,N,N1,M1,X,Y,NUM1,WAVE,IPP)
C......CALL SUBROUTINE TO SOLVE THE MATRIX
       CALL CGECO(A,100,N,KPVT,RC,FINC)
       XK=2.*3.141592654/WAVE
       IF (KODE.NE.0) GO TO 70
       NINC=1
       NBIT=1+IFIX((LAST-FIRST)/INK)
       GO TO 80
  70   NBIT=1
       NINC=1+IFIX((LAST-FIRST)/INK)
  80   WRITE (6,400) IPOL(IPP),NINC,NBIT,WAVE
       IF(KODE.EQ.1) WRITE(6,600)
       IF(KODE.EQ.1) CANG=FIRST
  90   TETA=RED*CANG
       CT=COS(TETA)
       ST=SIN(TETA)
       DO 100 I=1,N
```

```
      HOLD=XK*(CT*X(I)+ST*Y(I))
  100 FINC(I)=CMPLX(COS(HOLD),SIN(HOLD))
C..... COMPUTE NEAR FIELD (NODAL FIELD VALUES)
      CALL CGESL(A,100,N,KPVT,FINC,0)
      IF(IOPT.EQ.0) GOTO 101
      WRITE(6,700)
      DO 98 I=1,N
   98 WRITE(6,99) I,FINC(I),CABS(FINC(I))
   99 FORMAT(5X,I3,5X,2E14.4,5X,F12.4)
  101 CONTINUE
      CALL FARF1(FAR,FINC,N,M,X,Y,NUM,WAVE,FIRST,INK,NBIT,IPP)
      CALL FARF2(FAR,FINC,N,N1,M1,X,Y,NUM1,WAVE,FIRST,INK,NBIT,IPP)
      PI=3.141592654
      IF(KODE.EQ.0) WRITE(6,610) CANG
      DO 102 I=1,NBIT
      ANGLE=FIRST+INK*FLOAT(I-1)
      PMAG=CABS(FAR(I))
      SIGMA=10.*LOG10(2.*PMAG*PMAG/PI)
      PPHS=ATAN2(AIMAG(FAR(I)),REAL(FAR(I)))*180./PI
      WRITE(6,650) ANGLE,SIGMA,PPHS
  102 CONTINUE
      IF(KODE.EQ.1) THEN
      CANG=CANG+INK
      FIRST=CANG
      IF(CANG.LE.LAST) GOTO 90
      ELSE
      END IF
 1000 FORMAT (18A4)
 1005 FORMAT (1X,18A4)
 1010 FORMAT (I3,F10.5)
 1020 FORMAT (I3,I3,4F10.5)
 1030 FORMAT (2I3)
 1040 FORMAT (3X,2F10.5)
 1050 FORMAT (5X,8I3)
 1060 FORMAT(10X,'TOTAL NUMBER OF DISCRETE POINTS',5X,I3/
     & 10X,' I',10X,'X(I)',10X,'Y(I)'/)
 1070 FORMAT(//10X,'TOTAL NUMBER OF AREA ELEMENTS',5X,I3/
     & 10X,' L',5X,'N(1,L)',2X,'N(2,L)',2X,'N(3,L)',2X,'N(4,L)',
     & 2X,'N(5,L)',2X,'N(6,L)',2X,'N(7,L)',2X,'N(8,L)'/)
 1080 FORMAT(//10X,'TOTAL NUMBER OF LINE ELEMENTS',5X,I3/
     & 10X,' L',5X,'N(1,L)',2X,'N(2,L)',2X,'N(3,L)'/)
  400 FORMAT (//25X,14HKEY PARAMETERS//
     &10X,21HINCIDENT POLARIZATION,22X,1A1/
     &10X,35HNUMBER OF INCIDENT FIELD DIRECTIONS,I9/
     &10X,29HNUMBER OF BISTATIC DIRECTIONS,I15/
     &10X,10HWAVELENGTH,F34.5)
  600 FORMAT (///,20X,28HBACKSCATTERING CROSS SECTION/17X,
     &36HTHETA   10*LOG(SIGMA/LAMBDA)   PHASE/)
  610 FORMAT (///,19X,33HBISTATIC SCATTERING CROSS SECTION/18X,
     &29HFOR INCIDENT FIELD DIRECTION=,F7.2/17X,
     &36HTHETA   10*LOG(SIGMA/LAMBDA)   PHASE/)
  650 FORMAT (9X,F13.2,F15.2,F16.1)
  700 FORMAT(//20X,'FIELD VALUES AT NODES',/
     &5X,'NODE          REAL       IMAGINARY          MAGNITUDE'/)
      STOP
      END
```

```
      SUBROUTINE EMFUN(X,Y,EPS,MU,IPP)
      COMPLEX EPS,MU,EXCH
C..... SPECIFY PERMITTIVITY AND PERMEABILITY
      EPS=(72.,-162.)
      MU=(1.0,0.0)
      IF(IPP.EQ.2) RETURN
      EXCH=EPS
      EPS=MU
      MU=EXCH
      RETURN
      END



      SUBROUTINE DRFUN(X,Y,DXEPS,DYEPS,IPP)
      COMPLEX DXEPS,DYEPS,DXMU,DYMU
C..... SPECIFY THE DERIVATIVES OF PERMITTIVITY AND PERMEABILITY
      DXEPS=(0.,0.)
      DYEPS=(0.,0.)
      DXMU=(0.,0.)
      DYMU=(0.,0.)
      IF(IPP.EQ.2) RETURN
      DXEPS=DXMU
      DYEPS=DYMU
      RETURN
      END
```

```
      SUBROUTINE MATRIX1(A,N,M,X,Y,NUM,WAVE,IPP)
      COMPLEX A(100,100),AE,AIJ,EPS,MU,B(8)
      REAL X(N),Y(N),W(3),T(3),NE(8),NEXI(8),NETA(8)
      REAL X1(8),Y1(8)
      INTEGER NUM(8,M)
      DATA W/0.5555555556,0.8888888889,0.5555555556/
      DATA T/-0.7745966692,0.,0.7745966692/
      DO 100 I=1,N
      DO 100 J=1,N
  100 A(I,J)=CMPLX(0.,0.)
      DO 120 I=1,N
      CALL EMFUN(X(I),Y(I),EPS,MU,IPP)
  120 A(I,I)=1./EPS
      DO 900 L=1,M
      DO 150 I1=1,8
      X1(I1)=X(NUM(I1,L))
  150 Y1(I1)=Y(NUM(I1,L))
      DO 700 J=1,3
      WJ=W(J)
      XI=T(J)
      DO 600 K=1,3
      WK=W(K)
      ETA=T(K)
      CALL CALNE(NE,XI,ETA)
      XX=0.
      YY=0.
      DO 200 I1=1,8
      XX=XX+NE(I1)*X1(I1)
  200 YY=YY+NE(I1)*Y1(I1)
      CALL CALNEXI(NEXI,XI,ETA)
      CALL CALNETA(NETA,XI,ETA)
      XXI=0.
      YXI=0.
      XETA=0.
      YETA=0.
      DO 300 I1=1,8
      XXI=XXI+X1(I1)*NEXI(I1)
      YXI=YXI+Y1(I1)*NEXI(I1)
      XETA=XETA+X1(I1)*NETA(I1)
  300 YETA=YETA+Y1(I1)*NETA(I1)
      DETJ=ABS(XXI*YETA-XETA*YXI)
      DO 1000 II=1,N
      CALL CALAE(AE,X(II),Y(II),XX,YY,WAVE,IPP)
      DO 400 I=1,8
  400 B(I)=WJ*WK*NE(I)*AE*DETJ
      DO 1000 I=1,8
      JJ=NUM(I,L)
      A(II,JJ)=A(II,JJ)+B(I)
 1000 CONTINUE
  600 CONTINUE
  700 CONTINUE
  800 CONTINUE
  900 CONTINUE
      RETURN
      END
```

```
      SUBROUTINE MATRIX2(A,N,N1,M1,X,Y,NUM1,WAVE,IPP)
      COMPLEX A(100,100),BE,AIJ,EPS,MU,B(3)
      REAL X(N),Y(N),W(4),T(4),NE(3),NEXI(3),X1(3),Y1(3)
      INTEGER NUM1(3,M1)
      DATA W/0.3478548451,0.6521451549,0.6521451549,0.3478548451/
      DATA T/-0.8611363116,-0.3399810436,0.3399810436,0.8611363116/
      DO 100 I=1,N1
      CALL EMFUN(X(I),Y(I),EPS,MU,IPP)
  100 A(I,I)=A(I,I)+0.5*(1.-1./EPS)
      DO 900 L=1,M1
      DO 150 I1=1,3
      X1(I1)=X(NUM1(I1,L))
  150 Y1(I1)=Y(NUM1(I1,L))
      DO 700 J=1,4
      WJ=W(J)
      XI=T(J)
      CALL CALNE1(NE,XI)
      XX=0.
      YY=0.
      DO 200 I1=1,3
      XX=XX+NE(I1)*X1(I1)
  200 YY=YY+NE(I1)*Y1(I1)
      CALL CALNEXI1(NEXI,XI)
      XXI=0.
      YXI=0.
      DO 300 I1=1,3
      XXI=XXI-X1(I1)*NEXI(I1)
  300 YXI=YXI+Y1(I1)*NEXI(I1)
      DETJ=SQRT(XXI*XXI+YXI*YXI)
      XXI=XXI/DETJ
      YXI=YXI/DETJ
      DO 1000 II=1,N
      CALL CALBE(BE,X(II),Y(II),XX,YY,XXI,YXI,WAVE,IPP)
      DO 400 I=1,3
  400 B(I)=WJ*NE(I)*BE*DETJ
      DO 1000 I=1,3
      JJ=NUM1(I,L)
      A(II,JJ)=A(II,JJ)+B(I)
 1000 CONTINUE
  700 CONTINUE
  800 CONTINUE
  900 CONTINUE
      RETURN
      END
```

```
      SUBROUTINE FARF1(FAR,F,N,M,X,Y,NUM,WAVE,FIRST,DANG,NBIT,IPP)
      COMPLEX F(100),AE,AIJ,EPS,MU,B(8),FAR(1)
      REAL X(N),Y(N),W(3),T(3),NE(8),NEXI(8),NETA(8)
      REAL X1(8),Y1(8)
      INTEGER NUM(8,M)
      DATA W/0.5555555556,0.8888888889,0.5555555556/
      DATA T/-0.7745966692,0.,0.7745966692/
      DO 170 I=1,NBIT
  170 FAR(I)=CMPLX(0.,0.)
      DO 900 L=1,M
      DO 150 I1=1,8
      X1(I1)=X(NUM(I1,L))
  150 Y1(I1)=Y(NUM(I1,L))
      DO 700 J=1,3
      WJ=W(J)
      XI=T(J)
      DO 600 K=1,3
      WK=W(K)
      ETA=T(K)
      CALL CALNE(NE,XI,ETA)
      XX=0.
      YY=0.
      DO 200 I1=1,8
      XX=XX+NE(I1)*X1(I1)
  200 YY=YY+NE(I1)*Y1(I1)
      CALL CALNEXI(NEXI,XI,ETA)
      CALL CALNETA(NETA,XI,ETA)
      XXI=0.
      YXI=0.
      XETA=0.
      YETA=0.
      DO 300 I1=1,8
      XXI=XXI+X1(I1)*NEXI(I1)
      YXI=YXI+Y1(I1)*NEXI(I1)
      XETA=XETA+X1(I1)*NETA(I1)
  300 YETA=YETA+Y1(I1)*NETA(I1)
      DETJ=ABS(XXI*YETA-XETA*YXI)
      DO 1000 II=1,NBIT
      ANG=(FIRST+FLOAT(II-1)*DANG)*3.141592654/180.
      CALL CALAE1(AE,ANG,XX,YY,WAVE,IPP)
      DO 400 I=1,8
      JJ=NUM(I,L)
  400 FAR(II)=FAR(II)+WJ*WK*NE(I)*AE*DETJ*F(JJ)
 1000 CONTINUE
  600 CONTINUE
  700 CONTINUE
  800 CONTINUE
  900 CONTINUE
      RETURN
      END
```

```
      SUBROUTINE FARF2(FAR,F,N,N1,M1,X,Y,NUM1,WAVE,FIRST,DANG,NBIT,IPP)
      COMPLEX F(100),BE,AIJ,EPS,MU,FAR(1)
      REAL X(N),Y(N),W(4),T(4),NE(3),NEXI(3),X1(3),Y1(3)
      INTEGER NUM1(3,M1)
      DATA W/0.3478548451,0.6521451549,0.6521451549,0.3478548451/
      DATA T/-0.8611363116,-0.3399810436,0.3399810436,0.8611363116/
      DO 900 L=1,M1
      DO 150 I1=1,3
      X1(I1)=X(NUM1(I1,L))
  150 Y1(I1)=Y(NUM1(I1,L))
      DO 700 J=1,4
      WJ=W(J)
      XI=T(J)
      CALL CALNE1(NE,XI)
      XX=0.
      YY=0.
      DO 200 I1=1,3
      XX=XX+NE(I1)*X1(I1)
  200 YY=YY+NE(I1)*Y1(I1)
      CALL CALNEXI1(NEXI,XI)
      XXI=0.
      YXI=0.
      DO 300 I1=1,3
      XXI=XXI-X1(I1)*NEXI(I1)
  300 YXI=YXI+Y1(I1)*NEXI(I1)
      DETJ=SQRT(XXI*XXI+YXI*YXI)
      XXI=XXI/DETJ
      YXI=YXI/DETJ
      DO 1000 II=1,NBIT
      ANG=(FIRST+FLOAT(II-1)*DANG)*3.141592654/180.
      CALL CALBE1(BE,ANG,XX,YY,XXI,YXI,WAVE,IPP)
      DO 400 I=1,3
      JJ=NUM1(I,L)
  400 FAR(II)=FAR(II)+WJ*NE(I)*BE*DETJ*f(jj)
 1000 CONTINUE
  700 CONTINUE
  900 CONTINUE
      RETURN
      END
```

```
      SUBROUTINE CALAE(AE,X,Y,XP,YP,WAVE,IPP)
      COMPLEX AE,EPS,MU,HZERO,HONE,DXEPS,DYEPS
      PI=3.141592654
      XK=2.*PI/WAVE
      XJI=X-XP
      YJI=Y-YP
      RJI=SQRT(XJI*XJI+YJI*YJI)
      RKO=XK*RJI
      CALL HANKZ2(RKO,2,HZERO,HONE)
      CALL EMFUN(XP,YP,EPS,MU,IPP)
      CALL DRFUN(XP,YP,DXEPS,DYEPS,IPP)
      AE=XK*XK*(MU-1./EPS)*HZERO*CMPLX(0.,0.25)-(DXEPS*XJI/RJI+
     & DYEPS*YJI/RJI)/(EPS*EPS)*XK*HONE*CMPLX(0.,0.25)
      RETURN
      END



      SUBROUTINE CALAE1(AE,ANG,XP,YP,WAVE,IPP)
      COMPLEX AE,EPS,MU,HZERO,HONE,DXEPS,DYEPS
      PI=3.141592654
      XK=2.*PI/WAVE
      RP=SQRT(XP*XP+YP*YP)
      IF(RP.EQ.0.) GOTO 1
      COP=XP/RP
      SIP=YP/RP
      COT=COS(ANG)
      SIT=SIN(ANG)
1     HOLD=XK*RP*(COT*COP+SIT*SIP)
      HZERO=CMPLX(COS(HOLD),SIN(HOLD))
      HONE=CMPLX(0.,1.)*HZERO
      CALL EMFUN(XP,YP,EPS,MU,IPP)
      CALL DRFUN(XP,YP,DXEPS,DYEPS,IPP)
      AE=XK*XK*(MU-1./EPS)*HZERO*CMPLX(0.,0.25)+(DXEPS*COT+
     & DYEPS*SIT)/(EPS*EPS)*XK*HONE*CMPLX(0.,0.25)
      RETURN
      END
```

```
      SUBROUTINE CALBE(BE,X,Y,XP,YP,XXI,YXI,WAVE,IPP)
      COMPLEX BE,EPS,MU,HZERO,HONE
      PI=3.141592654
      XK=2.*PI/WAVE
      XJI=X-XP
      YJI=Y-YP
      RJI=SQRT(XJI*XJI+YJI*YJI)
      RKO=XK*RJI
      CALL HANKZ2(RKO,1,HZERO,HONE)
      CALL EMFUN(XP,YP,EPS,MU,IPP)
      BE=(1.-1./EPS)*(XJI/RJI*YXI+YJI/RJI*XXI)*HONE*XK*CMPLX(0.,0.25)
      RETURN
      END



      SUBROUTINE CALBE1(BE,ANG,XP,YP,XXI,YXI,WAVE,IPP)
      COMPLEX BE,EPS,MU,HZERO,HONE
      PI=3.141592654
      XK=2.*PI/WAVE
      RP=SQRT(XP*XP+YP*YP)
      COP=XP/RP
      SIP=YP/RP
      COT=COS(ANG)
      SIT=SIN(ANG)
1     HOLD=XK*RP*(COT*COP+SIT*SIP)
      HZERO=CMPLX(COS(HOLD),SIN(HOLD))
      HONE=CMPLX(0.,1.)*HZERO
      CALL EMFUN(XP,YP,EPS,MU,IPP)
      BE=(1.-1./EPS)*(COT*YXI+SIT*XXI)*HONE*XK*CMPLX(0.,0.25)
      RETURN
      END
```

```
SUBROUTINE CALNE(NE,XI,ETA)
REAL NE(8)
NE(1)=-0.25*(1.-XI)*(1.-ETA)*(XI+ETA+1.)
NE(2)=0.25*(1.+XI)*(1.-ETA)*(XI-ETA-1.)
NE(3)=0.25*(1.+XI)*(1.+ETA)*(XI+ETA-1.)
NE(4)=0.25*(1.-XI)*(1.+ETA)*(-XI+ETA-1.)
NE(5)=0.5*(1.-XI*XI)*(1.-ETA)
NE(6)=0.5*(1.+XI)*(1.-ETA*ETA)
NE(7)=0.5*(1.-XI*XI)*(1.+ETA)
NE(8)=0.5*(1.-XI)*(1.-ETA*ETA)
RETURN
END


SUBROUTINE CALNEXI(NEXI,XI,ETA)
REAL NEXI(8)
NEXI(1)=0.25*(1.-ETA)*(XI+ETA+1.)-0.25*(1.-XI)*(1.-ETA)
NEXI(2)=0.25*(1.-ETA)*(XI-ETA-1.)+0.25*(1.+XI)*(1.-ETA)
NEXI(3)=0.25*(1.+ETA)*(XI+ETA-1.)+0.25*(1.+XI)*(1.+ETA)
NEXI(4)=-0.25*(1.+ETA)*(-XI+ETA-1.)-0.25*(1.-XI)*(1.+ETA)
NEXI(5)=-XI*(1.-ETA)
NEXI(6)=0.5*(1.-ETA*ETA)
NEXI(7)=-XI*(1.+ETA)
NEXI(8)=-0.5*(1.-ETA*ETA)
RETURN
END


SUBROUTINE CALNETA(NETA,XI,ETA)
REAL NETA(8)
NETA(1)=0.25*(1.-XI)*(XI+ETA+1.)-0.25*(1.-XI)*(1.-ETA)
NETA(2)=-0.25*(1.+XI)*(XI-ETA-1.)-0.25*(1.+XI)*(1.-ETA)
NETA(3)=0.25*(1.+XI)*(XI+ETA-1.)+0.25*(1.+XI)*(1.+ETA)
NETA(4)=0.25*(1.-XI)*(-XI+ETA-1.)+0.25*(1.-XI)*(1.+ETA)
NETA(5)=-0.5*(1.-XI*XI)
NETA(6)=-ETA*(1.+XI)
NETA(7)=0.5*(1.-XI*XI)
NETA(8)=-ETA*(1.-XI)
RETURN
END
```

```
SUBROUTINE CALNE1(NE,XI)
REAL NE(3)
NE(1)=-0.5*(1.-XI)*XI
NE(2)=0.5*(1.+XI)*XI
NE(3)=1.-XI*XI
RETURN
END


SUBROUTINE CALNEXI1(NEXI,XI)
REAL NEXI(3)
NEXI(1)=0.5*XI-0.5*(1.-XI)
NEXI(2)=0.5*XI+0.5*(1.+XI)
NEXI(3)=-2.*XI
RETURN
END
```